NASA
Technical
Paper
2691

July 1987

Flight Investigation of the Effects of an Outboard Wing-Leading-Edge Modification on Stall/Spin Characteristics of a Low-Wing, Single-Engine, T-Tail Light Airplane

H. Paul Stough III,
Daniel J. DiCarlo,
and James M. Patton, Jr.

NASA

NASA Technical Paper 2691

1987

Flight Investigation of the Effects of an Outboard Wing-Leading-Edge Modification on Stall/Spin Characteristics of a Low-Wing, Single-Engine, T-Tail Light Airplane

H. Paul Stough III,
Daniel J. DiCarlo,
and James M. Patton, Jr.

Langley Research Center
Hampton, Virginia

National Aeronautics and Space Administration

Scientific and Technical Information Office

Contents

List of Figures

Summary

Flight tests were performed to investigate the change in stall/spin characteristics due to the addition of an outboard wing-leading-edge modification to a four-place, low-wing, single-engine, T-tail, general aviation research airplane. Stalls and attempted spins were performed for various weights, center-of-gravity positions, power settings, flap deflections, and landing-gear positions. Both stall behavior and spin resistance were improved compared with the baseline airplane. The baseline airplane would readily spin for all combinations of power settings, flap deflections, and aileron inputs, but the modified airplane did not spin at idle power or with flaps extended. With maximum power and flaps retracted, the modified airplane did enter spins with abused loadings or for certain combinations of maneuver and control input. The modified airplane tended to spin at a higher angle of attack than the baseline airplane.

Introduction

In response to the need for improving the stall/spin characteristics of general aviation airplanes, the National Aeronautics and Space Administration (NASA) is conducting a comprehensive program to develop new stall/spin technology for this class of airplane (ref. 1). The program incorporates spin-tunnel model tests, static- and rotary-balance wind-tunnel tests, analytic studies, and airplane and model flight tests for a number of configurations representative of typical general aviation airplanes weighing under 4000 lb.

Stalling and spinning are major causal factors in general aviation accidents (refs. 2 through 4). Examination of the circumstances involved suggests that the majority of these stall/spin accidents occur at low altitude and involve inadvertent loss of longitudinal or lateral-directional control, spin entry, and ground impact before the spin becomes fully developed. In recognition of the potential danger associated with the inadvertent stalls at low altitude, studies are being conducted at the NASA Langley Research Center to define concepts which improve the stall characteristics and spin resistance of light airplanes. Because the inadvertent spin usually occurs at low altitude, emphasis is being placed on spin resistance rather than spin recovery.

Lateral stability and controllability at the stall of airplanes with unswept wings are characterized by the tendency of such wings to experience unstable damping in roll and autorotation near the stall. Unstable damping in roll can result in rapid rolling and yawing motions which the pilot may find difficult to control. High angular rates may result from unstable damping in roll and may lead to autorotation at higher angular rates and at angles of attack at which the vehicle may exhibit a developed spin mode.

Wing-leading-edge devices such as slots, slats, or flaps can significantly improve the damping-in-roll characteristics of wings near the stall. Early research of the National Advisory Committee for Aeronautics (NACA) by Weick, et al. (refs. 5 through 9) identified the potential aerodynamic benefit of such wing modifications; however, many of the concepts proposed by the early research efforts proved impractical because of attendant degradation in aerodynamic performance, complexity of construction, excessive maintenance, and cost. Also, certain types of leading-edge, high-lift devices improved stall behavior but aggravated spin characteristics and degraded spin recovery.

Model tests at NASA Langley more fully explored the effects of these and several other wing-leading-edge modifications. Promising modifications were selected for flight testing based on the criteria that, for practical application to light aircraft, such a modification should have a minimum adverse effect on airplane performance below the stall, should be lightweight, should be passive (not require sensors and actuators or pilot activation), should require a minimum of maintenance, and should be low cost.

A discontinuous, outboard wing-leading-edge droop modification which appears to meet these requirements was conceived and flight tested on an airplane with an untwisted rectangular wing (ref. 10). Subsequently, a similar wing modification was developed (ref. 11) for the twisted, tapered wing of the low-wing, T-tail airplane of reference 12.

This report presents results of flight tests of the low-wing, T-tail airplane with the wing leading edge modified to increase spin resistance. Stall characteristics and the results of attempted spin entries are presented along with the effects of center-of-gravity position, power, flaps, and control inputs on these characteristics. Comparisons are made with the stall/spin characteristics of the airplane prior to modification of the wing.

Symbols and Abbreviations

Measurements are referred to the set of body axes with the origin at the airplane center of gravity, as shown in figure 1. Measurements were made and quantities are presented in U.S. Customary Units. Symbols in parentheses refer to labels on computer-generated figures.

a_N	(NORM ACC)	normal acceleration at center of gravity (positive in negative Z_b direction), g units
	(ALTITUDE)	pressure altitude, ft
BL		butt line; lateral displacement from centerline of fuselage, in.
b		wing span, ft
C_D		drag coefficient, $\frac{\text{Drag}}{\frac{1}{2}\rho V^2 S}$
C_L		lift coefficient, $\frac{\text{Lift}}{\frac{1}{2}\rho V^2 S}$
$\bar{c}$		mean aerodynamic chord, ft
c.g.		center of gravity
FS		fuselage station; longitudinal coordinate measured along waterline, positive moving aft, in.
g		acceleration due to gravity, 32.2 ft/sec^2
I_x, I_y, I_z		moment of inertia about X_b, Y_b, and Z_b body axis, respectively, slug-ft^2
L.E.		leading edge
	(LAT ACC)	lateral acceleration at center of gravity (positive in positive Y_b direction), g units
	(LAT FORCE)	lateral wheel force (positive for forces tending to rotate wheel clockwise), lb
	(LONG ACC)	longitudinal acceleration at center of gravity (positive in positive X_b direction), g units
	(LONG FORCE)	longitudinal wheel force (positive for forces tending to pull wheel aft), lb
m		mass of airplane, slugs
	(MPR)	engine manifold pressure, in. Hg
p	(ROLL RATE)	roll rate (positive for rolling right wing down), deg/sec
	(PROP SPEED)	propeller and engine speed, rpm
q	(PITCH RATE)	pitch rate (positive for pitching nose up), deg/sec
R		spin radius, ft; $R \approx \frac{g}{\left(\frac{\Omega}{57.3}\right)^2 \tan \alpha}$, ft
R/S		rate of sink, ft/sec
r	(YAW RATE)	yaw rate (positive for yawing nose right), deg/sec
	(RES ACC)	resultant linear acceleration, (LONG ACC^2 + LAT ACC^2 + NORM ACC^2)$^{1/2}$, g units
	(RUD FORCE)	rudder pedal force (positive for forces tending to push right pedal forward), lb
S		wing area, ft^2
T		period of spin, $\approx \frac{360}{\Omega}$, sec
	(THRUST)	propeller thrust determined using engine performance chart and assumed propeller efficiency of 0.85, lb
V	(SPEED)	true airspeed, ft/sec (see fig. 1)
WL		waterline; vertical coordinate in airplane plane of symmetry measured perpendicular to reference line (reference line is WL 40.00 and passes through propeller shaft centerline at back of spinner), in.
WS		wing station, in.
X_b, Y_b, Z_b		body axes through airplane c.g. (see fig. 1)
x		distance rearward from leading edge of mean aerodynamic chord to center of gravity, ft

y		distance between center of gravity and fuselage centerline (positive when center of gravity is right of centerline), ft
z		distance between center of gravity and fuselage reference line (positive when center of gravity is below line), ft
α	(ALPHA CG)	true angle of attack at airplane center of gravity, deg (see fig. 1)
α_L		angle of attack at left-wing tip boom location, deg
α_m		measured angle of attack at instrumentation boom, deg
α_R		angle of attack at right-wing tip boom location, deg
α_T		true angle of attack at instrumentation boom, deg
β	(BETA CG)	angle of sideslip at airplane center of gravity, deg (see fig. 1)
δ_a	(AILERON)	average aileron deflection (positive for right aileron trailing edge down), 1/2 (Right aileron deflection + Left aileron deflection), deg (see fig. 1)
δ_e	(STABILATOR)	stabilator deflection (positive for trailing edge down), deg (see fig. 1)
δ_f		flap deflection (positive for trailing edge down), deg
δ_r	(RUDDER)	rudder deflection (positive for trailing edge left), deg (see fig. 1)
μ		airplane relative density, $\frac{m}{\rho S b}$
ρ		air density, slugs/ft^3
ϕ		bank angle (positive for right wing down), deg
Ω	(TURN RATE)	total angular velocity of airplane, $(p^2+q^2+r^2)^{1/2}$, with sign of r, deg/sec

Description of Airplane

The test airplane was a four-place, low-wing, single-engine, retractable-gear, T-tail design. This airplane was a one-of-a-kind research airplane, but it was considered representative of this class of aircraft. A photograph and three-view drawing of the airplane are presented as figures 2 and 3, respectively; physical characteristics of the baseline airplane are presented in table 1. The mass characteristics and inertia parameters for representative loadings tested with the modified wing are presented in table 2.

The baseline wing incorporated a modified NACA 65_2-415 airfoil section. The leading edge of the tapered portion of the wing was drooped and transitioned smoothly from no droop at the start of the taper to maximum droop at the wing tip. The wing had slotted trailing-edge flaps and plain ailerons. The horizontal tail was mounted on the vertical tail at the top of the rudder and consisted of a stabilator with a geared antiservo tab to provide longitudinal trim. An adjustable spring in the rudder control cables served to trim out rudder forces. Aileron trim was not adjustable in flight. The airplane was equipped with a spin-recovery parachute system (ref. 13), a quick-release door on the right side, and a pyrotechnic egress panel in the absence of a door on the left side (ref. 14).

The baseline wing was modified by installation of a glove over the forward part of the airfoil to provide a 2.9-percent chord extension and droop, which increased the leading-edge camber and radius, as shown in figure 4. The droop geometry duplicated the leading-edge airfoil configuration developed in reference 11 as a means of improving lateral stability at the stall. Transition from the original airfoil section to the drooped leading edge was an abrupt discontinuity. Coordinates of the baseline wing sections are presented in table 3; coordinates of the new airfoil sections created by addition of the glove are presented in table 4. The modified wing-leading-edge geometry varied linearly in the spanwise direction from the inboard end to the tip end of the modification.

Tests were conducted at center-of-gravity positions from $0.2394\bar{c}$ to $0.3207\bar{c}$ (12.66 to 4.53 percent static margin) at test weights of 2438 to 2829 lb (take off weights of 2498 to 2889 lb). Figure 5 shows the test loadings relative to the design c.g. envelope. The inertia yawing-moment parameter, calculated from measured moments of inertia, varied from -62×10^{-4} to -24×10^{-4}.

Instrumentation

The airplane was instrumented to measure and record flow angles and true airspeed ahead of each wing tip, linear accelerations along the body axes, angular rates about the body axes, control surface positions, control wheel and rudder pedal forces, engine power parameters, altitude, and spin-recovery parachute load. The onboard data system was supplemented by ground-based telephoto video and movie cameras and by cockpit- and wing-tip-mounted cameras. Pilot comments were recorded on the ground-based videotape. All data were time correlated and provided a continuous time history from maneuver entry through recovery. The data were telemetered to a ground station and were monitored in real time along with a video display of the airplane. For debriefing purposes, the videotape and telemetry records were reviewed shortly after each flight.

Linear accelerations and flow measurements were corrected to indicate conditions at the airplane center of gravity using the techniques reported in reference 15. Angle-of-attack measurements were corrected for upwash by applying the flow correction presented in figure 6 (taken from ref. 12). Because true angles of attack from both wing tips were averaged, corrections to angle of attack due to sidewash at the wing tips have a tendency to cancel out. Likewise, because measurements from both wing tips were averaged, corrections to sideslip due to upwash at the wing tips have a tendency to cancel out (ref. 16).

Evaluation Procedure

The results of the investigation were based on pilot comments, time-history records of airplane motions and controls, and films and videotapes of the tests. The majority of maneuvers were flown by three NASA research pilots. Maneuvers were also flown by three industry test pilots and two FAA test pilots.

Initial tests evaluated airplane stall and departure characteristics. Maneuvers included $1g$ and accelerated (banked) stalls with various combinations of engine power, bank angle, and sideslip as shown in table 5.

Spin tests were performed at the NASA Wallops Flight Facility. Test altitudes ranged from 12 000 to 6000 ft. Most spins were entered at an altitude of about 10 000 ft, which corresponds to a Reynolds number at the stall of about 3×10^6. Spin-entry conditions included combinations of acceleration, roll, pitch, yaw, and power. Pro-spin controls were applied at or just before the stall. The control positions at entry were wheel back with pro-spin rudder and ailerons either neutral, with the spin (right wheel for a right spin), or against the spin (left wheel for a right spin). In some instances, additional control inputs were made during the post-stall gyrations in an effort to drive the airplane into a spin. Spin entry was also attempted from the conditions of the stall/spin scenarios described in reference 4, as representative of typical inadvertent spin entries.

The effects of center-of-gravity position, weight, power level, and flap position were investigated individually and in combination. Stall/spin characteristics were evaluated by NASA pilots over the weight and c.g. range. Test pilots from three light-airplane manufacturers and from the FAA evaluated the airplane stall/spin characteristics at the aft c.g. ($0.2804\bar{c}$) and at a gross weight of 2690 lb.

Results and Discussion

Stall Characteristics

Airplane stall characteristics with the wing-leading-edge modification are presented in table 5 and are illustrated via time histories in figures 7 and 9 through 15. Comparisons are made with the unmodified airplane where data are available. Qualitatively, the baseline airplane stall characteristics had been described as "good" and more docile than those of most current airplanes of this class (ref. 12). The pilots described the modified airplane stall characteristics at the aft-center-of-gravity ($0.2804\bar{c}$) gross-weight loading as "outstanding", "very docile", "benign", and "controllable". Good controllability throughout the stall and excellent aileron control at minimum speed conditions with the control wheel full back were also noted.

Stall characteristics of the modified airplane were evaluated with flaps and gear retracted, with flaps extended 10° and 40°, and with flaps and gear extended. Stalls were entered from level flight, from left and right turns, and from pullups with and without sideslip at idle power, power for level flight (75 percent), and maximum power. Both the slow (1 knot/sec) and rapid (3 to 5 knots/sec) deceleration rates to the stall, as specified in reference 17, were used. For the modified airplane, no uncontrollable motions were encountered during the 127 stalls performed over the loading range tested (0.2394 to $0.3207\bar{c}$). Airplane stalling characteristics met the requirements of FAR Part 23 (ref. 17).

Idle-power stalls. For the baseline airplane, slow deceleration to a $1g$, wings-level stall with near-zero sideslip resulted in a Dutch-roll-type motion with the airplane flying in and out of the stall. The baseline airplane stalled at about 20° angle of attack (2° trailing-edge-up stabilator deflection

at a center-of-gravity position of about 28 percent $\bar{c}$). Additional trailing-edge-up stabilator deflection beyond that required to stall the airplane generally resulted in a roll-off to the left. This roll-off was often initially uncontrollable even with full rudder and aileron inputs against the roll. Stalls from coordinated 30° and 60° banked turns produced little roll-off tendency. When stalled with sideslip, the airplane rolled away from the slip; that is, right sideslip produced a left roll.

For the modified airplane, slow deceleration to a 1g, wings-level stall with near-zero sideslip (fig. 7) resulted in a small pitching oscillation (nose bobble) with roll- and yaw-rate oscillations that the pilot perceived to be less throughout the maneuver than for the unmodified airplane. The modified airplane stall was sensed at 20° angle of attack (about 4° trailing-edge-up stabilator deflection at a center-of-gravity position of about 28 percent $\bar{c}$) and was usually accompanied by the onset of small pitch-rate oscillations; however, the modified wing outer panels did not stall until the local angle of attack reached 36° as indicated by tufts on the wing. Figure 8 shows tufts on the modified wings during an attempted spin entry as photographed from a camera inside the airplane cabin. At the instant of this picture, the outer panel of the left wing was just at stall (36° angle of attack); the outer panel of the right wing was at 31° angle of attack. Additional trailing-edge-up stabilator deflection beyond that required to stall the modified airplane generally resulted in a slight roll tendency that was easily controlled with small aileron and rudder inputs. Figure 9 compares the characteristics of the modified airplane with the roll-off tendency of the unmodified airplane (ref. 12) for full trailing-edge-up stabilator deflection.

Stalls from coordinated 30° banked turns were very docile with the modified wing (fig. 10). When stalled with sideslip, the modified airplane exhibited little or no roll-off tendency (fig. 11). Roll tendency, if any, was away from the slip; that is, left sideslip produced a right-roll tendency.

Power-on stalls. When stalled with maximum power and near-zero sideslip, the baseline airplane usually rolled to the right. Stalls from 30° and 60° banked left and right turns resulted in roll-offs to the right. When stalled with sideslip, the baseline airplane rolled away from the slip. These rolls often could not be controlled with rudder and aileron until the airplane was unstalled by reducing the up-stabilator deflection.

When stalled with maximum power and near-zero sideslip, the modified airplane was very docile. Any rolling tendency was controllable with ailerons, and bank could be easily controlled with ailerons and rudder (fig. 12).

For the modified airplane, stalls from coordinated 30° and 60° banked left and right turns produced an easily controllable right-roll tendency. When stalled with sideslip, the modified airplane exhibited easily controllable roll tendencies away from the slip. Figure 13 illustrates the controllable roll tendency of the modified airplane when stalled in a 30° banked skidding left turn.

With power for level flight, straight-ahead stalls of the modified airplane were docile. Stalls from coordinated 30° banked left and right turns resulted in a tendency for the modified airplane to roll opposite the direction of the turn. Stalls from slipping or skidding 30° banked turns resulted in a tendency for the modified airplane to roll away from the slip.

Full-flaps stalls. With flaps deflected 40°, the baseline airplane tended to roll to the right at the stall for both idle- and maximum-power cases. For maximum-power cases, the rolling tendency could be countered by large rudder and aileron inputs.

For the modified airplane, slow deceleration to a 1g stall at idle power with flaps deflected 40° did not provide any stall warning; only a mild departure tendency resulted, and this tendency was easily controllable with rudder and aileron inputs. Stalls from coordinated 30° banked left and right turns were docile.

With the modified wing leading edge, slow deceleration to a 1g stall at maximum power with flaps deflected 40° produced a very light stall break with a little more roll tendency than at idle power, but the airplane was easily controllable with coordinated rudder and aileron inputs (fig. 14). Stalls from coordinated 30° banked left and right turns produced easily controllable right-roll tendencies. When stalled in skidding turns, the modified airplane exhibited easily controllable roll tendencies away from the slip (fig. 15).

For the modified airplane, slow deceleration to a 1g stall at the power required for level flight with flaps deflected 40° produced a docile stall with good aileron control. When stalled with sideslip, the modified airplane tended to roll away from the slip.

Spin Characteristics

A total of 244 spins were attempted during 25 evaluation flights with the modified wing. Of these, 13 (5 percent) resulted in spins and 231 (95 percent) resulted in spirals or failed to produce a spin or a spiral. The modified airplane had a markedly increased resistance to spin entry compared with the baseline airplane, which, as reported in reference 12, entered a spin in 173 (83 percent) of 209 spin attempts.

Figures 16 through 20 illustrate the predominant airplane response to pro-spin control inputs by comparing motions with and without the wing modification. The baseline airplane would readily spin from 1g flight, power-on or power-off, with the application of normal pro-spin controls. It spun at about 43° angle of attack. Application of recovery controls did not always stop the spin. With the modified wing leading edge, no spins were obtained for idle-power settings or with flaps deflected; spins were obtained only with maximum power and flaps retracted.

When intentional spins were attempted at either idle power or maximum power by applying aft-stick, full-rudder deflection, and with ailerons neutral (fig. 16), with (fig. 17), or against (fig. 18) the rudder input, the modified airplane typically entered a steep, controlled spiral with a slow turn rate and a high sink rate. Angle of attack was above that at which the basic wing stalled but below that at which the outer wing panel stalled. Tufts showed that the outboard part of the wing remained unstalled. Loss of lift on the inboard wing panels and airframe buffeting from the separated flow on the inboard wing panels provided the pilot with cues similar to a conventional stall, although the wing outer panels continued to operate below stall and maintain roll damping. Rotation stopped if the controls were not held in the pro-spin position.

Typically, as the spiral progressed, the stabilator rotated off the trailing-edge-up stop, even though the pilot exerted increased stick force. The reduced control-surface deflection is attributed to increased stabilator hinge moment with increased dynamic pressure and to control-system flexibility. With full pro-spin controls, the typical motion of the modified airplane is somewhat spiral-like and somewhat spin-like. The root section of the wing is stalled, which gives buffet and drag as in a spin. The tip panels are attached and produce roll damping and lateral control much like in a spiral. The modified airplane reaches a steady terminal velocity at a speed much higher than in a spin. The terminal velocity of the spiral-like motion is dependent upon the magnitude of the trailing-edge-up stabilator deflection, which determines how high an angle of attack is achieved in the maneuver.

For the modified airplane, attempted spins with flaps deflected typically produced a bucking spiral as shown in figure 19, or, with maximum power applied, a spiral as shown in figure 20. With flaps up or flaps down, relaxing the controls returned the modified airplane to normal flight.

Table 6 presents the configurations and entry maneuvers of the modified airplane for the 13 spins that were achieved. Table 7 presents representative spin characteristics, and table 8 summarizes the modified-airplane spin tendencies.

With the modified wing, spin entry from 1g flight was achieved only for loadings outside the design center-of-gravity envelope (beyond aft-center-of-gravity position or over gross weight) and involved full trailing-edge-up stabilator deflection, full-rudder deflection, and ailerons neutralized at the stall (figs. 21 and 22). For these loadings, no special control inputs were required to achieve spin entry. After one turn or more of sustained pro-spin controls, the airplane would quickly pitch up into a spin. In one instance, a left spin at maximum power with the center of gravity at 0.3207$\bar{c}$, recovery control inputs were unable to stop the spin, and the spin-recovery parachute was deployed (fig. 21). Because the baseline airplane occasionally failed to respond to initial spin-recovery control inputs, and because the baseline airplane was not tested with a center-of-gravity position as far aft as 0.3207$\bar{c}$, it is not known whether the baseline airplane would have exhibited an unrecoverable spin under these conditions.

For loadings of the modified airplane near the design aft-center-of-gravity position (0.2804$\bar{c}$), spins could be entered at maximum power from a 30° banked right turn by applying full trailing-edge-up stabilator, full right rudder, and neutral ailerons (fig. 23).

Spins were obtained for loadings of the modified airplane within the design loading envelope by using a zoom maneuver. With maximum power, the modified airplane was put into a dive to build up speed. It was then pulled up into a steep climb to bleed off speed and achieve an extreme nose-high pitch attitude at the stall. Pro-spin controls were applied at the stall with aileron deflection against the spin. Only left spins were obtained from zoom maneuvers (figs. 24 through 26).

At the forward center-of-gravity position tested (0.2395$\bar{c}$), spins were attempted with the modified airplane loaded with 30 gal more fuel in the right wing tank than in the left wing tank (200 lb right wing heavy). Airplane spin tendencies were not degraded by this severe loading asymmetry as shown in table 8.

For the few maneuvers that resulted in spin entries, the modified airplane spun at a higher angle of attack than the baseline airplane (table 7). Spin angle of attack increased as the center of gravity was moved aft and as weight was increased. Spin-entry tendency also increased as the center of gravity was moved aft and as weight was increased (table 8).

The motions of the modified airplane following application of pro-spin control inputs were compared with those of the baseline airplane in terms of the

time required for the airplane to rotate 360° in heading or in roll (fig. 27). All maneuvers for which the modified airplane completed one turn of rotation, whether in a spin or spiral, were included. In general, the modified airplane provided the pilot more time to make corrective control inputs before completing one turn of rotation.

Analysis of Spin Resistance

Initial analysis of the spin resistance of the airplane with the outboard-wing modification was based on the assumptions that (1) an airplane would be highly spin resistant if roll damping could be maintained for all maneuvers, and (2) roll damping could be maintained if the outer wing panel did not stall. Conceptually, spin resistance was thus related to the difference between the maximum attainable angle of attack and the stall angle of attack. The maximum attainable angle of attack was defined as the maximum local angle of attack of the wing outer panel, including dynamic effects; the stall angle of attack was defined as the local angle of attack at which the outer-panel flow separated. For analysis purposes, maximum attainable angle of attack was divided into a baseline trim angle of attack and increments due to center-of-gravity changes, power effects, and dynamic effects (fig. 28). If the summation of these increments did not exceed the outer-panel stall angle of attack, the airplane was not expected to spin. An airplane whose maximum attainable angle of attack greatly exceeded the stall angle of attack was expected to enter a spin more readily than an airplane whose maximum attainable angle of attack just slightly exceeded the stall angle of attack. During many maneuvers, the stall angle of attack was exceeded temporarily without leading to a spin entry. The length of time that the stall angle of attack is exceeded, as well as the magnitude of the increment in angle of attack beyond that required for stall, may be a factor in spin entry.

The static trim angles of attack with full nose-up pitch-control input were measured for a range of center-of-gravity positions. These were measured at maximum gross weight with maximum power, 50 percent power, and idle power for the modified airplane with flaps retracted and deflected 40°. Results are presented in figure 29 as plots of static trim angle of attack versus center-of-gravity position. The maximum angle of attack presented in figure 30 is the peak value of the first transient in local angle of attack at the outer wing panel after pro-spin control inputs. The region between the curves of the maximum angle of attack and the trim angle of attack represents the transient effects of the dynamics associated with the spin-entry maneuver. The first peak in angle of attack was used because it is the closest to the initial conditions of the test maneuver. This would best enable the influence of such variables as static margin, power, control inputs, and control phasing to be readily detected. The extreme angles of attack that can be achieved by means of zoom maneuvers are also shown in figure 30, but such maneuvers are not considered typical of inadvertent spin entries.

The outer wing stall angle of attack was determined from measured angle-of-attack data and from corresponding films of tufts on the wings. These values for the basic and modified-airplane configurations are indicated by the horizontal lines in figure 30. Flight-test results indicated that the baseline wing outer panel stalled at 20° angle of attack. The intersections of the outer wing angle-of-attack curves and the stall angle-of-attack curves suggest center-of-gravity positions forward of which the airplane should not spin and aft of which it would have the potential to spin. For example, the airplane with the basic wing would be expected to spin for all center-of-gravity positions shown, regardless power, since the maximum angles of attack exceed the stall value of the basic wing. Indeed, the airplane with the basic wing did readily enter spins at about 28 percent $\bar{c}$ (the only center-of-gravity position tested for the baseline airplane) for both idle and maximum power.

The modified wing outer panel stalled at 36° angle of attack. As shown in figure 30, the airplane with the modified wing would not be expected to spin at idle power until the center-of-gravity position was aft of about 28 percent $\bar{c}$.

The modified airplane was tested at center-of-gravity positions of $0.238\bar{c}$ to $0.32\bar{c}$, and it did not spin with idle power. Figure 30 also indicates that the airplane would be expected to spin with the use of maximum power, but spin tendencies would be small until the center of gravity was aft of about 28 percent $\bar{c}$. With maximum power, spin entries were obtained for all loadings tested, including 24 percent $\bar{c}$; however, it became increasingly difficult to enter a spin as the center of gravity was moved forward, and very deliberate, prolonged inputs of a zoom maneuver were required to utilize the dynamic effects to cause spin entry for center-of-gravity positions forward of about 28 percent $\bar{c}$.

The stall-margin concept of figure 28 and its quantification, such as shown in figure 30, may help an airplane designer assess trade-offs and their relative impact on spin resistance. The consequences of increasing control deflection, extending the center-of-gravity envelope, or increasing the installed power are easy to visualize. For example, the change in stall

margin due to an increase in power could be offset somewhat by moving the aft-center-of-gravity limit forward. Likewise, changes which reduce the stall margin tend to reduce spin resistance. If a point is reached where the outer wing-panel stall angle of attack can be exceeded with subsequent loss of roll damping, the airplane could spin. With the modified wing, this airplane would be expected to spin at a higher angle of attack and may be more difficult to stop than the airplane with the baseline wing.

Effect of Wing Modification on Airplane Lift and Drag

Airplane lift and drag were measured for both the baseline and modified airplane configurations by conducting level flight runs at constant airspeeds from maximum level flight speed to near stall onset. As shown in figure 31, there was no discernible difference in lift up to about 10° angle of attack. As shown in figure 32, within the measurement accuracy, no difference was found in airplane drag for lift coefficients typical of cruising flight. For lift coefficients between about 0.5 to 1.0, the modified wing had increased drag.

Summary of Results

Flight tests were conducted to evaluate the change in spin resistance caused by the addition of an outboard wing-leading-edge modification to a low-wing, single-engine, T-tail, general aviation research airplane. Tests were conducted at weights of 2438 to 2829 lb (89 to 103 percent of maximum gross weight) with center-of-gravity positions of 0.2394 to 0.3207 mean aerodynamic chord (12.66 to 4.53 percent static margin). The following results were indicated:

1. Addition of the modification increased stall angle of attack of the outer wing to 36°, which was approximately twice the stall angle of attack of the basic wing (20°).
2. The modified airplane had improved stall behavior and increased spin resistance compared with the baseline airplane.
3. Spin resistance has been related to the variation in attainable outer wing-panel angle of attack with center-of-gravity position, power level, and dynamic effects.
4. For the few maneuvers that did produce spins with the wing modification, the modified airplane tended to spin at a higher angle of attack than the baseline airplane.
5. Airplane cruise drag was unchanged by addition of the wing modification.

NASA Langley Research Center
Hampton, Virginia 23665-5225
April 2, 1987

References

1. Chambers, Joseph R.: Overview of Stall/Spin Technology. AIAA-80-1580, Aug. 1980.
2. Silver, Brent W.: Statistical Analysis of General Aviation Stall Spin Accidents. [Preprint] 760480, *Soc. Automotive Engineers,* Apr. 1976.
3. Ellis, David R.: *A Study of Lightplane Stall Avoidance and Suppression.* FAA-RD-77-25, Feb. 1977.
4. Hoffman, William C.; and Hollister, Walter M.: *General Aviation Pilot Stall Awareness Training Study.* Rep. No. FAA-RD-77-26, Sept. 1976. (Available from DTIC as AD A041 310/4.)
5. Weick, Fred E.; and Wenzinger, Carl J.: *Effect of Length of Handley Page Tip Slots on the Lateral-Stability Factor, Damping in Roll.* NACA TN 423, 1932.
6. Weick, Fred E.; and Wenzinger, Carl J.: *Wind-Tunnel Research Comparing Lateral Control Devices, Particularly at High Angles of Attack. VII—Handley Page Tip and Full-Span Slots With Ailerons and Spoilers.* NACA TN 443, 1933.
7. Weick, Fred E.; and Wenzinger, Carl J.: *Wind-Tunnel Research Comparing Lateral Control Devices, Particularly at High Angles of Attack. I—Ordinary Ailerons on Rectangular Wings.* NACA Rep. 419, 1932.
8. Weick, Fred E.; Sevelson, Maurice S.; McClure, James G.; and Flanagan, Marion D.: *Investigation of Lateral Control Near the Stall—Flight Investigation With a Light High-Wing Monoplane Tested With Various Amounts of Washout and Various Lengths of Leading-Edge Slot.* NACA TN 2948, 1953.
9. Weick, Fred E.; and Abramson, H. Norman: *Investigation of Lateral Control Near the Stall. Flight Tests With High-Wing and Low-Wing Monoplanes of Various Configurations.* NACA TN 3676, 1956.
10. Staff of Langley Research Center: *Exploratory Study of the Effects of Wing-Leading-Edge Modifications on the Stall/Spin Behavior of a Light General Aviation Airplane.* NASA TP-1589, 1979.
11. White, E. Richard: *Wind-Tunnel Investigation of Effects of Wing-Leading-Edge Modifications on the High Angle-of-Attack Characteristics of a T-Tail Low-Wing General-Aviation Aircraft.* NASA CR-3636, 1982.
12. Stough, H. Paul, III; DiCarlo, Daniel J.; and Patton, James M., Jr.: *Flight Investigation of Stall, Spin, and Recovery Characteristics of a Low-Wing, Single-Engine, T-Tail Light Airplane.* NASA TP-2427, 1985.
13. Bradshaw, Charles F.: A Spin-Recovery Parachute System for Light General-Aviation Airplanes. *14th Aerospace Mechanisms Symposium,* NASA CP-2127, 1980, pp. 195–209.
14. Bement, Laurence J.: *Emergency In-Flight Egress Opening for General Aviation Aircraft.* NASA TM-80235, 1980.
15. Sliwa, Steven M.: Some Flight Data Extraction Techniques Used on a General Aviation Spin Research Aircraft. AIAA Paper 79-1802, Aug. 1979.
16. Moul, Thomas M.: *Determination of Corrections to Flow Direction Sensor Measurements Over an Angle-of-Attack Range From 0° to 85°.* NASA TM-86402, 1985.
17. Airworthiness Standards: Normal, Utility, and Acrobatic Category Airplanes. Federal Aviation Regulations, vol. III, pt. 23, Federal Aviation Administration, June 1974.

Table 1. Physical Characteristics of Baseline Airplane

Overall dimensions:	
Span, ft	35.43
Length, ft	27.80
Height, ft	8.26
Powerplant:	
Type	Reciprocating, four cylinder horizontally opposed
Rated power at sea level, hp	200
Rated continuous speed, rpm	2700
Propeller:	
Type	Two blades, constant speed
Diameter, in.	76
Pitch (variable), deg	14 to 31
Wing:	
Area, ft^2	173.7
Root chord, in.	74.0
Chord of constant section, in.	63.0
Tip chord, in.	42.2
Mean aerodynamic chord, in.	62.16
Aspect ratio	7.24
Dihedral, deg	7.0
Incidence at root, deg	2.0
Incidence at tip, deg	−1.0
Airfoil section	NACA 65_2-415 modified
Flap:	
Chord, in.	12.26
Span, in.	85.50
Area (each), ft^2	7.3
Hinge line, percent flap chord	20.0
Deflection, deg	40 down
Aileron:	
Mean chord, in.	10.01
Span, in.	100.05
Area (each), ft^2	6.95
Deflection, deg	30 up, 16 down
Stabilator:	
Area (including tab), ft^2	25.0
Chord (constant), in.	30.0
Aspect ratio	4.0
Dihedral, deg	0
Hinge line, percent stabilator chord	26.97
Deflection, deg	10 up, 10 down
Airfoil section	NACA 0012

Table 1. Concluded

Tab:	
Chord (constant), in.	6.0
Span, in.	106.2
Area, ft^2	4.4
Tab hinge line to stabilator hinge line, in.	15.91
Vertical tail:	
Area (including rudder), ft^2	17.6
Root chord, in.	54.52
Tip chord, in.	28.62
Mean aerodynamic chord, in.	42.91
Span, in.	60.84
Aspect ratio	1.47
Leading-edge sweep back, deg	33.91
Rudder:	
Area, ft^2	5.8
Average chord aft of hinge line, in.	11.85
Span (parallel to hinge line), in.	61.6
Deflection, deg	28 left, 28 right
Test weight at altitude, lb	2420
Relative density μ at 9000 ft altitude	6.7
Representative center-of-gravity position:	
FS, in.	95.85 ($0.2782\bar{c}$)
BL, in.	−0.56
WL, in.	38.15
Moments of inertia about body axes (based on represenative center-of-gravity position):	
I_x, slug-ft^2	1789
I_y, slug-ft^2	2486
I_z, slug-ft^2	3796
Inertia yawing-moment parameter, $\frac{I_x - I_y}{mb^2}$	-74×10^{-4}

Table 2. Modified-Airplane Mass Characteristics and Inertia Parameters for Representative Loadings Tested

Parameter									
Test weight at altitude, lb	2678	[a]2683	2823	2678	2438	2677	2829	2690	2690
Relative density μ at 9000 ft	7.5	7.5	7.9	7.5	6.8	7.5	7.9	7.5	7.5
Center-of-gravity position:									
$x/\bar{c}$	0.2397	0.2395	0.2394	0.2594	0.2777	0.2823	0.2787	0.2998	0.3207
$y/\bar{c}$	−.001	.093	−.001	−.008	−.009	−.006	−.004	−.003	.001
$z/\bar{c}$	−.041	−.041	−.048	−.039	−.030	−.045	−.047	−.045	−.046
Moments of inertia, slug-ft^2:									
I_x	1981	1973	2173	2137	1892	2242	2250	2146	2046
I_y	2551	2551	2555	2530	2486	2498	2568	2529	2562
I_z	4042	4035	4233	4181	3899	4252	4327	4186	4118
Inertia yawing moment parameter $\times 10^4$ . . .	−55	−55	−35	−38	−62	−24	−29	−37	−49

[a]200 lb right wing heavy.

Table 3. Coordinates of Basic-Wing Airfoil Sections in Percent Chord

Upper station	Surface ordinate for —				Lower station	Surface ordinate for —			
	WS 22.78	WS 106.19	WS 157.00	WS 211.575		WS 22.78	WS 106.19	WS 157.00	WS 211.575
0	0	0	−0.585	−0.813	0	0	0	−0.585	−0.813
.313	.922	1.208	.481	.334	.687	−.811	−1.008	−1.992	−2.405
.542	1.164	1.480	.868	.664	.958	−.946	−1.200	−2.171	−2.630
1.016	1.481	1.900	1.469	1.261	1.484	−1.163	−1.472	−2.429	−2.891
2.231	2.097	2.680	2.426	2.329	2.769	−1.528	−1.936	−2.832	−3.223
4.697	2.995	3.863	3.804	3.791	5.303	−2.052	−2.599	−3.228	−3.412
7.184	3.725	4.794	4.767	4.829	7.816	−2.420	−3.098	−3.398	−3.472
9.682	4.327	5.578	5.546	5.616	10.318	−2.745	−3.510	−3.625	−3.649
14.697	5.334	6.842	6.834	6.872	15.303	−3.279	−4.150	−4.150	−4.150
19.726	6.138	7.809	7.809	7.809	20.274	−3.678	−4.625	−4.625	−4.625
24.764	6.785	8.550	8.550	8.550	25.236	−3.989	−4.970	−4.970	−4.970
29.807	7.294	9.093	9.093	9.093	30.193	−4.232	−5.205	−5.205	−5.205
34.854	7.693	9.455	9.455	9.455	35.146	−4.408	−5.335	−5.335	−5.335
39.903	7.984	9.639	9.639	9.639	40.097	−4.529	−5.355	−5.355	−5.355
44.953	8.168	9.617	9.617	9.617	45.047	−4.597	−5.237	−5.237	−5.237
50.000	8.246	9.374	9.374	9.374	50.000	−4.549	−4.962	−4.962	−4.962
55.043	8.126	8.910	8.910	8.910	54.957	−4.394	−4.530	−4.530	−4.530
60.079	7.758	8.260	8.260	8.260	59.921	−4.027	−3.976	−3.976	−3.976
65.106	7.157	7.462	7.462	7.462	64.894	−3.489	−3.342	−3.342	−3.342
70.124	6.408	6.542	6.542	6.542	69.876	−2.866	−2.690	−2.654	−2.654
75.131	5.476	5.532	5.532	5.532	74.869	−2.231	−2.048	−2.028	−2.028
80.126	4.448	4.447	4.476	4.476	79.874	−1.595	−1.397	−1.366	−1.366
85.109	3.327	3.320	3.403	3.403	84.891	−1.082	−1.103	−1.073	−1.073
90.080	2.231	2.175	2.330	2.330	89.920	−.759	−.786	−.771	−.771
95.040	1.134	1.058	1.257	1.257	94.960	−.449	−.468	−.469	−.469
100.000	.027	.317	.176	.176	100.000	−.135	−.159	−.176	−.176
Chord, in.	73.960	63.000	52.971	42.200					
L.E. radius, percent	1.030	1.505	1.790	2.240					

Table 4. Coordinates of Modified Leading-Edge Contour in Percent Chord of Basic-Wing Airfoil Sections

WS 114.07

Station	Ordinate
2.441	2.816
2.181	2.726
1.953	2.666
1.709	2.549
1.465	2.432
1.221	2.295
.977	2.148
.732	2.021
.488	1.855
.244	1.689
.000	1.543
−.244	1.348
−.488	1.172
−.732	.977
−.977	.771
−1.221	.498
−1.465	.273
−1.709	.000
−1.953	−.285
−2.197	−.674
−2.441	−1.172
−2.686	−1.758
−2.832	−2.441
−2.686	−3.076
−2.441	−3.525
−2.197	−3.760
−1.953	−3.926
−1.709	−4.053
−1.465	−4.131
−1.221	−4.199
−.977	−4.238
−.732	−4.287
−.488	−4.297
−.244	−4.307
.000	−4.316
.977	−4.326
1.953	−4.346
2.930	−4.375
4.883	−4.414
6.836	−4.473
8.789	−4.521
10.742	−4.580
12.695	−4.619
14.648	−4.678
16.602	−4.736
18.555	−4.775
20.508	−4.824
22.461	−4.883
23.680	−4.919

Chord = 61.445 in.

WS 205.9

Station	Ordinate
3.424	3.093
3.080	2.872
2.737	2.666
2.392	2.449
2.049	2.168
1.706	1.888
1.362	1.649
1.018	1.362
.675	1.115
.332	.793
−.011	.346
−.353	.065
−.695	−.285
−1.036	−.746
−1.378	−1.192
−1.719	−1.681
−2.059	−2.252
−2.397	−3.004
−2.732	−4.116
−2.859	−5.225
−2.711	−6.055
−2.358	−6.743
−2.007	−7.183
−1.657	−7.470
−1.309	−7.646
−.961	−7.809
−.614	−7.902
−.267	−7.954
.080	−7.978
.426	−8.002
.773	−8.026
1.119	−8.022
1.465	−7.977
1.811	−7.946
2.157	−7.928
2.503	−7.883
2.848	−7.849
3.194	−7.820
3.540	−7.789
4.232	−7.740
5.616	−7.559
6.999	−7.433
9.767	−7.168
12.534	−6.862
15.301	−6.569
18.068	−6.262
20.835	−5.983
23.602	−5.705
26.369	−5.398
29.136	−5.092

Chord = 43.320 in.

Table 5. Modified-Airplane Stall Characteristics

δ_f, deg	Power	ϕ, deg	β, deg	Description of maneuver	Result
0	Idle	0	−5	Slow deceleration to 1g stall, then controls fixed	Stable; slight nose bobble
		0	−1 to 4	Slow deceleration to 1g stall, then wheel full back and controls fixed	Stable; slight left-roll tendency easily controllable with small right aileron and rudder inputs; very docile
		0	0	From level flight near stall, wheel abruptly pulled full back and controls fixed	Right or left-roll tendency controlled with small aileron and rudder inputs opposite to roll
		0	2	Slow deceleration to 1g stall, then wheel full back and controls fixed, then use ailerons and rudder	No roll-off tendency
		0	−18	1g stall with left sideslip (full right rudder)	No roll-off tendency; controllable
		−30	−20	Stall from slipping left turn (full right rudder)	Slight roll-off to the right; easily controllable
		−45	10	Stall from skidding left turn (3/4 left rudder)	Airplane stays in the bank; controllable
		−30	2	Stall from left turn	Mild roll to the left 4 sec after stall; countered with rudder and aileron inputs
		−30	0	Slow deceleration to stall in left turn, then wheel full back	Very docile
		30	4	Slow deceleration to stall in right turn, then wheel full back	Very docile
		0	−3	Pull-up to 1.5g accelerated stall	No roll-off tendency; docile
	For level flight	0	±12	Wheel back to stall, then use ailerons and rudder	Docile
		0	14	Wheel full back at stall with right sideslip	No large angular rates produced
		0	−10	Wheel full back at stall with left sideslip (full right rudder)	Very docile; only small roll and yaw oscillations
		30	2	Stall from right turn	Rolls to left
		−30	−2	Stall from left turn	Rolls to right
		30	−10	Stall from skidding right turn	Rolls to right
		−30	−13	Stall from slipping left turn	Rolls to right

Table 5. Continued

δ_f, deg	Power	ϕ, deg	β, deg	Description of maneuver	Result
0	Maximum	0	−2	Slow deceleration to 1g stall, then wheel full back	Very docile; rolling tendency controllable with ailerons; can control bank with ailerons and a little rudder
		0	2	Wheel abruptly pulled to full back and held	Easily controlled
		0	−10	1g stall with sideslip (full right rudder)	Tendency to roll off to right countered with ailerons
		30	3	Stall from right turn, then wheel full back	Slight right-roll tendency easily countered with normal controls; good control
		−30	−2	Stall from left turn, then wheel full back	Roll to the right easily countered
		30	−12	Stall from skidding right turn, then wheel full back	Roll to the right
		−30	12	Stall from skidding left turn, then wheel full back	Mild roll-off tendency; controllable with ailerons; good control
		30	13	Stall from slipping right turn, then wheel full back	Rolls level
		−30	−7	Stall from slipping left turn, then wheel full back	Roll to the right; controllable with ailerons; good control
		60	2	Stall from right turn, then wheel full back	Slight roll off to right, mild maneuver
		−60	−4	Stall from left turn, then wheel full back	Slight right-roll tendency; easily controllable
		60	−12	Stall from skidding right turn	Slight right roll-off tendency; easily recovered with ailerons
		−60	7	Stall from skidding left turn	Slight roll-off tendency; easily controllable
		0	2	Pull-up to stall, then wheel full back	Pronounced break; good control

Table 5. Concluded

δ_f, deg	Power	ϕ, deg	β, deg	Description of maneuver	Result
40	Idle	0	−2	Slow deceleration to 1g stall, then wheel full back	No stall warning; mild departure tendency; easily controlled with small rudder and aileron inputs; good control
		30	3	Stall in right turn, then wheel full back	Docile
		−30	−3	Stall in left turn, then wheel full back	Docile
		0	2	Rapid deceleration to stall, then wheel full back	Docile
	For level flight	0	−4	Slow deceleration to 1g stall, then wheel full back with full right rudder and left aileron	Docile; follows aileron input
		0	12	Slow deceleration to 1g stall with full left rudder and right aileron, then at full back wheel apply opposite rudder	Left roll and yaw changed to right roll and yaw
		30	14	Stall from slipping right turn (full left rudder)	Rolls to left
		−30	−15	Stall from slipping left turn (full right rudder)	Rolls to right
	Maximum	0	0	Slow deceleration to 1g stall, then wheel full back	Very light stall break; a little more roll tendency than with idle power and harder to control, rudder fixed; readily controlled with coordinated rudder and ailerons
		30	1	Stall from right turn, then wheel full back	Right-roll tendency easily countered
		−30	0	Stall from left turn, then wheel full back	Left then right-roll tendency easily countered
		30	−8	Stall from skidding right turn	Gentle roll to the right
		−30	9	Stall from skidding left turn	Roll to left easily recovered with rudder
		0	1	Zoom to stall, then wheel full back	Good control

Table 6. Conditions for Spin Entry of Modified Airplane

Center-of-gravity position, $x/\bar{c}$	Weight, lb	Power	Spin-entry maneuver	Number of seconds pro-spin input maintained	Number of turns pro-spin input maintained	Number of turns for recovery	Direction
0.2397	2678	Max	Zoom to stall; left rudder pulse prior to stall; pro-spin rudder and full trailing-edge-up stabilator at stall; ailerons against 1.2 sec after pro-spin input	10.5	2 1/2	2	Left
			Zoom to stall; left rudder pulse prior to stall; pro-spin rudder and full trailing-edge-up stabilator at stall; ailerons against 1.5 sec after pro-spin input	7.2	1 3/4	3	Left
.2594			Zoom to stall; pro-spin rudder and full trailing-edge-up stabilator at stall; ailerons against 3.2 sec after pro-spin input	17.0	4 1/8	1 1/8	Left
.2778	2656		Zoom to stall; full pro-spin rudder and trailing-edge-up stabilator at stall; ailerons against 2.8 sec after pro-spin input	12.5	2 1/2	1 1/2	Left
.2823	2677		Zoom to stall; pro-spin rudder and full trailing-edge-up stabilator at stall; ailerons against 2.0 sec after pro-spin input	6.7	3/4	3/4	Left
			Zoom to stall; pro-spin rudder and full trailing-edge-up stabilator at stall; ailerons against 2.9 sec after pro-spin input	10.7	2	1 1/2	Left
.2787	2829		1g, wings-level stall; pro-spin rudder and full trailing-edge-up stabilator at stall; ailerons neutral	27.1	8 1/2	2	Right
.2790	2690		Stall in 30° banked right turn; full pro-spin rudder and trailing-edge-up stabilator at stall; ailerons neutral	10.5	2 1/4	1/2	Right
.2842	2670			22.2	7 3/4	1 5/8	Right
.2998	2690		1g, wings-level stall; full pro-spin rudder and trailing-edge-up stabilator at stall; ailerons neutral	25.8	8	1 1/2	Right
.3207				19.8	5 7/8	1 1/2	Right
2				29.0	9	1 5/8	Right
				23.7	6	Chute	Left

Table 7. Airplane Spin Characteristics

Parameter	Baseline airplane	Modified airplane at various loadings (weight and c.g.)						
Weight, lb	2420	2678	2678	2677	2670	2690	2690	2829
c.g., $\frac{x}{c}$	0.2782	0.2397	0.2594	0.2823	0.2842	0.3207	0.3207	0.2787
Direction	Right	Left	Left	Left	Right	Right	Left	Right
Ailerons	Neutral	Against	Against	Against	Neutral	Neutral	Neutral	Neutral
α, deg	43 ± 4	48	49	52	50 ± 1	54 ± 5	53 ± 3	56 ± 2
β, deg	4 ± 5	2 ± 2	8	3 ± 7	4 ± 4	3 ± 7	-2 ± 5	3 ± 5
p, deg/sec	92 ± 25	-83 ± 5	-73 ± 8	-63 ± 13	76 ± 14	78 ± 18	-56 ± 26	75 ± 17
q, deg/sec	19 ± 16	22 ± 6	6 ± 4	14 ± 13	14 ± 11	19 ± 19	26 ± 17	11 ± 17
r, deg/sec	93 ± 5	-100	-90	-90	110 ± 4	100 ± 8	-86 ± 6	117 ± 5
Ω, deg/sec	135 ± 20	-128 ± 7	-115 ± 10	-107 ± 9	132 ± 2	130 ± 13	-110 ± 19	142 ± 7
T, sec	$2.67^{+0.46}_{-0.35}$	$2.81^{+.17}_{-.14}$	$3.13^{+.30}_{-.25}$	$3.36^{+.31}_{-.26}$	$2.73^{+.04}_{-.04}$	$2.77^{+.31}_{-.25}$	$3.27^{+.69}_{-.48}$	$2.53^{+.14}_{-.12}$
V, ft/sec . . .	127	130	120	125	123	114	114	115
R/S, ft/sec . . .	120	95	110	117	110	114	112	100
a_N, g units . . .	1.4 ± 0.2	1.5	1.4	1.4	1.4	$1.4 \pm .1$	1.4 ± 0.2	1.3
R, ft	6.2	5.8	6.9	7.2	5.1	4.5	6.6	3.5

Table 8. Modified-Airplane Spin Tendencies

Weight, lb	Center-of-gravity position, $x/\bar{c}$	Number of attempted spins	Number of spins obtained	Spins obtained / Spins attempted	Duration of pro-spin control input for attempts that did not produce spins		
					Attempts lasting 1 turn but < 7 sec	Attempts lasting 7 sec but < 1 turn	Attempts lasting < 1 turn and < 7 sec
2678	0.2397	27	2	7.4	0	19	6
[a]2683	.2395	16	0	0	2	13	1
2823	.2394	10	0	0	0	9	1
2678	.2594	12	1	8.3	1	10	0
2438	.2777	20	0	0	3	15	2
2677	.2823	137	5	3.6	24	103	5
2829	.2787	6	1	16.7	2	3	0
2690	.2998	6	1	16.7	0	5	0
2690	.3207	10	3	30.0	2	5	0
		244	13	5.3	34	182	15

[a]200 lb right wing heavy.

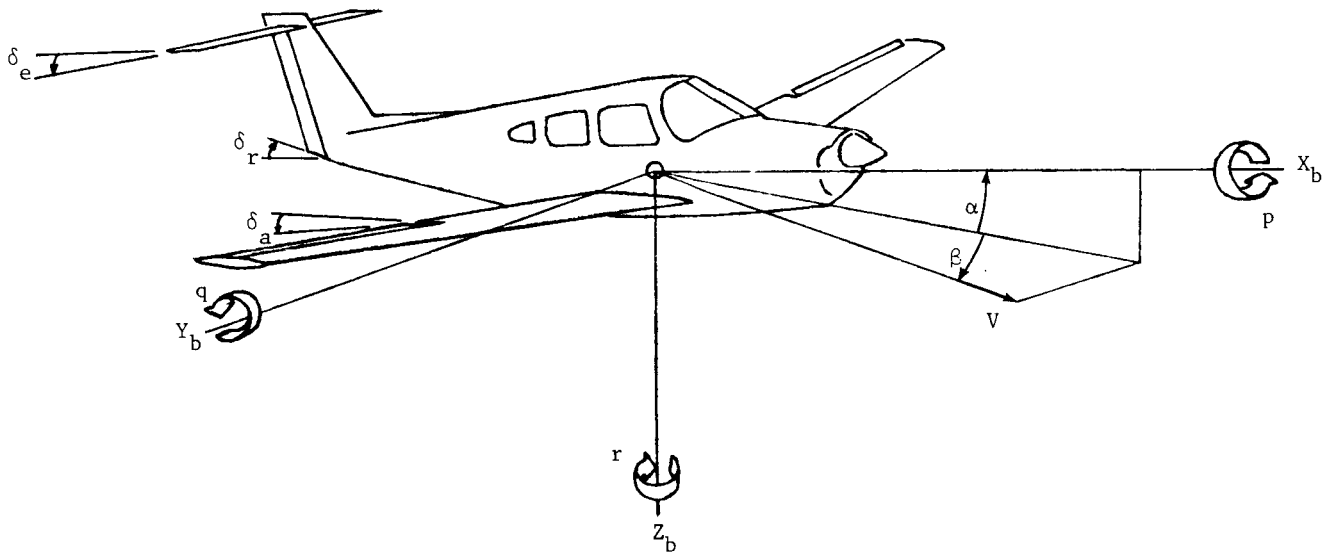

Figure 1. System of body axes. Arrows indicate positive direction of quantities.

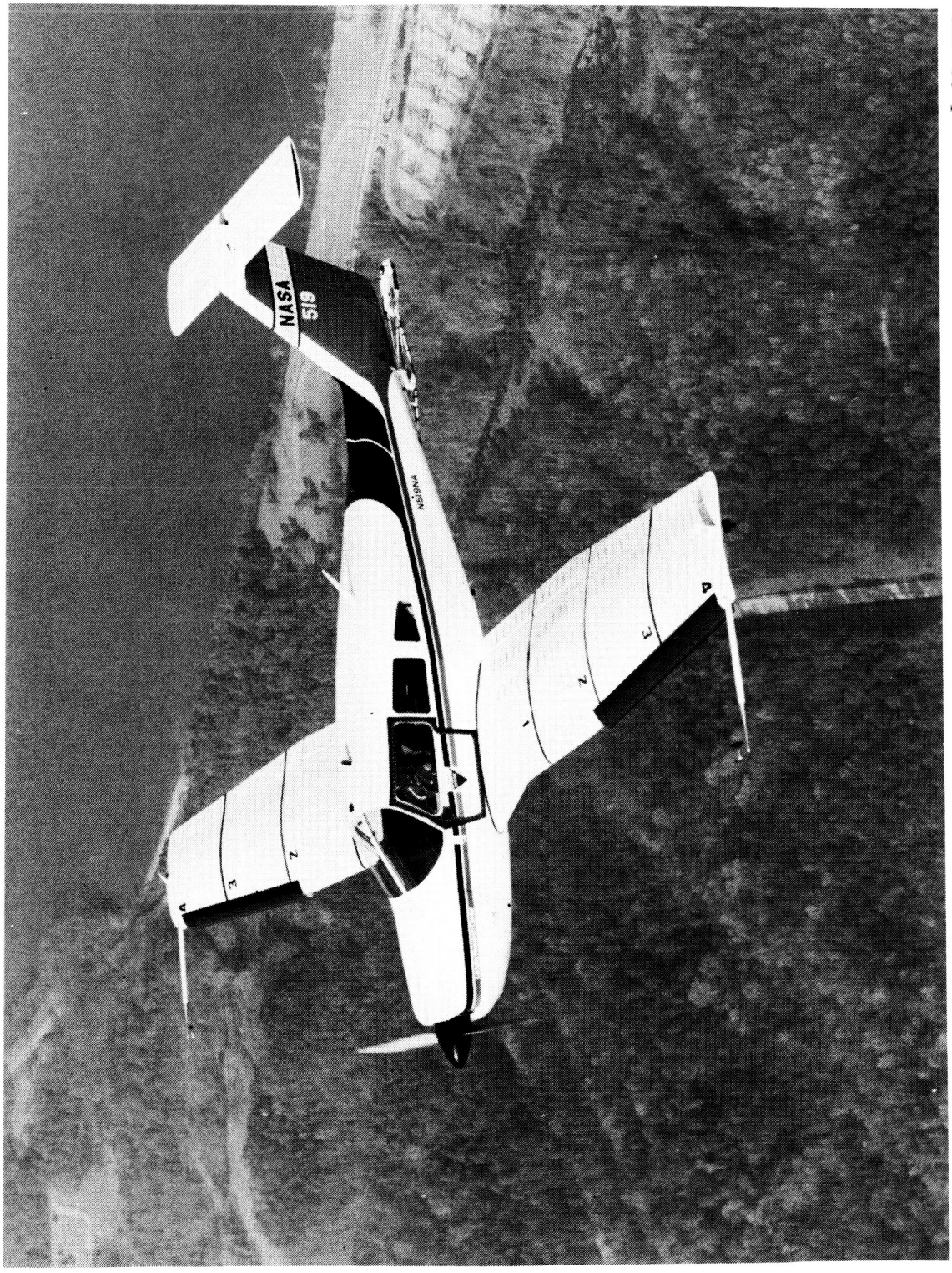

L-83-1568

Figure 2. Test airplane with modified wing leading edge.

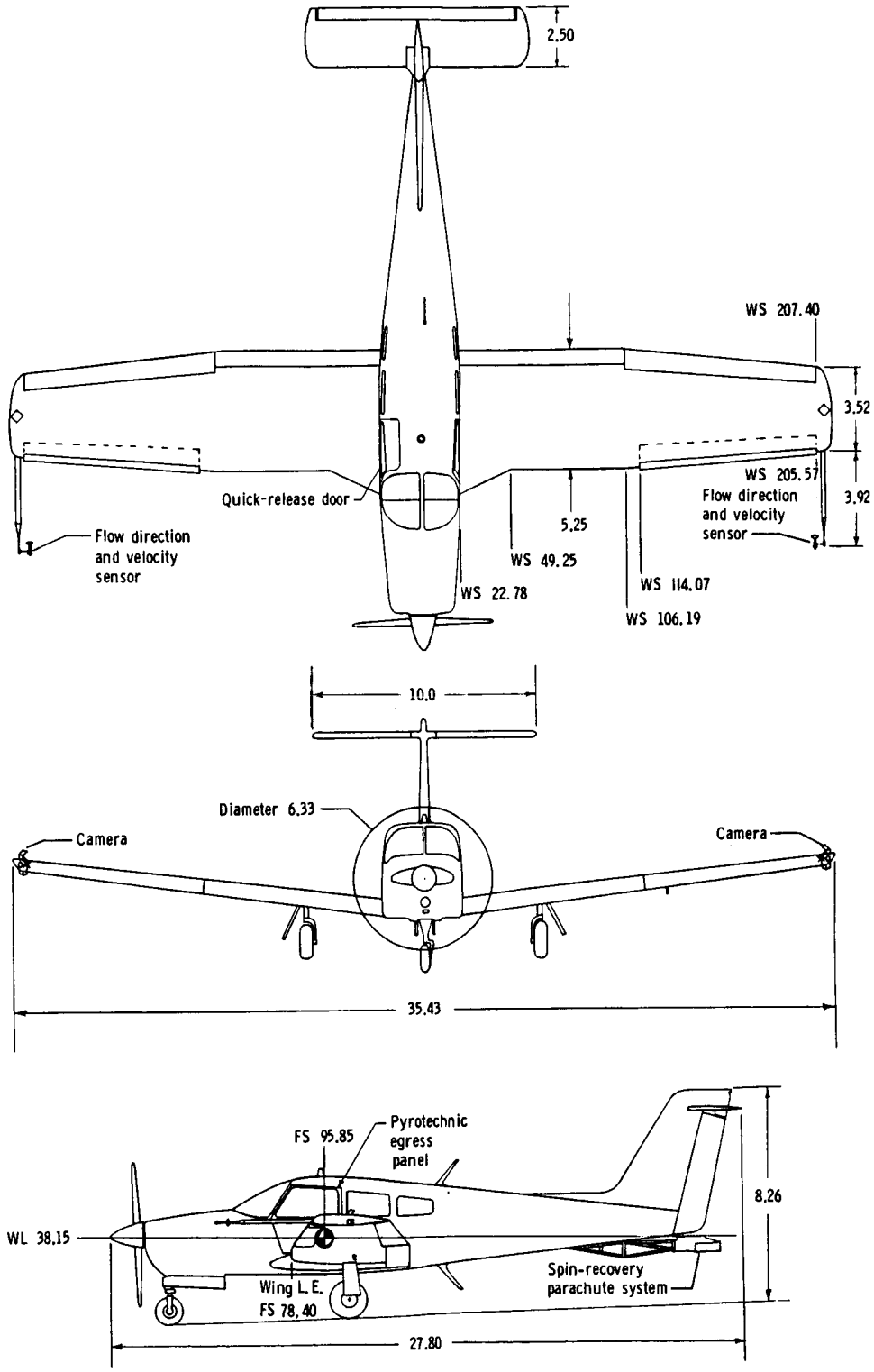

Figure 3. Three-view drawing of test airplane. Dimensions are in feet.

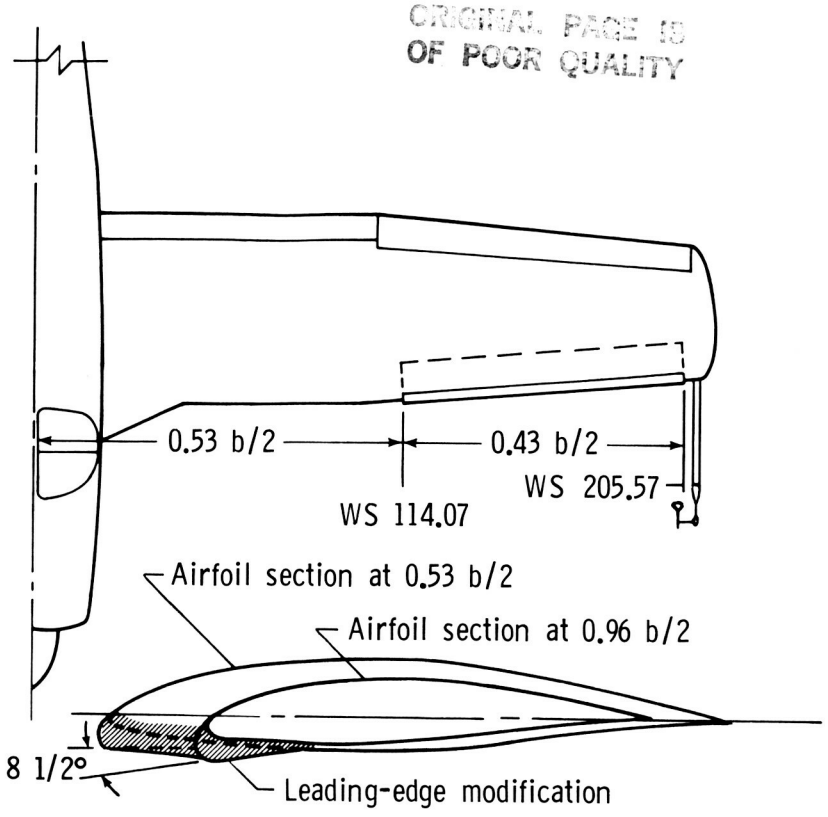

(a) Diagram.

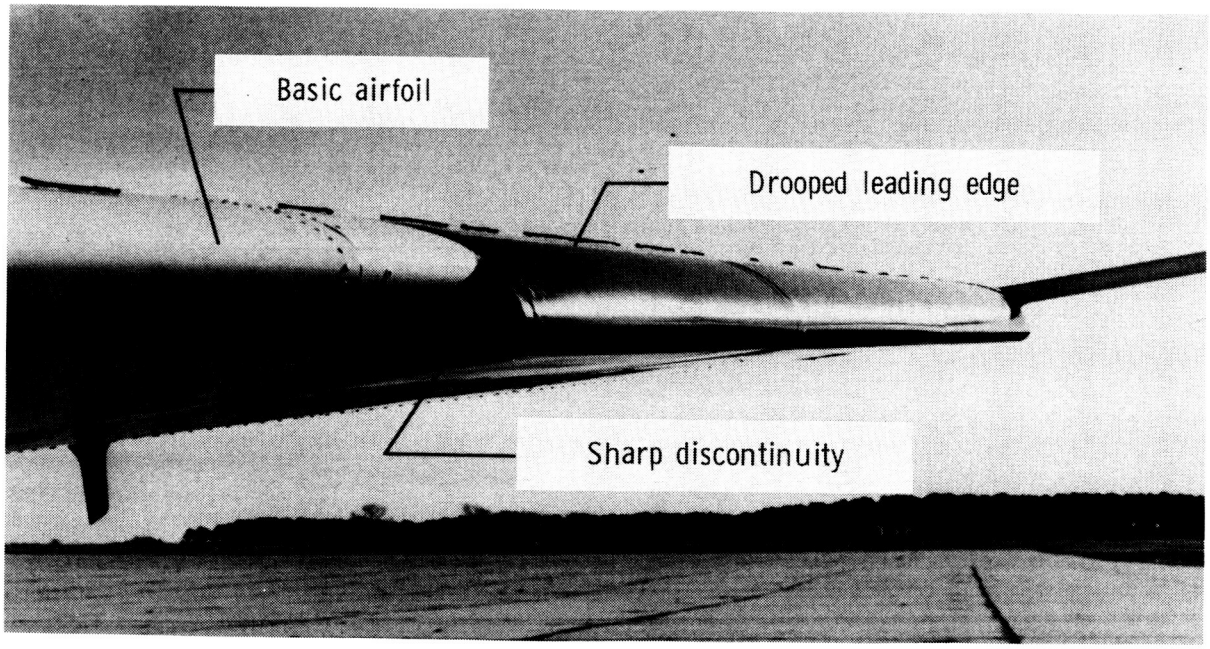

L-83-5680

(b) Photograph.

Figure 4. Wing-leading-edge modification.

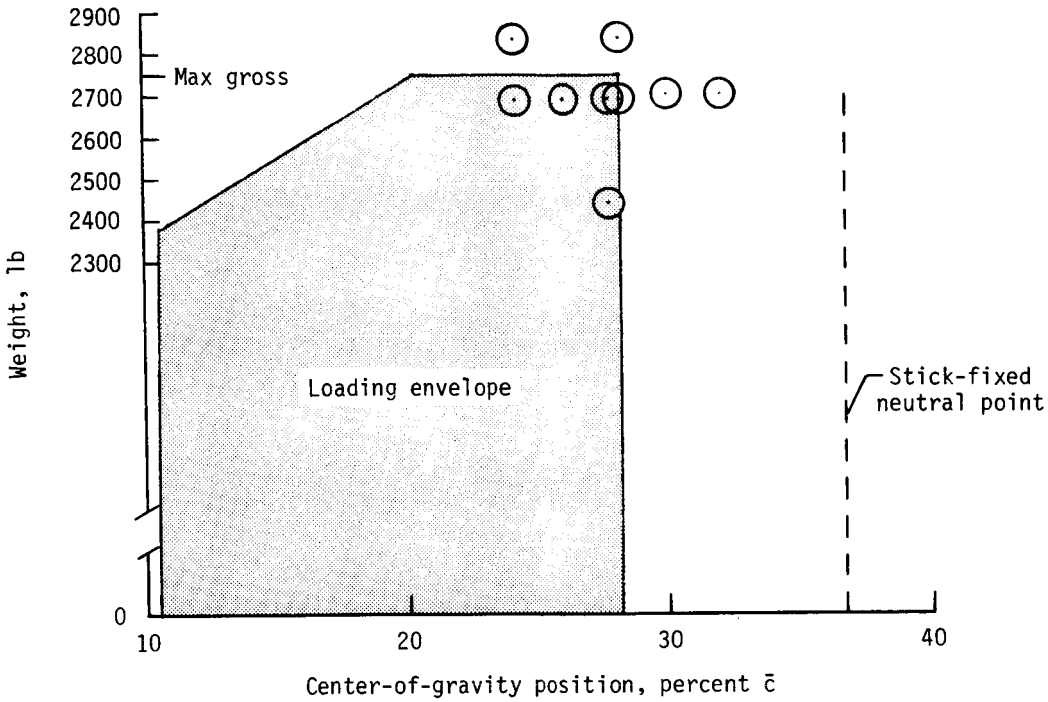

Figure 5. Airplane design center-of-gravity envelope showing loadings at test altitude.

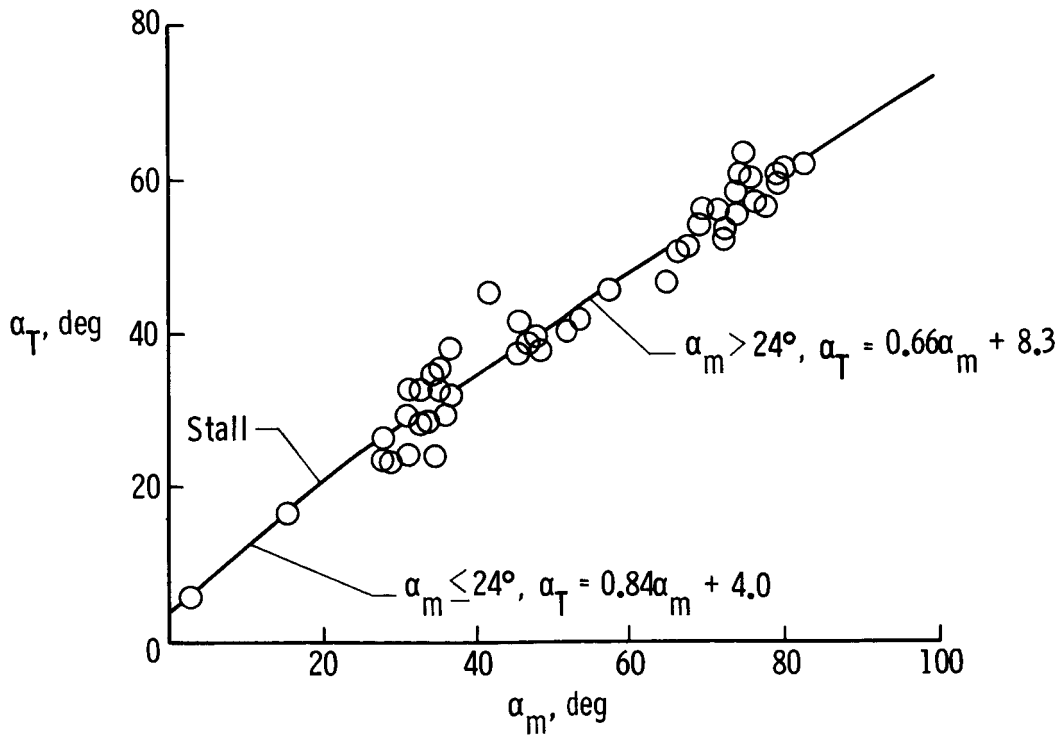

Figure 6. True angle of attack as a function of measured angle of attack at wing-tip boom location.

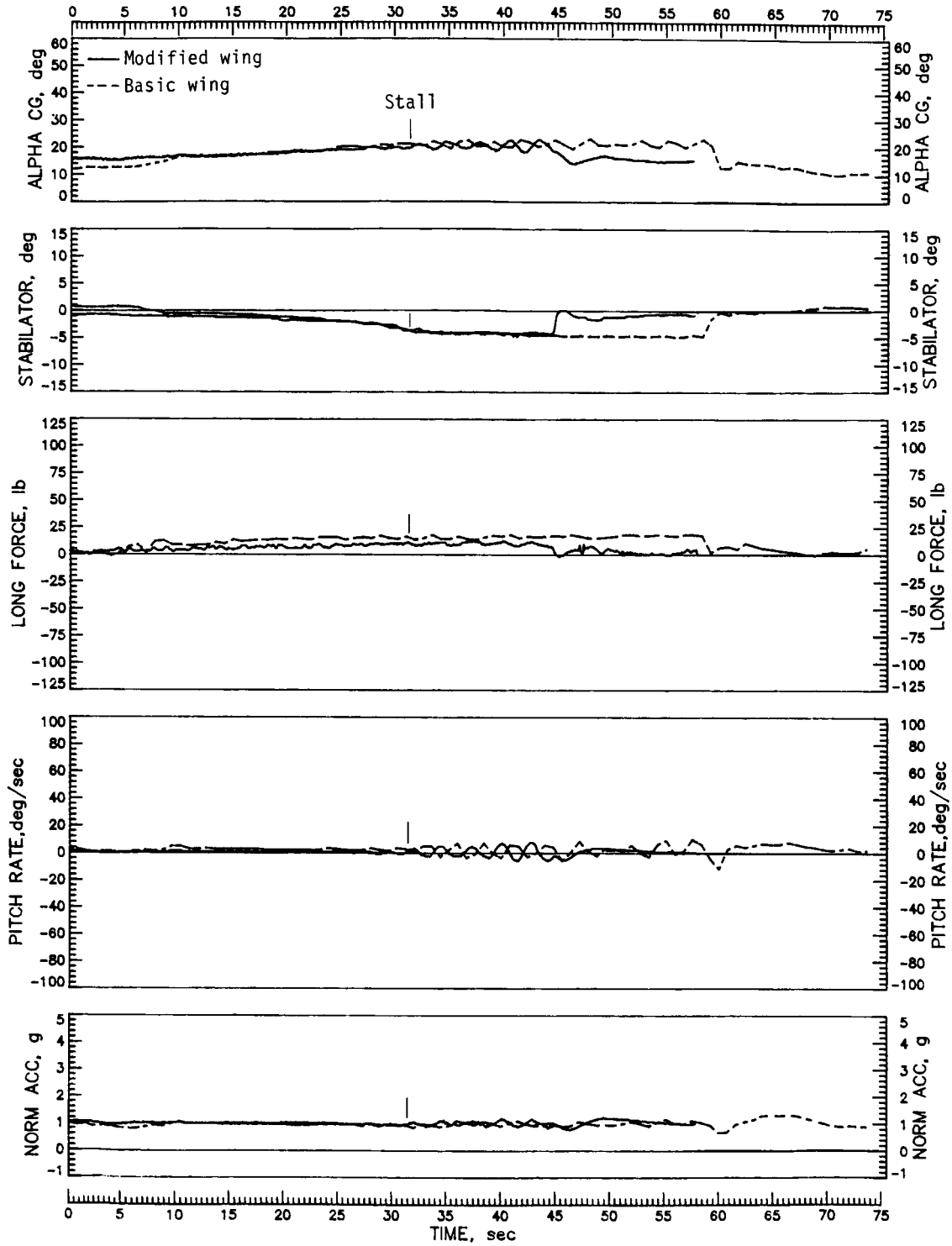

Figure 7. Slow deceleration to idle-power, 1g, wings-level stall with flaps and gear retracted. Test weight = 2438 lb; c.g. = 0.2777$\bar{c}$.

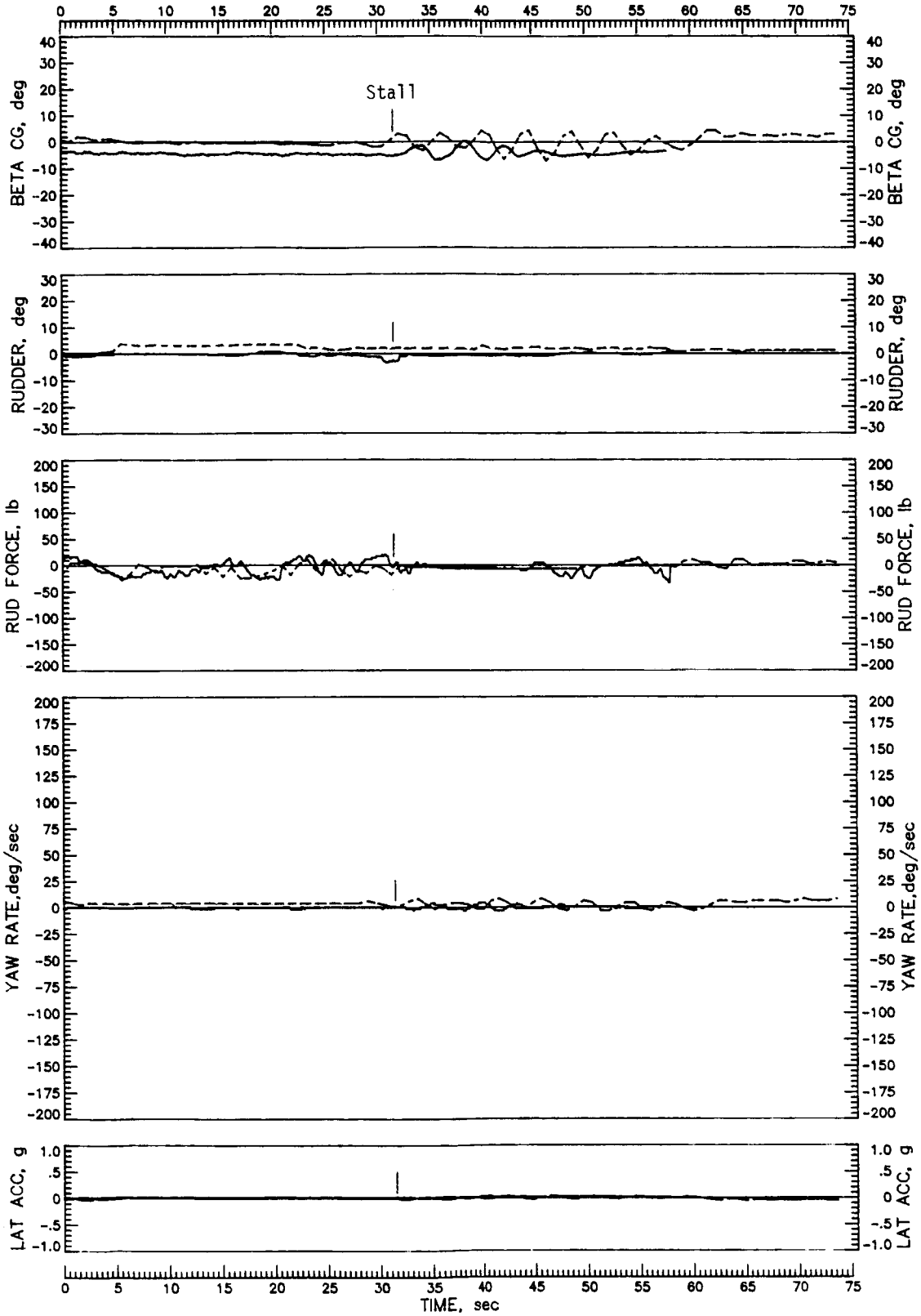

Figure 7. Continued.

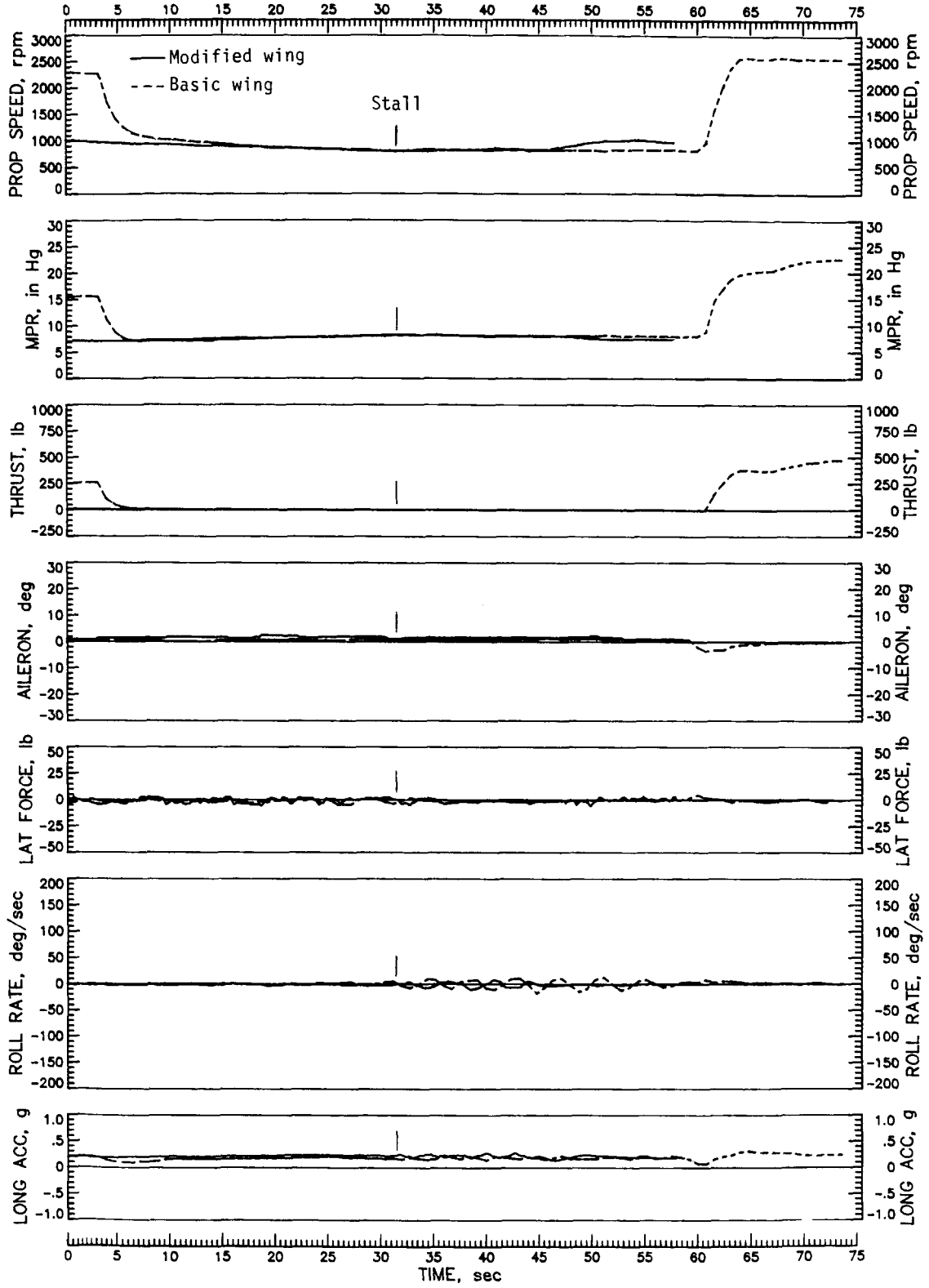

Figure 7. Continued.

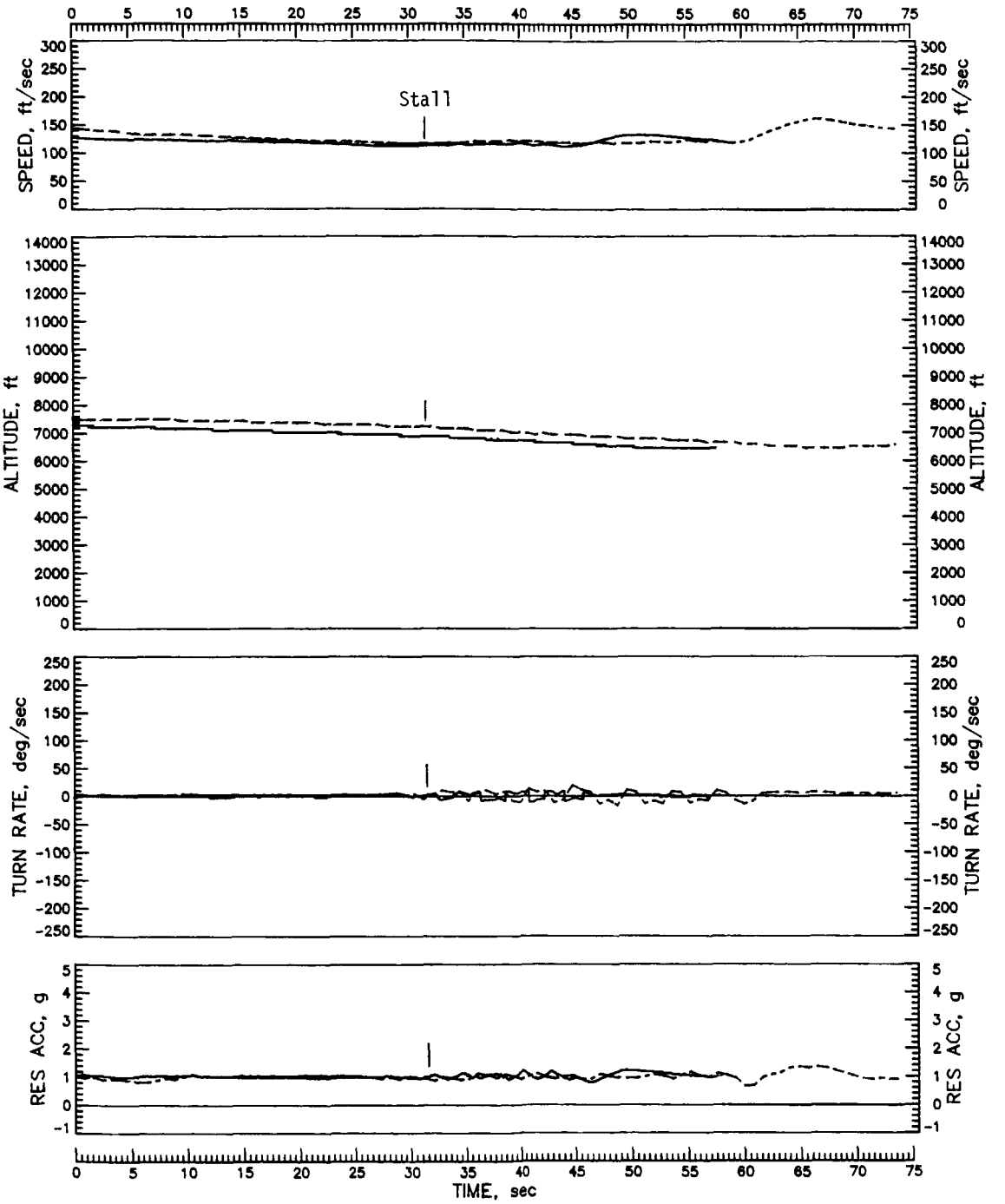

Figure 7. Concluded.

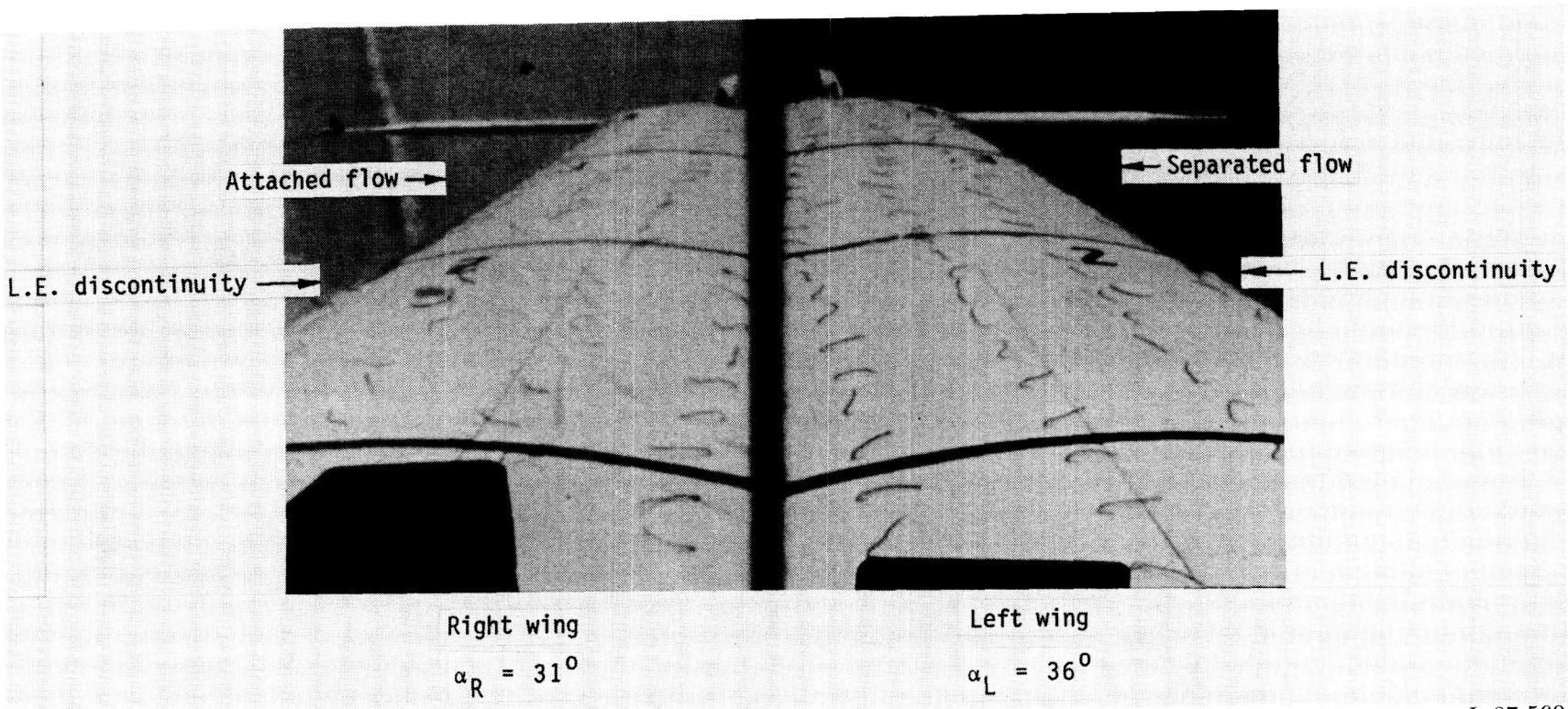

L-87-560

Figure 8. Visualization of flow over wings by means of tufts.

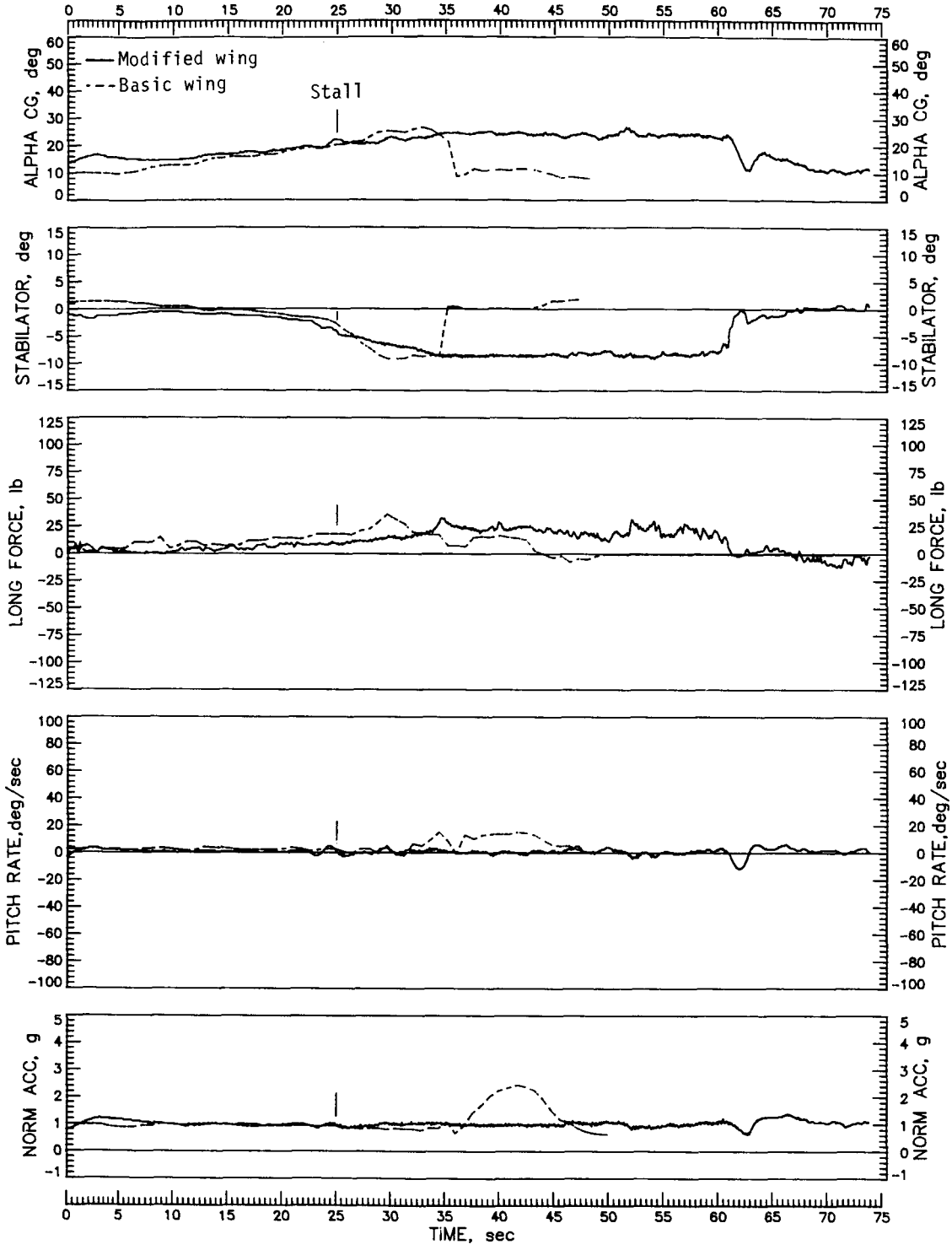

Figure 9. Idle-power, 1g, wings-level stall with maximum stabilator deflection, flaps and gear retracted. Test weight = 2438 lb; c.g. = 0.2777$\bar{c}$.

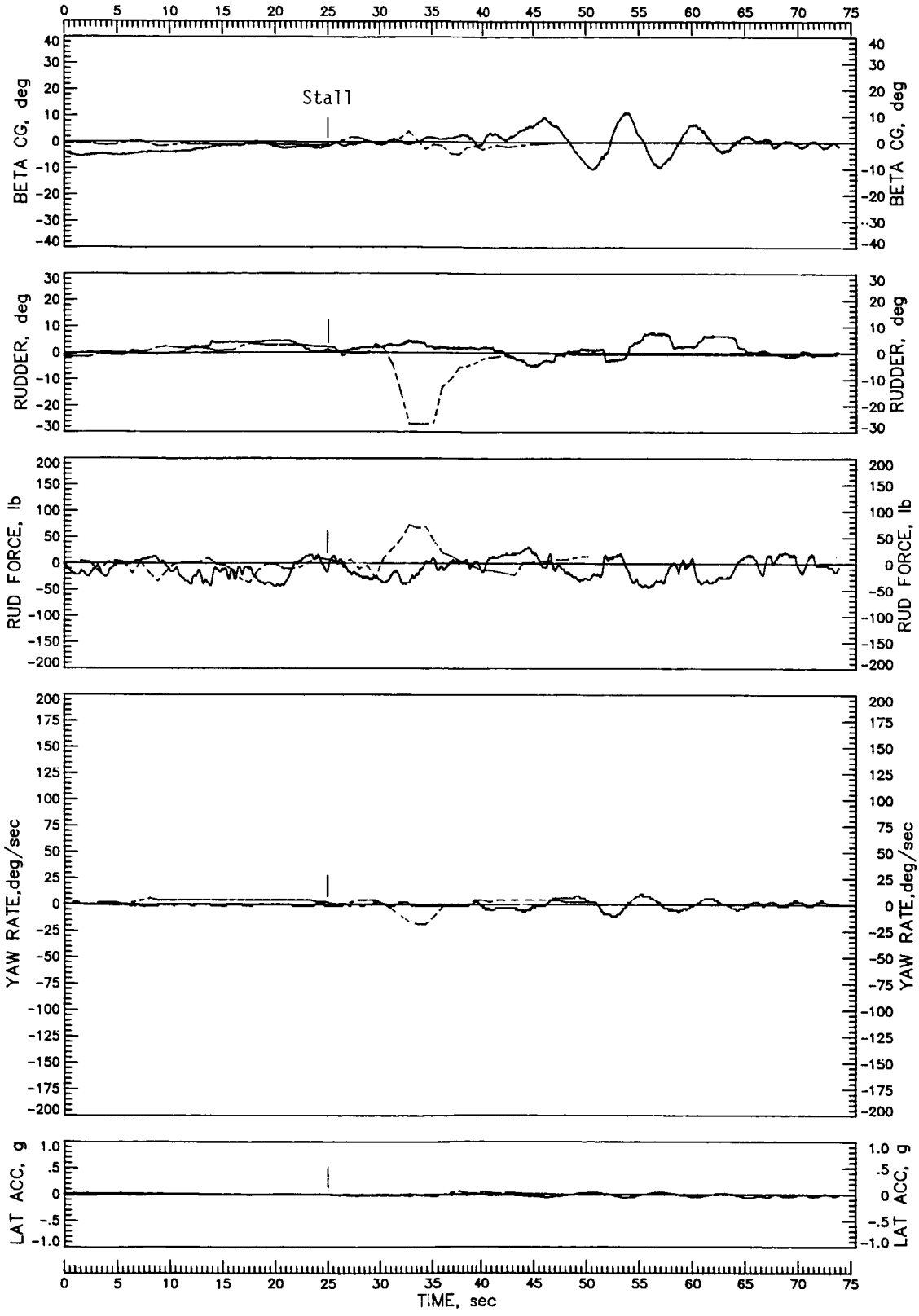

Figure 9. Continued.

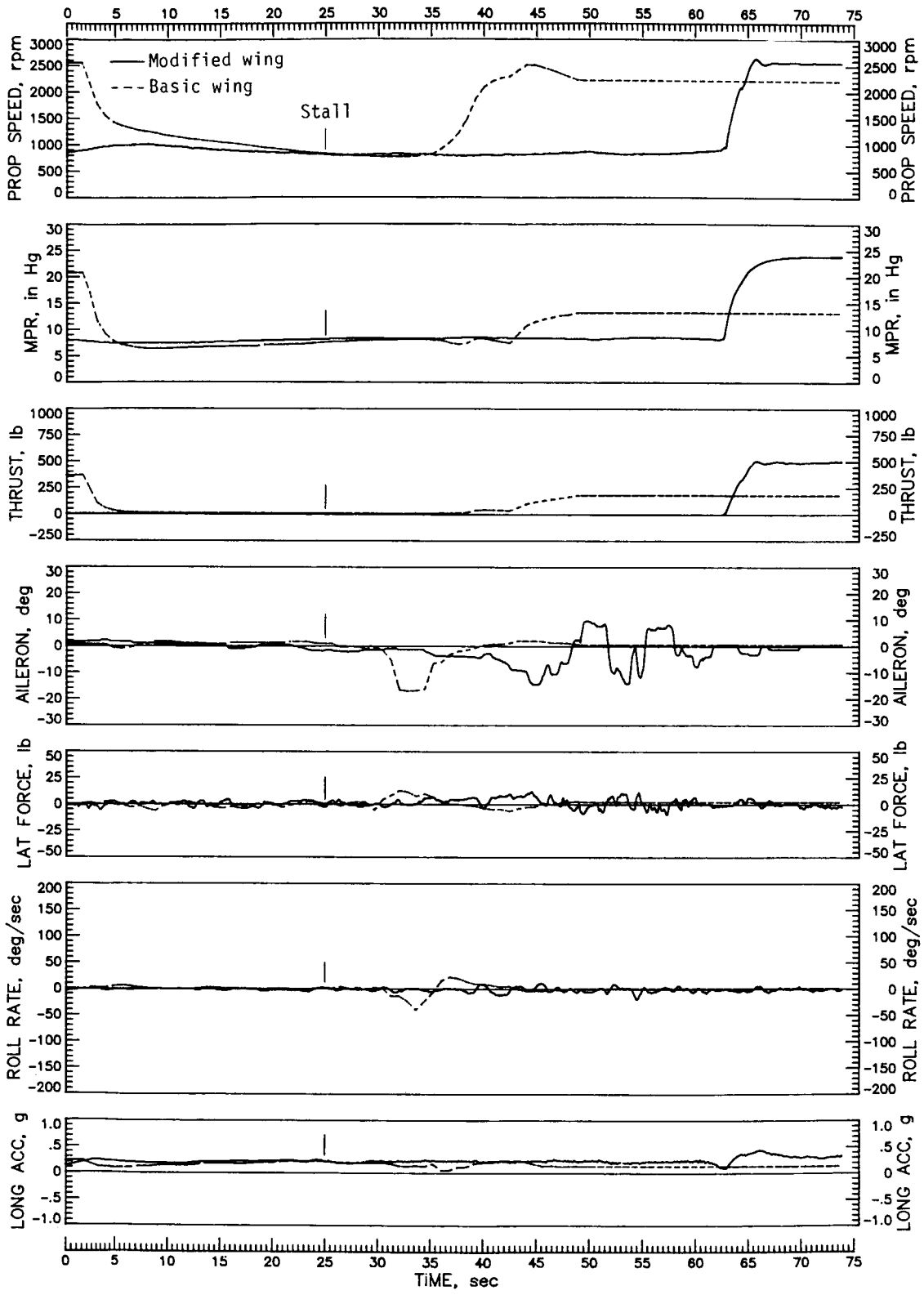

Figure 9. Continued.

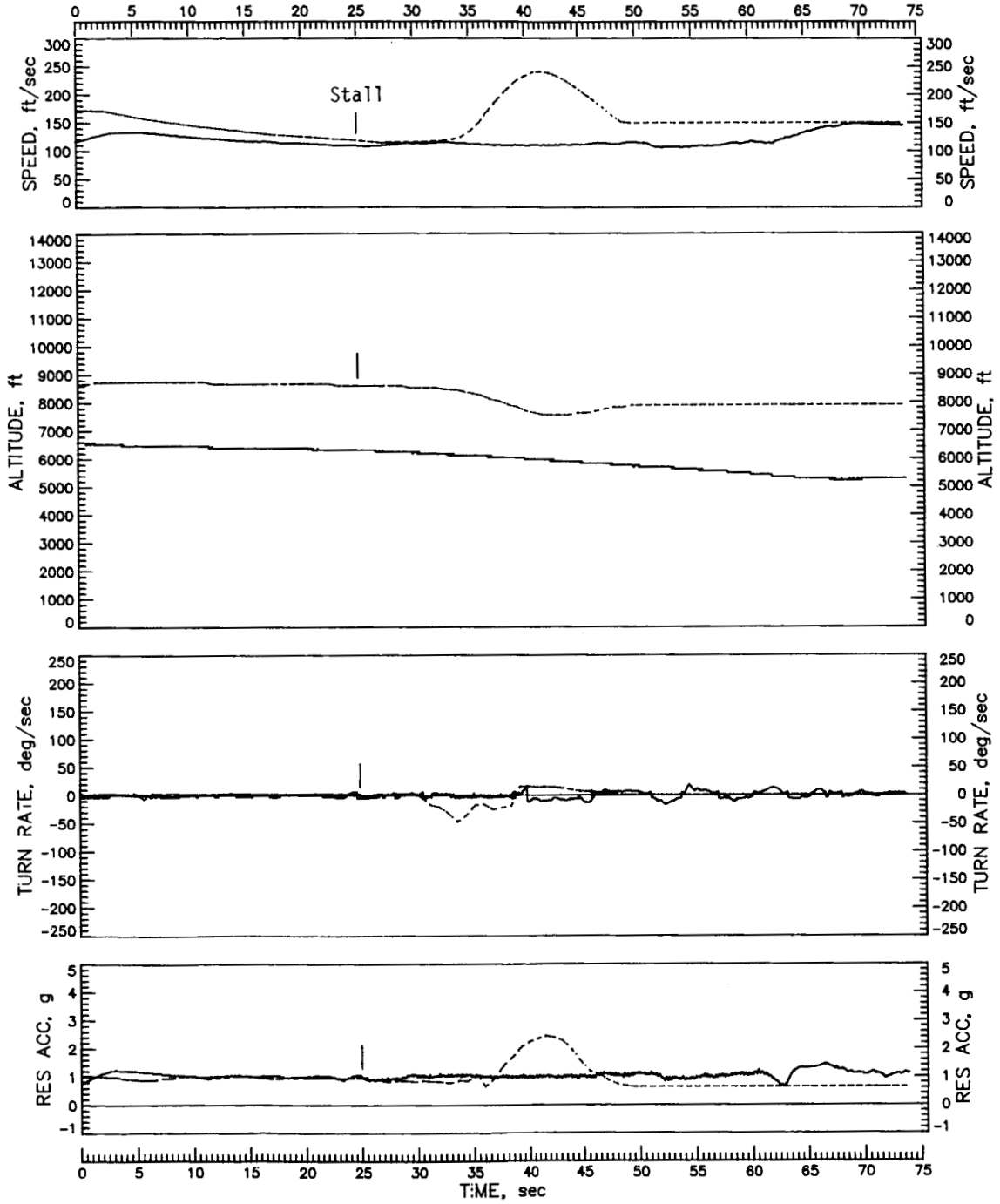

Figure 9. Concluded.

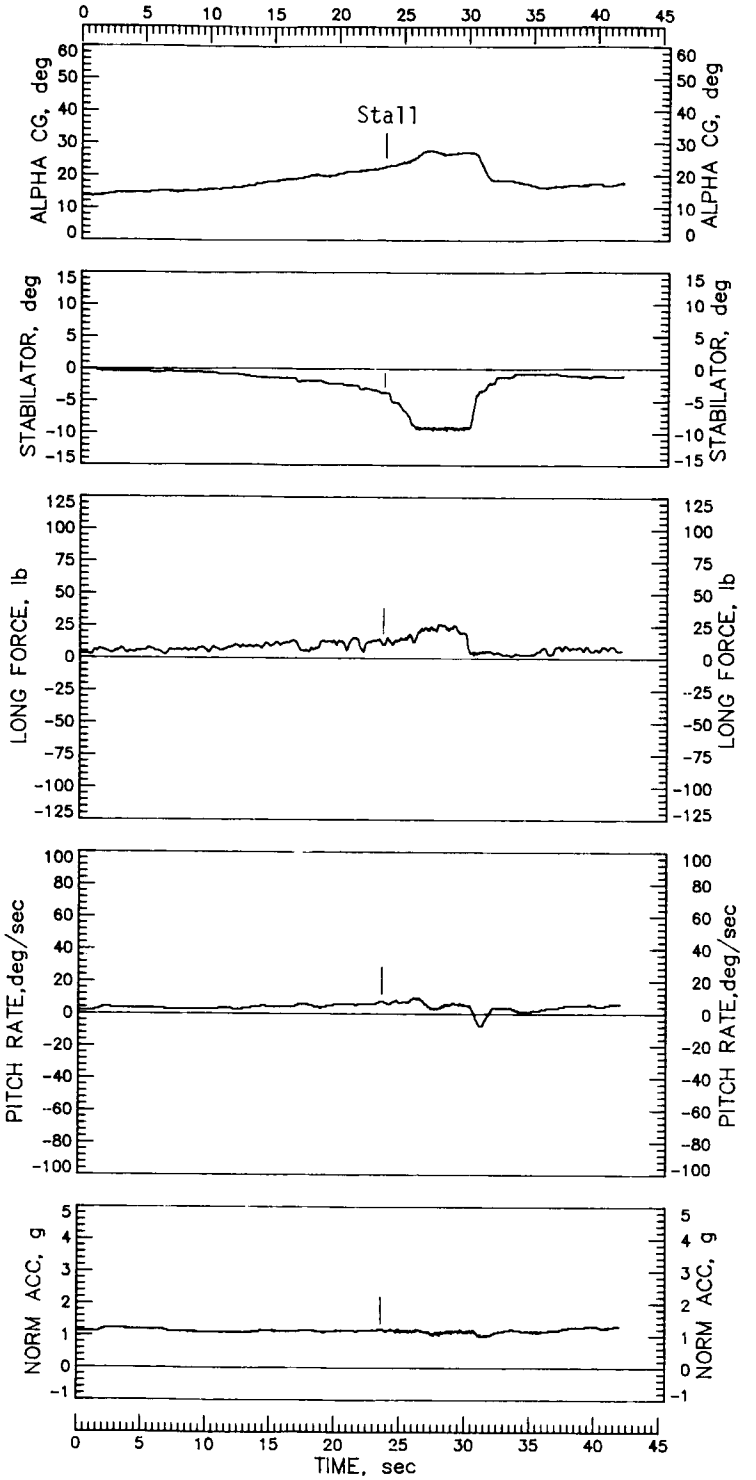

Figure 10. Idle-power stall of modified airplane from 30° banked left turn with flaps and gear retracted. Test weight = 2677 lb; c.g. = $0.2823\bar{c}$.

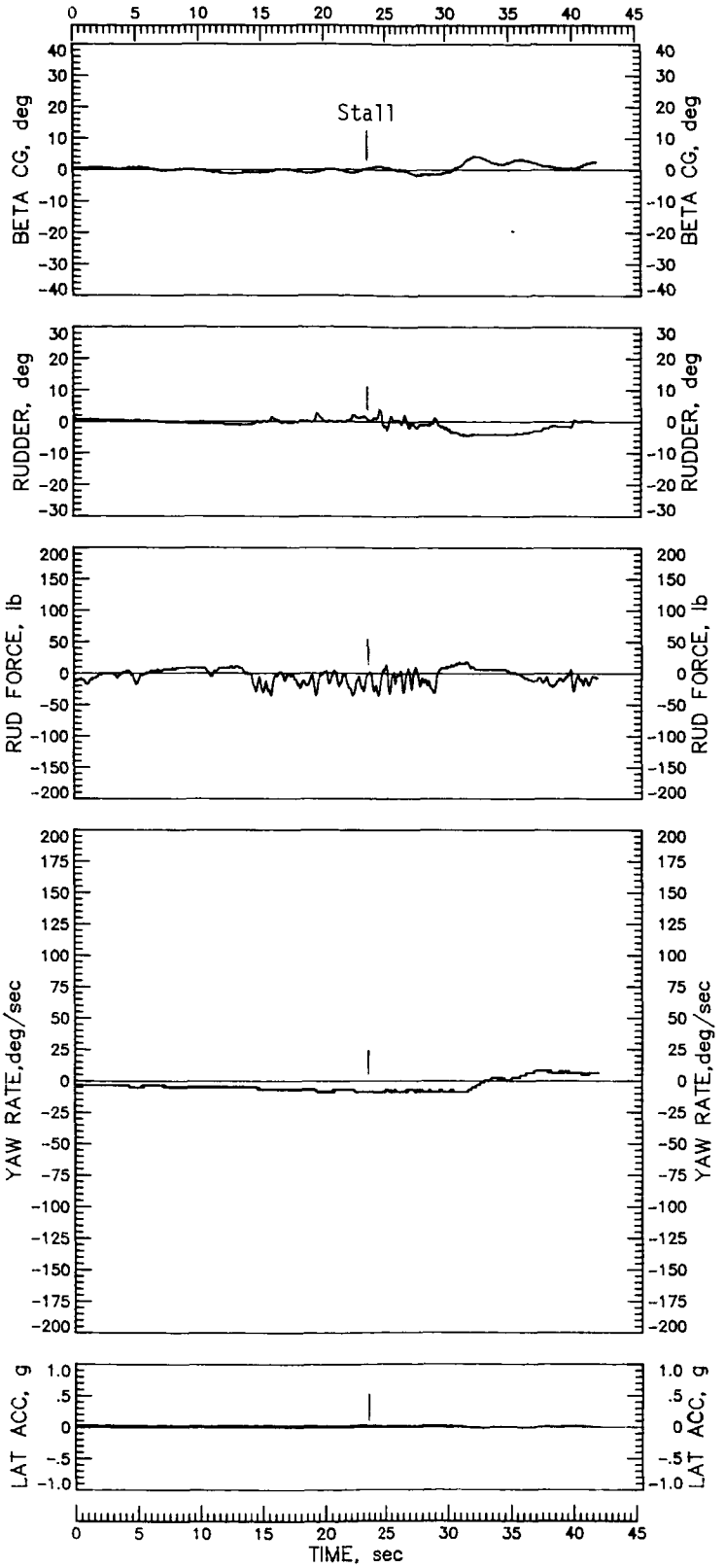

Figure 10. Continued.

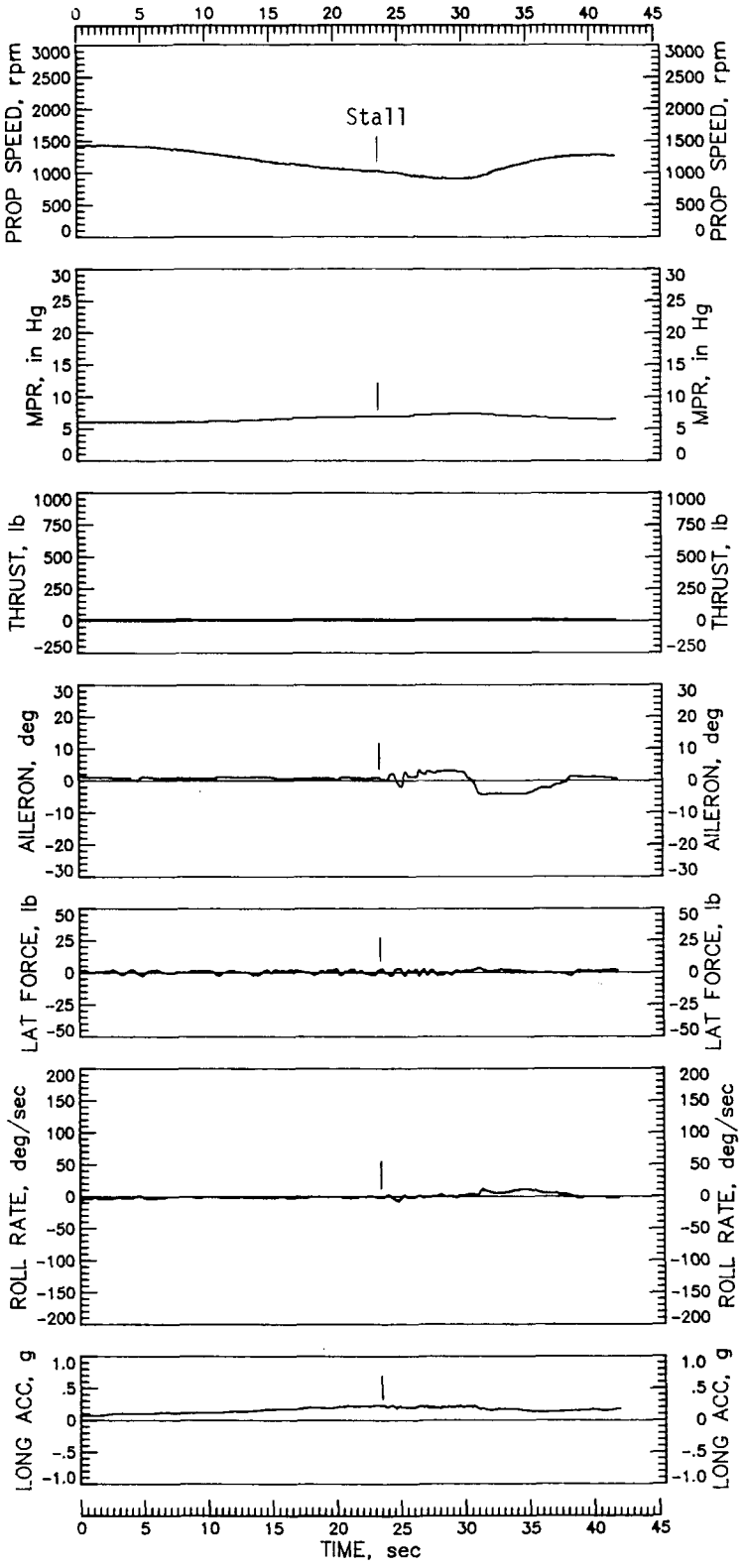

Figure 10. Continued.

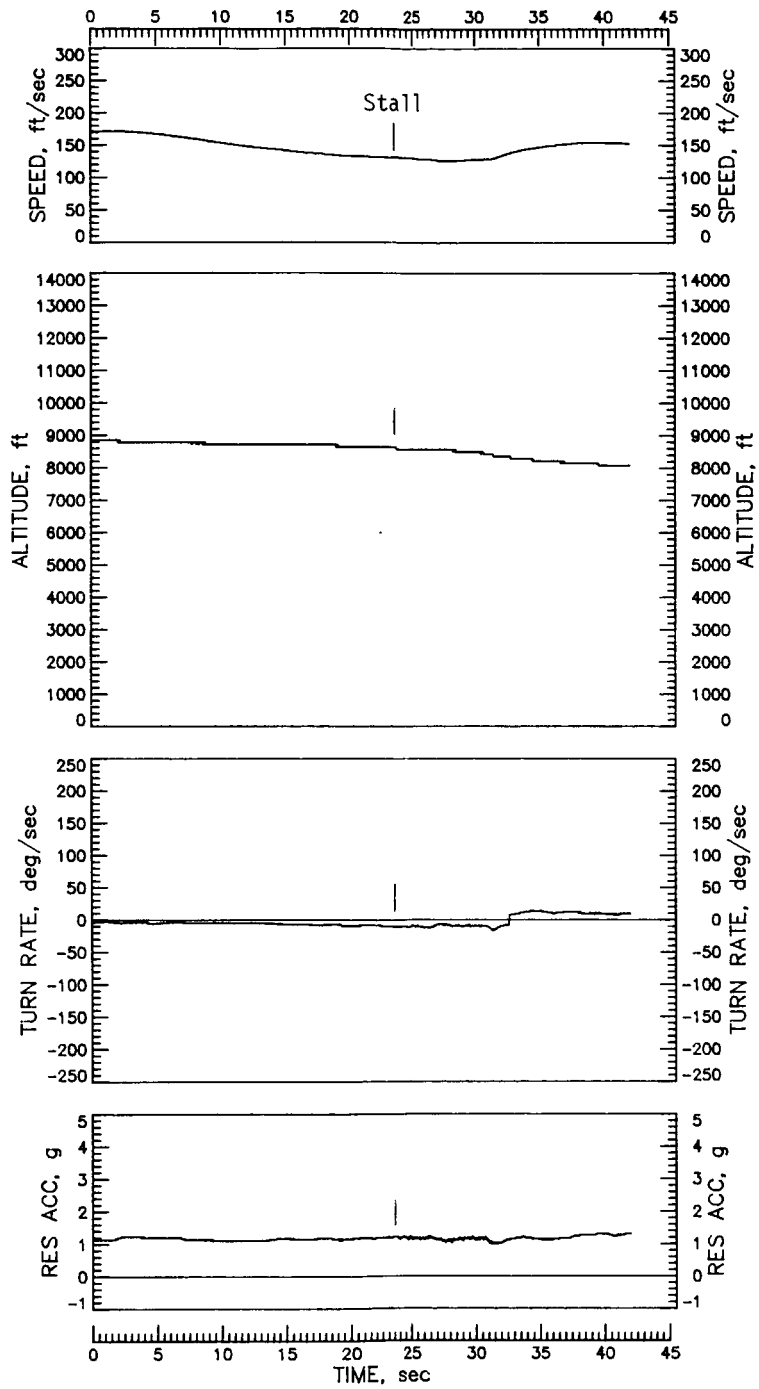

Figure 10. Concluded.

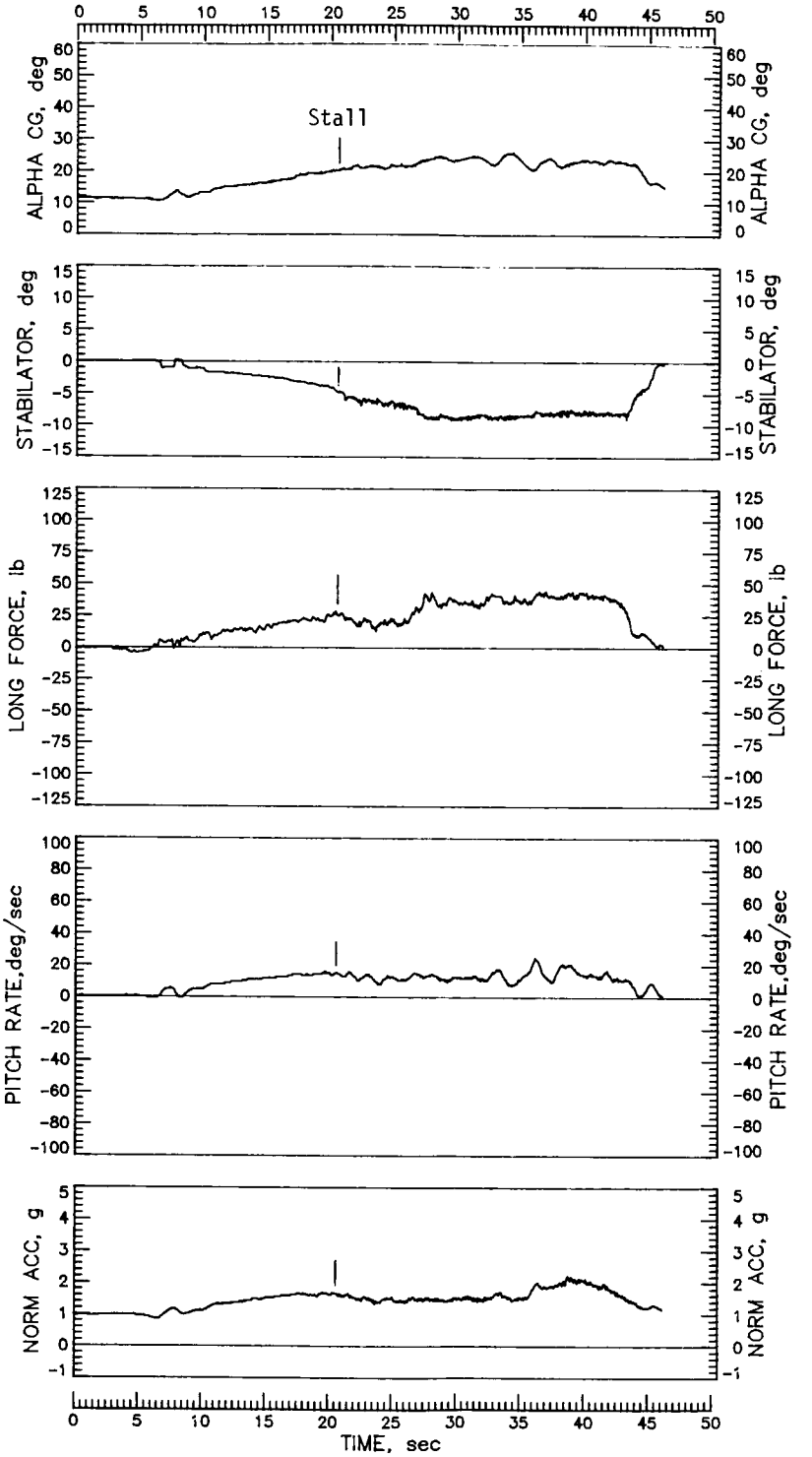

Figure 11. Idle-power stall of modified airplane from 45° banked skidding left turn with flaps and gear retracted. Test weight = 2677 lb; c.g. = $0.2823\bar{c}$.

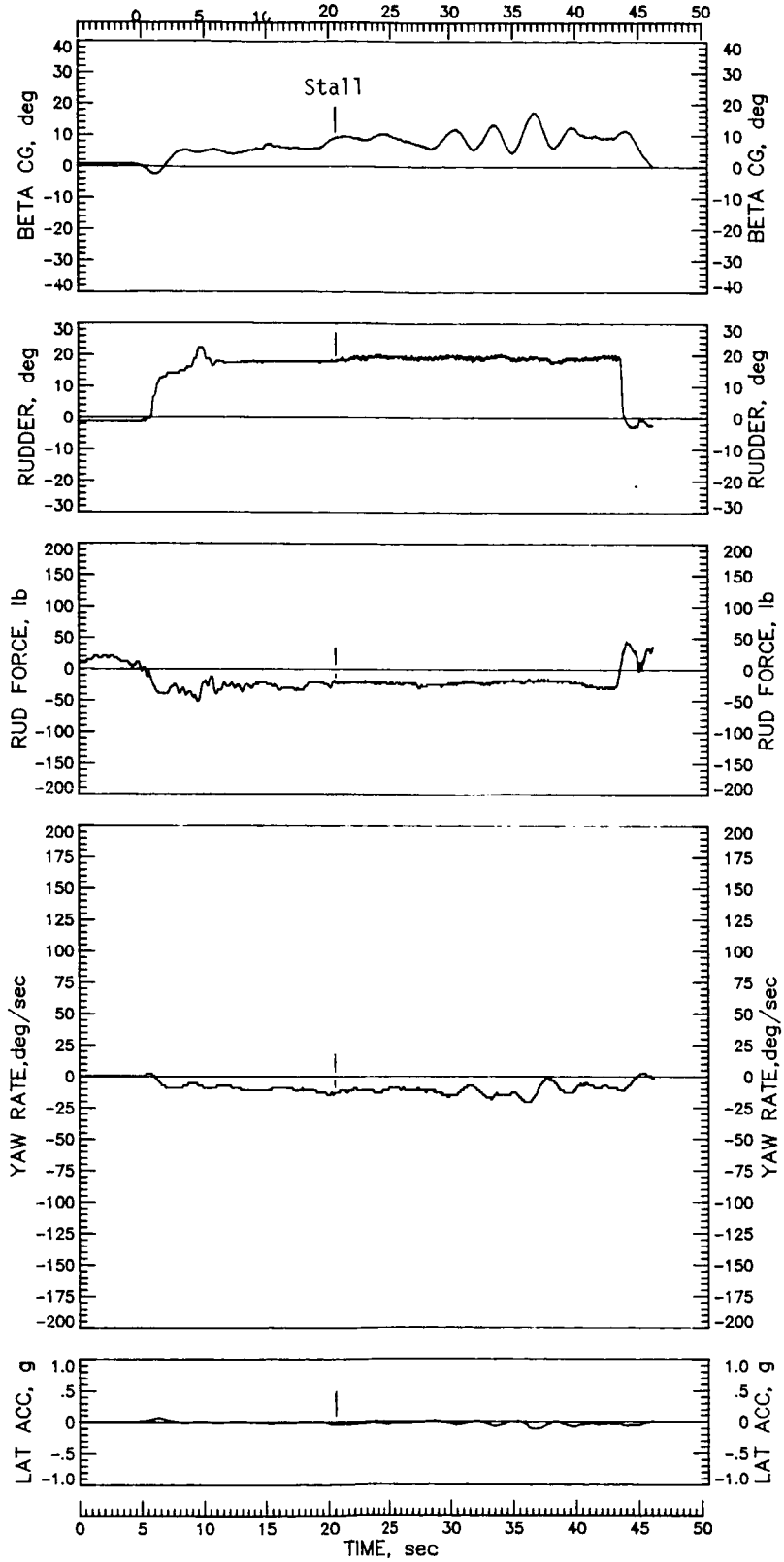

Figure 11. Continued.

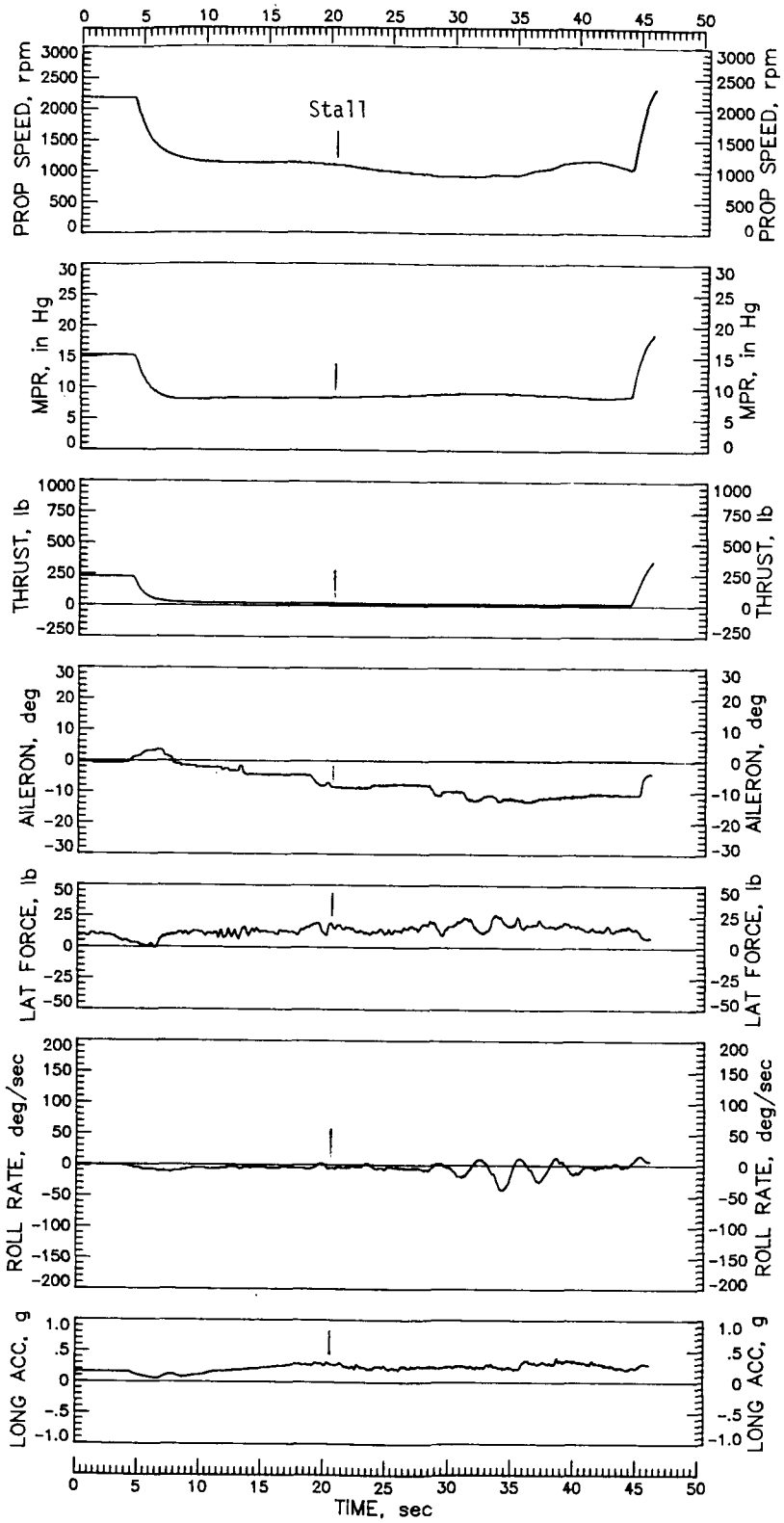

Figure 11. Continued.

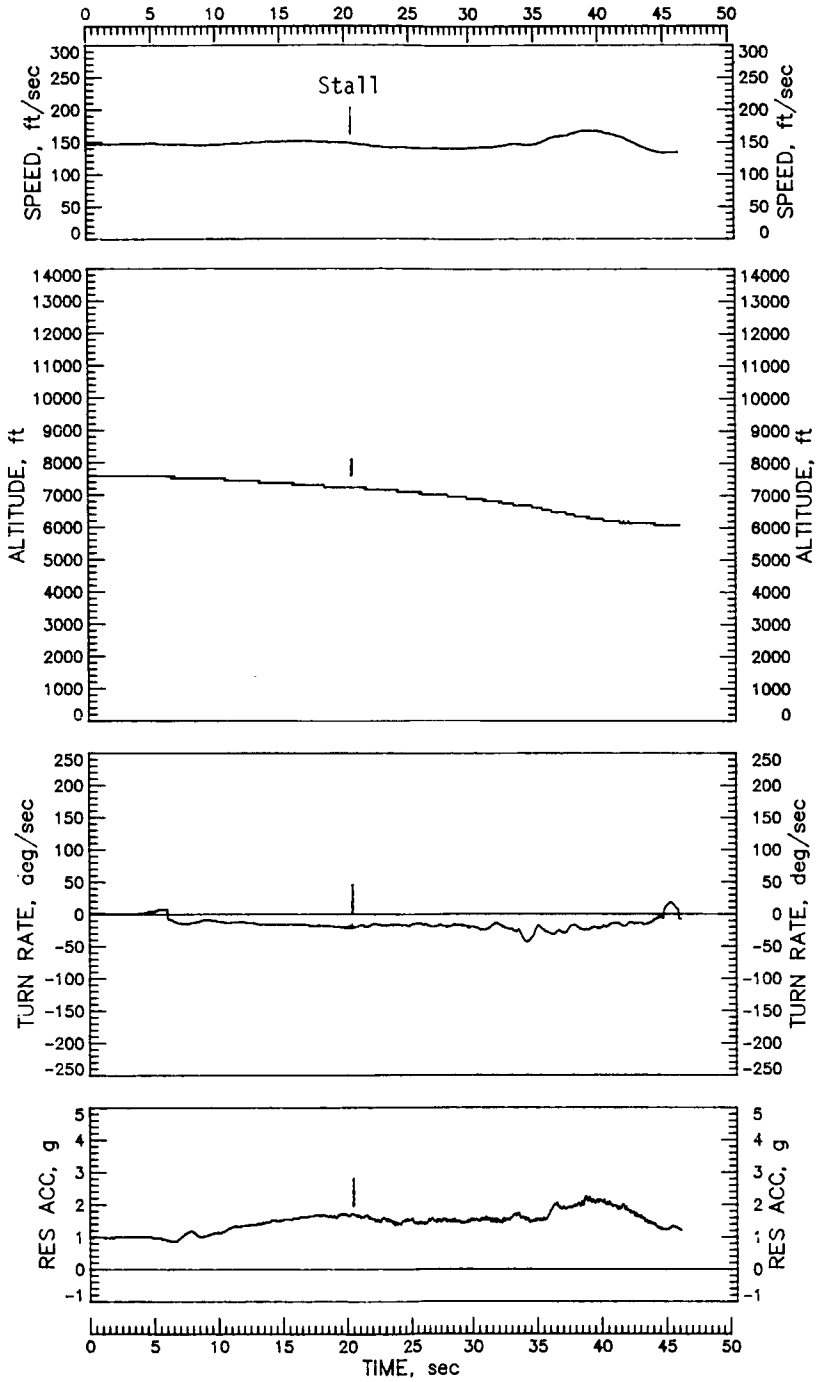

Figure 11. Concluded.

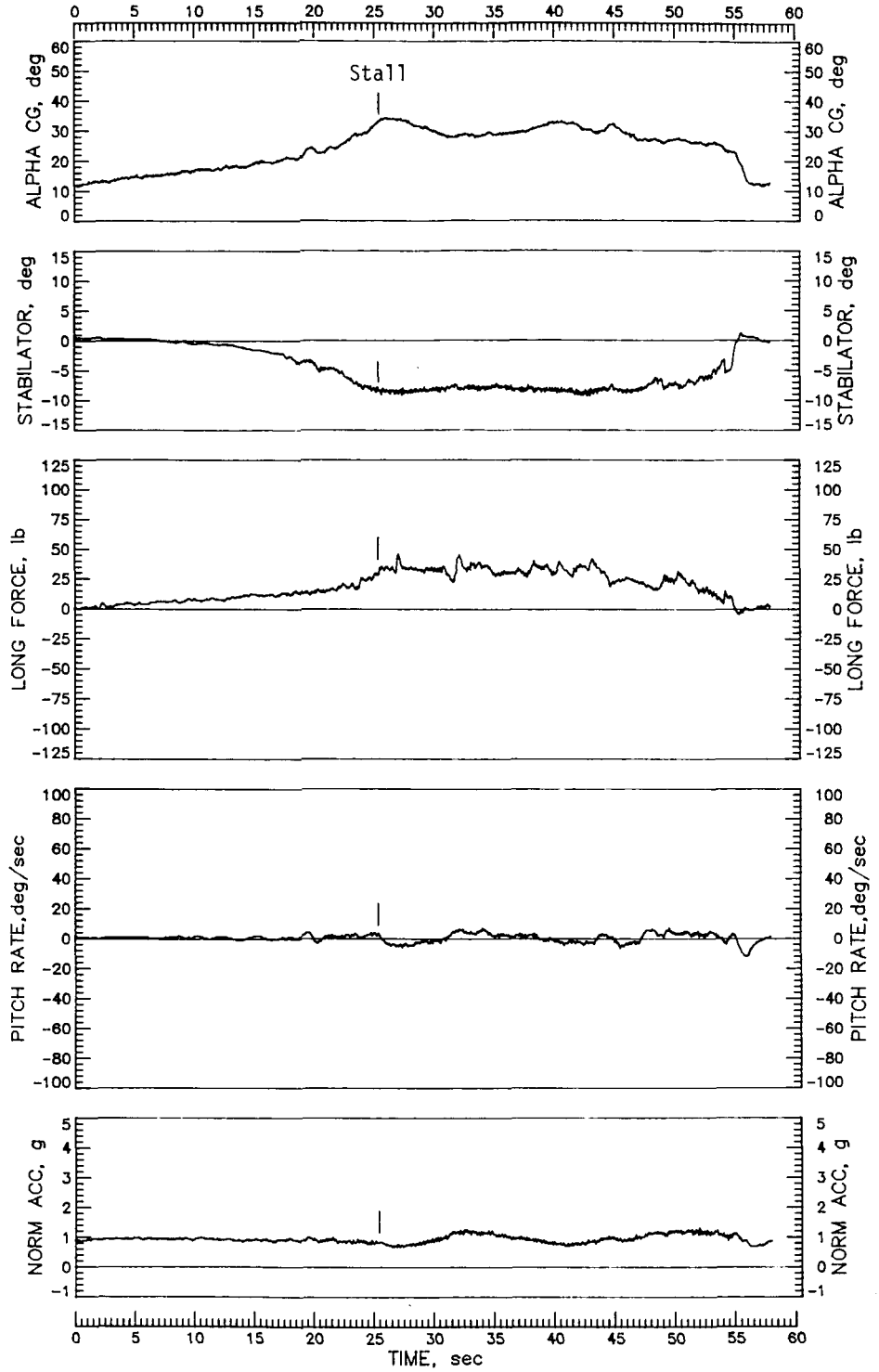

Figure 12. Maximum-power, 1g, wings-level stall of modified airplane with flaps and gear retracted. Test weight = 2438 lb; c.g. = 0.2777$\bar{c}$.

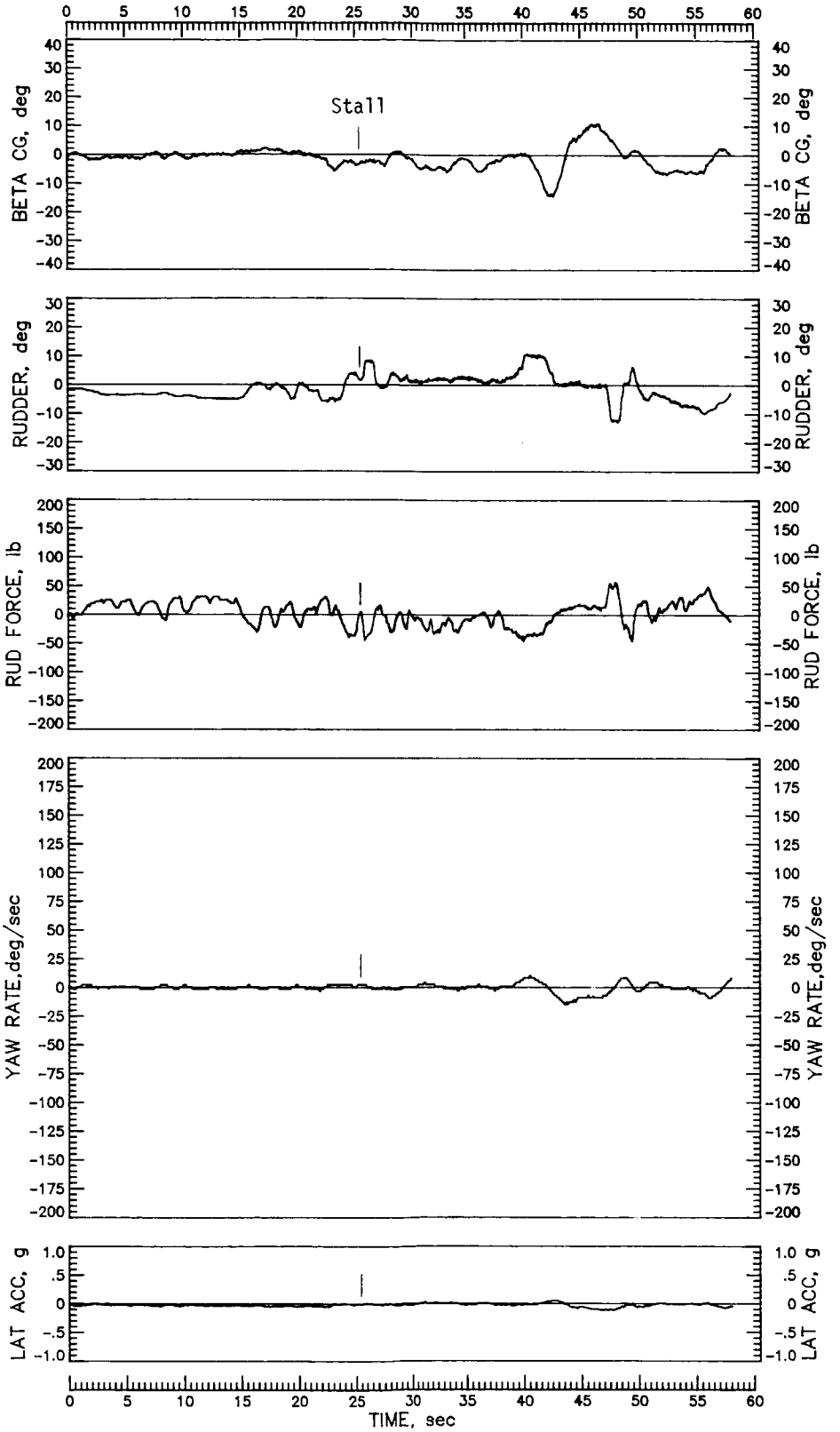

Figure 12. Continued.

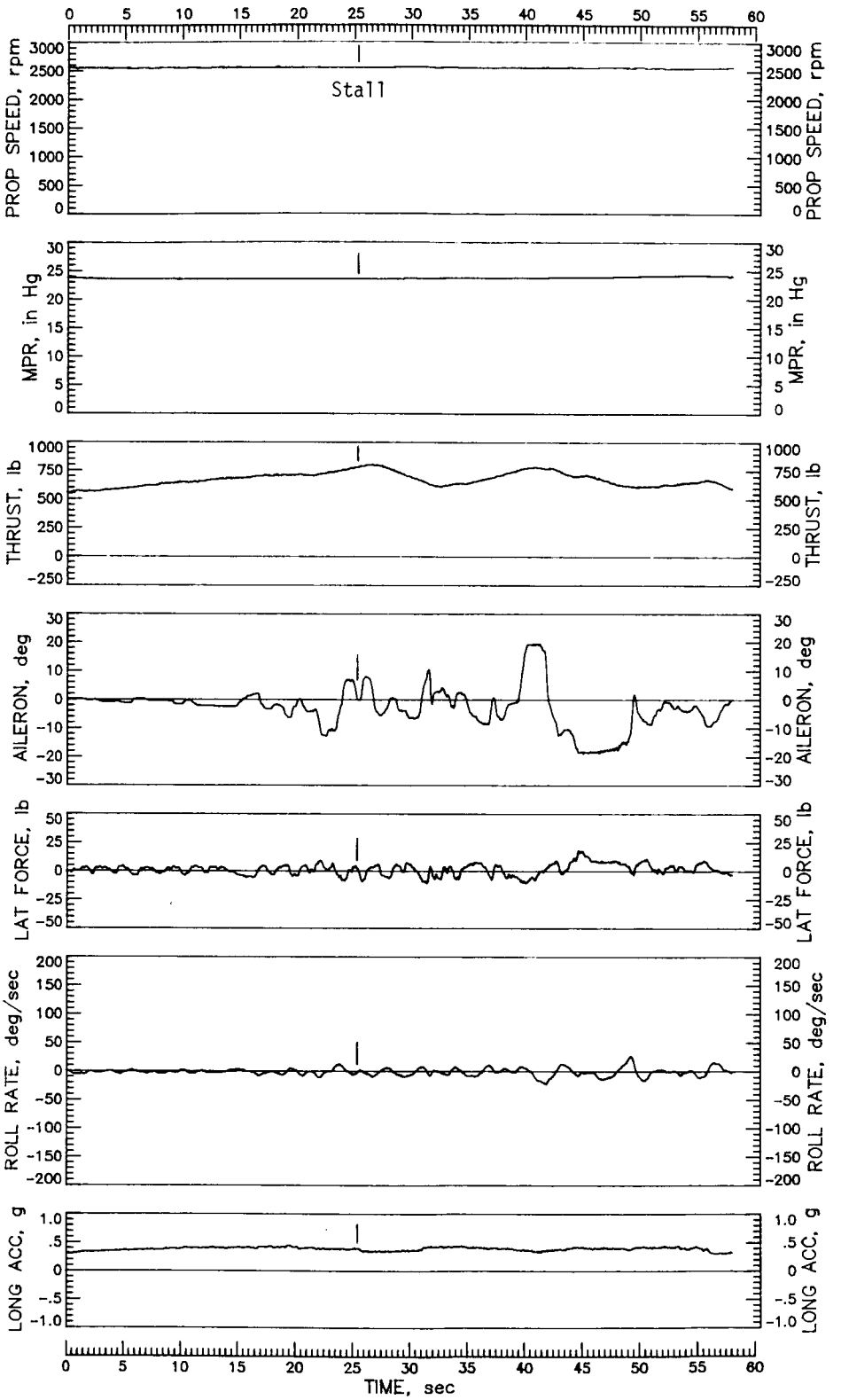

Figure 12. Continued.

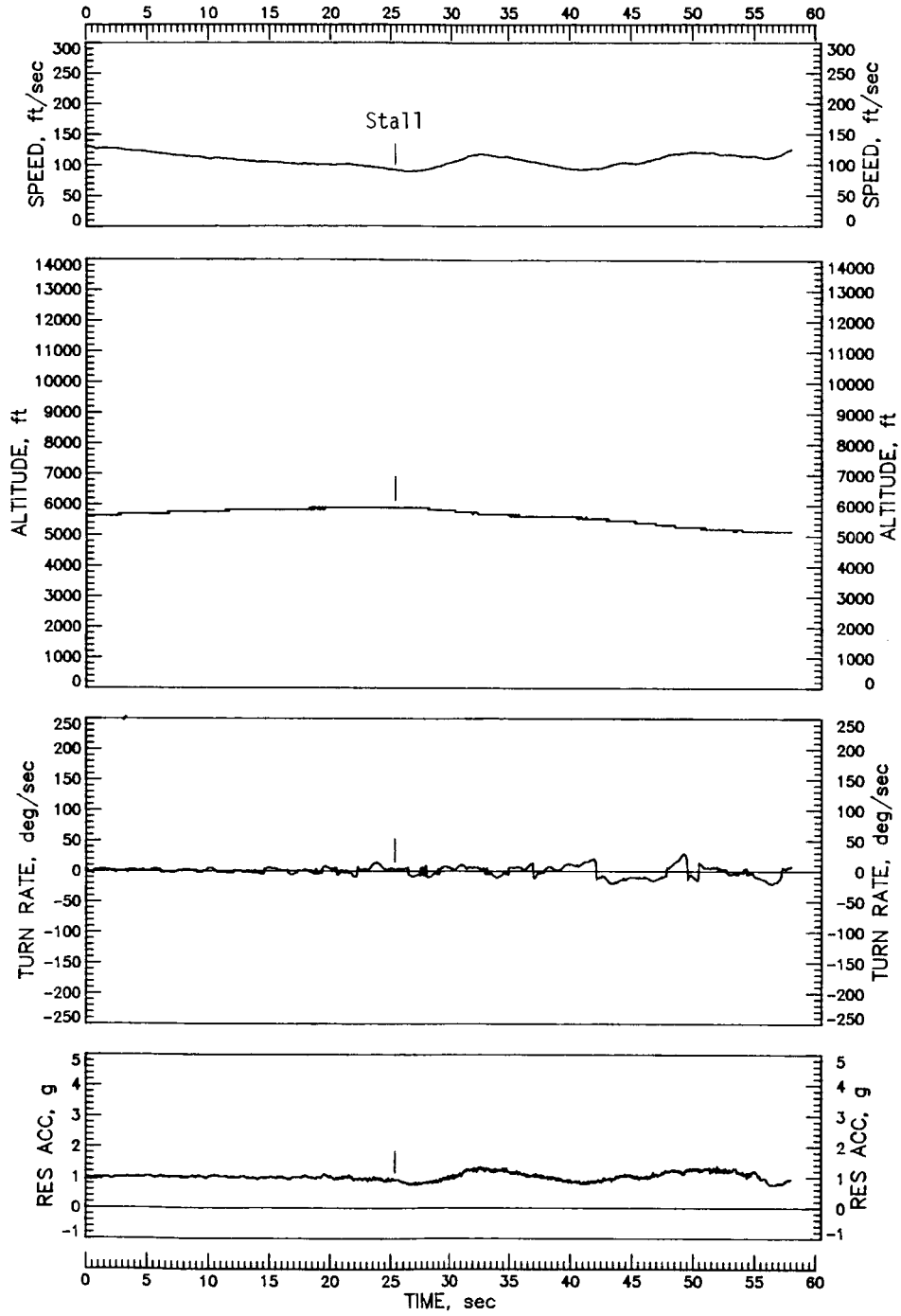

Figure 12. Concluded.

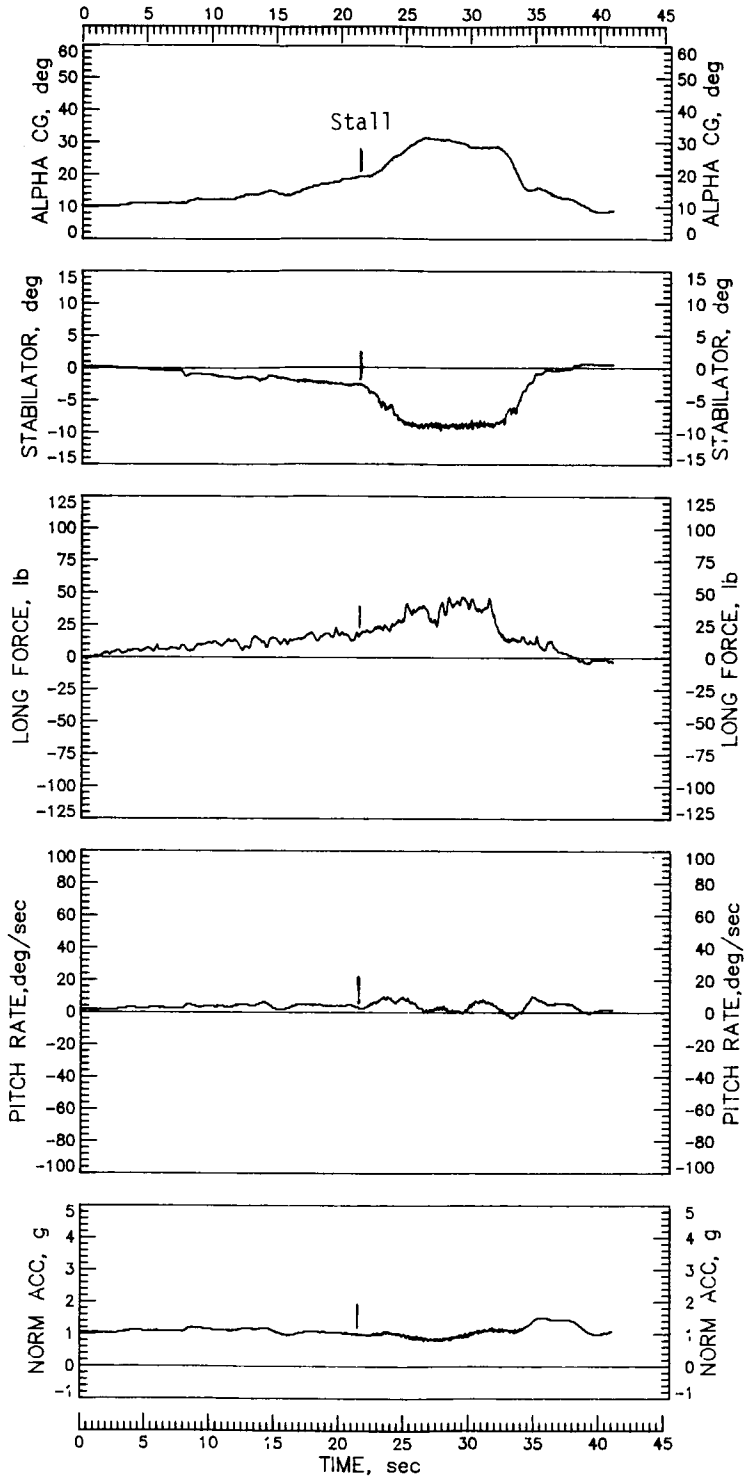

Figure 13. Maximum-power stall of modified airplane from 30° banked skidding left turn with flaps and gear retracted. Test weight = 2677 lb; c.g. = $0.2823\bar{c}$.

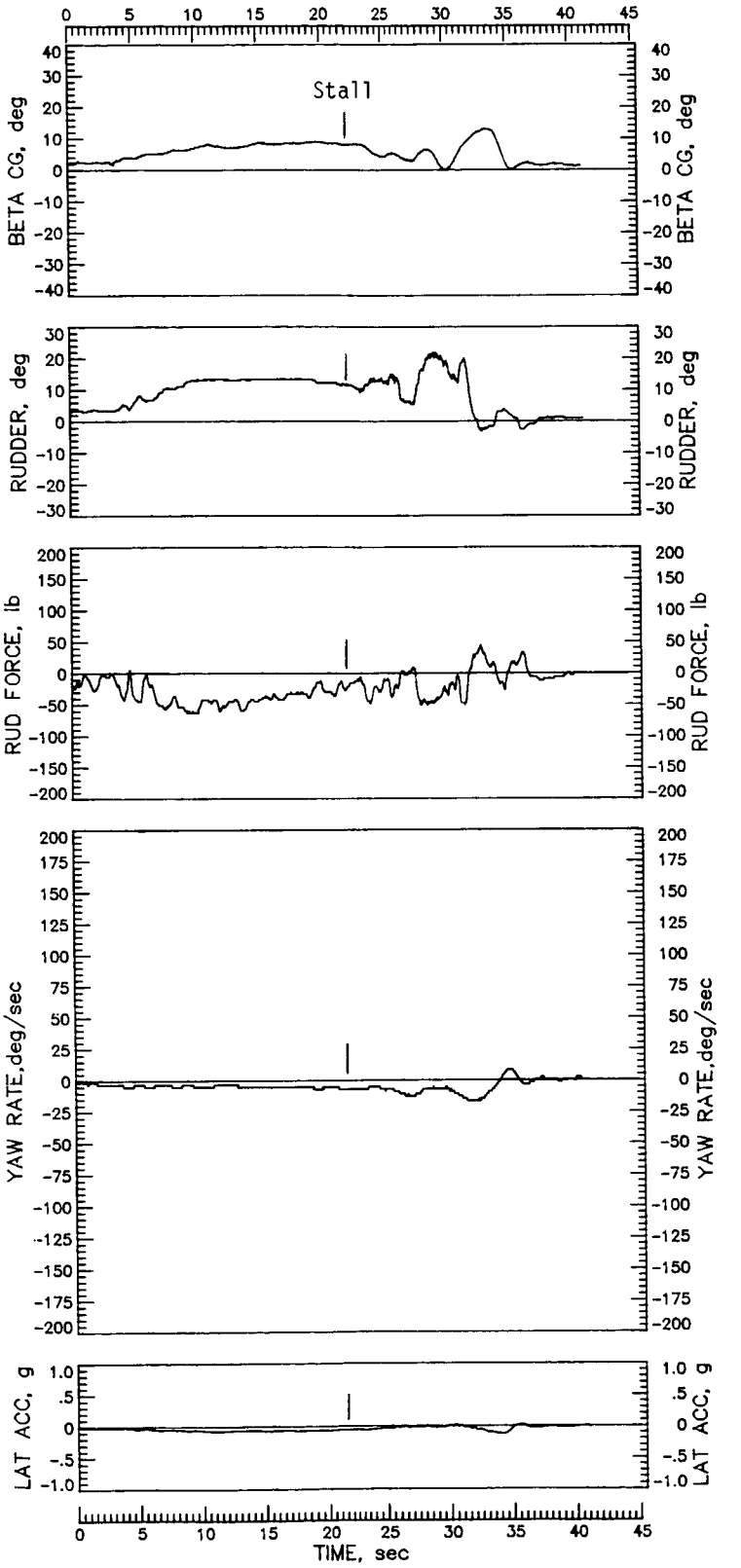

Figure 13. Continued.

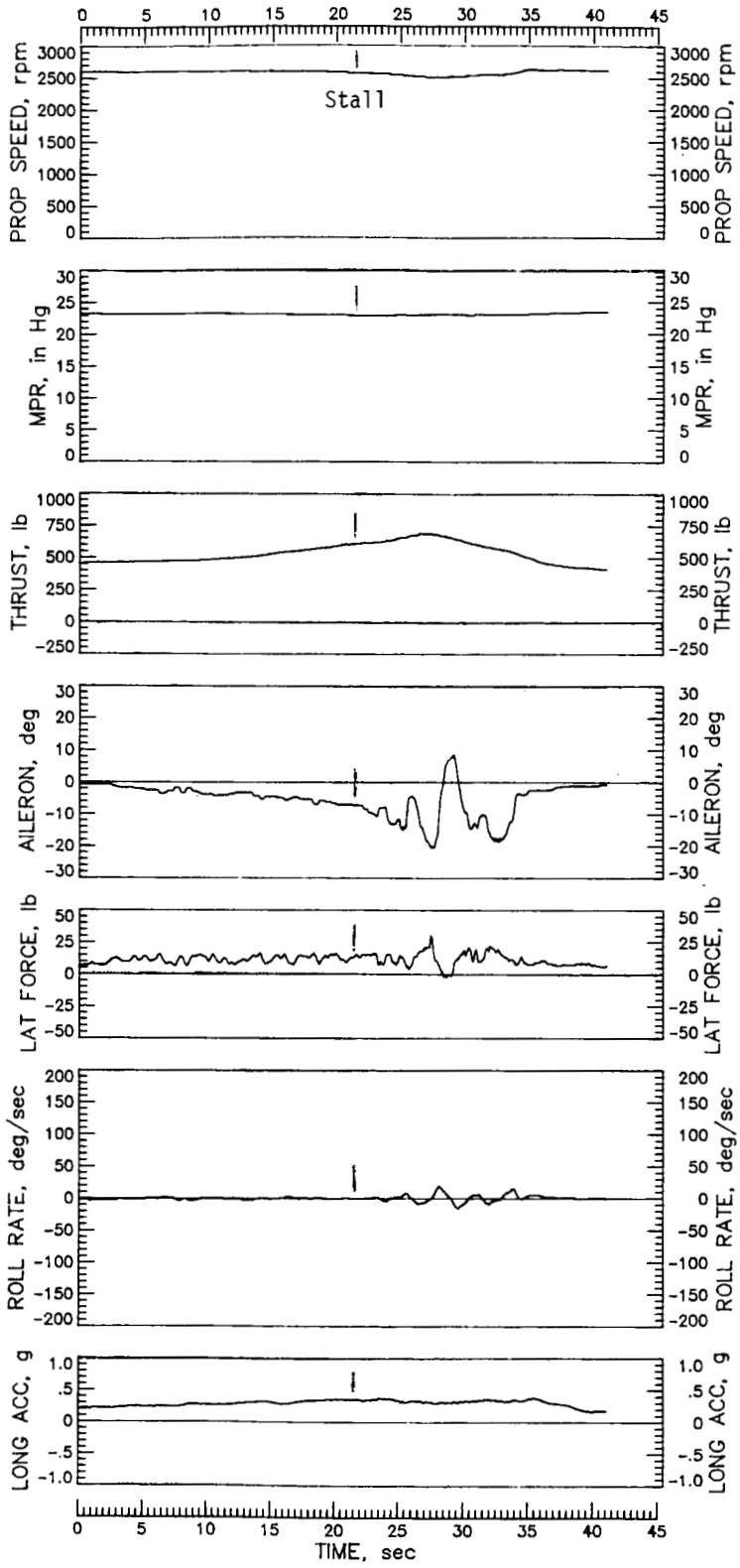

Figure 13. Continued.

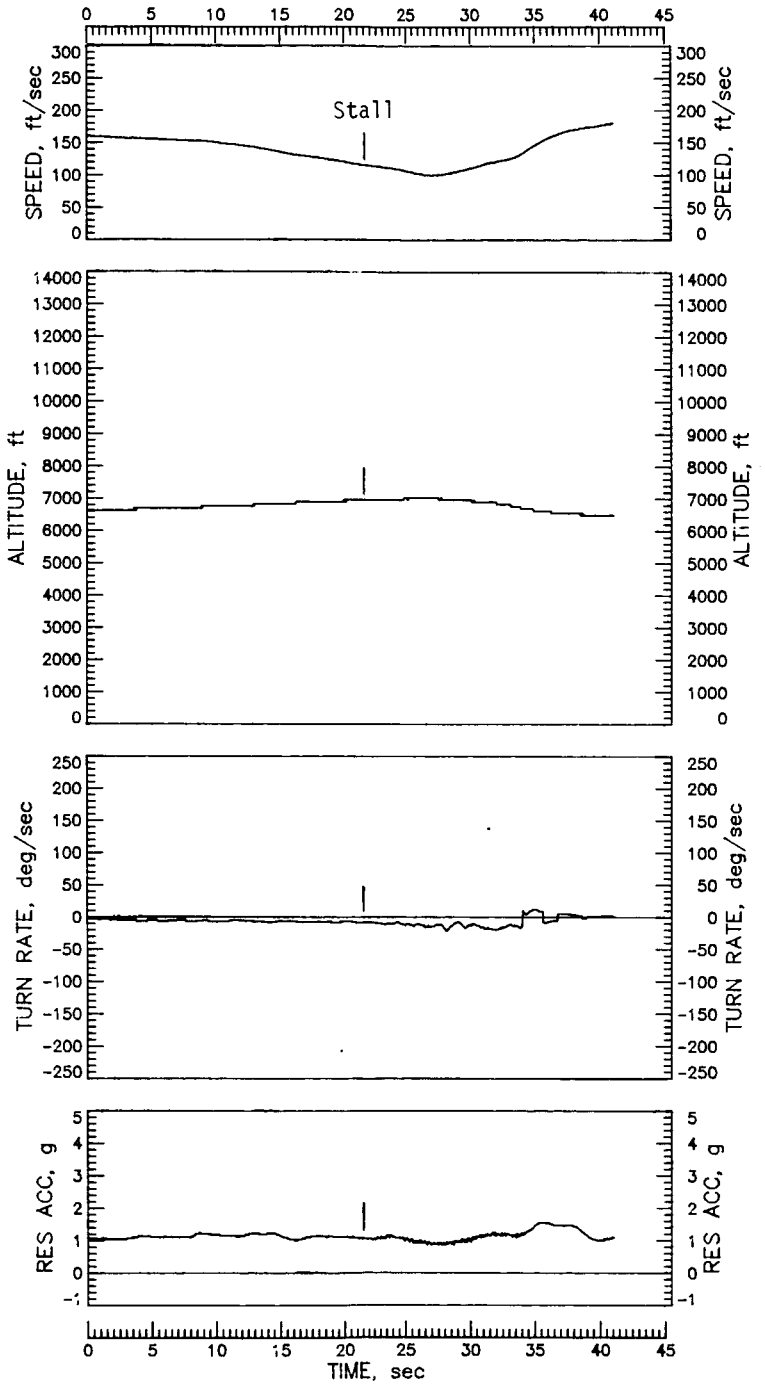

Figure 13. Concluded.

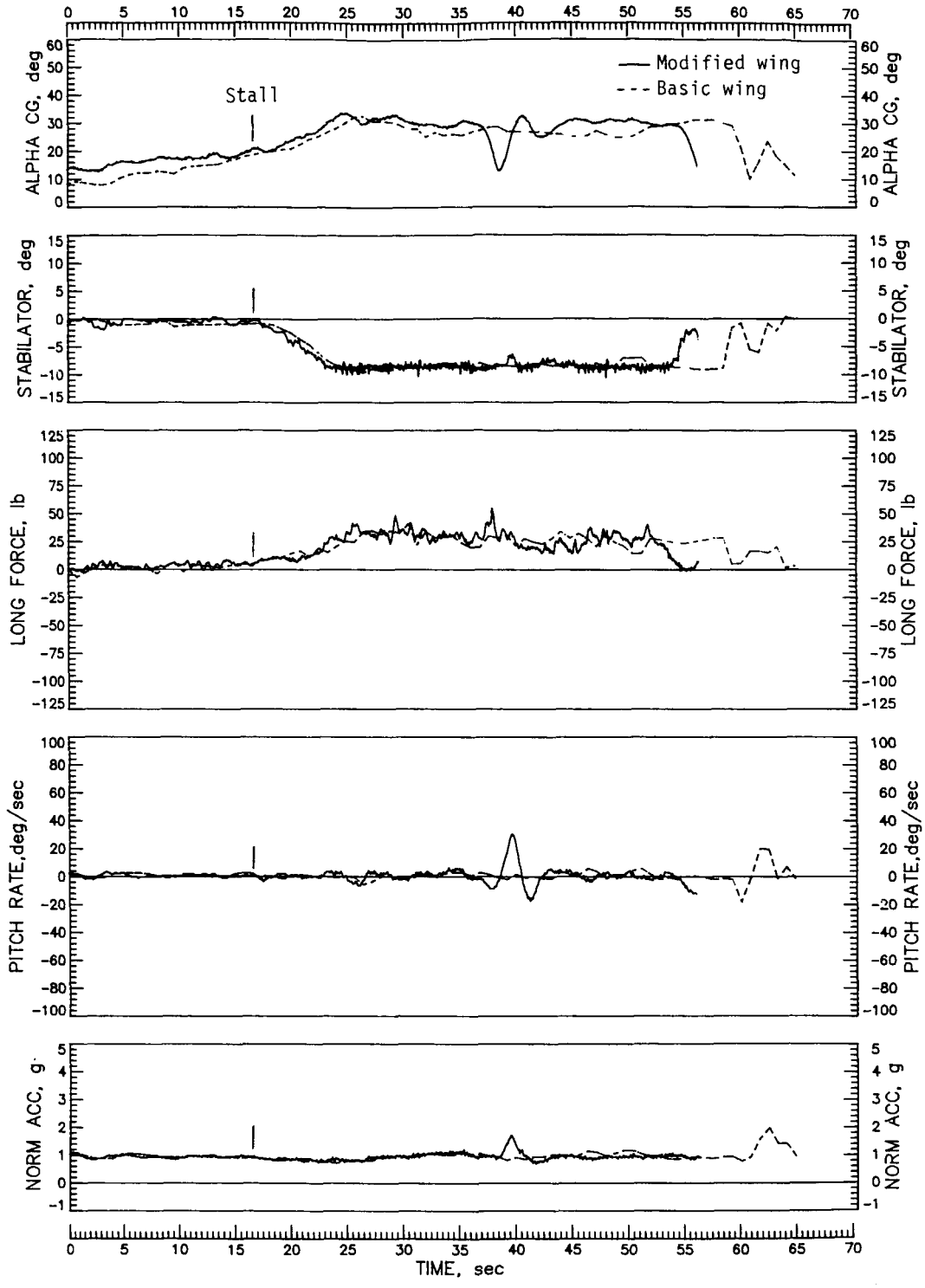

Figure 14. Maximum-power stall with flaps extended 40° and gear retracted. Test weight = 2438 lb; c.g. = $0.2777\bar{c}$.

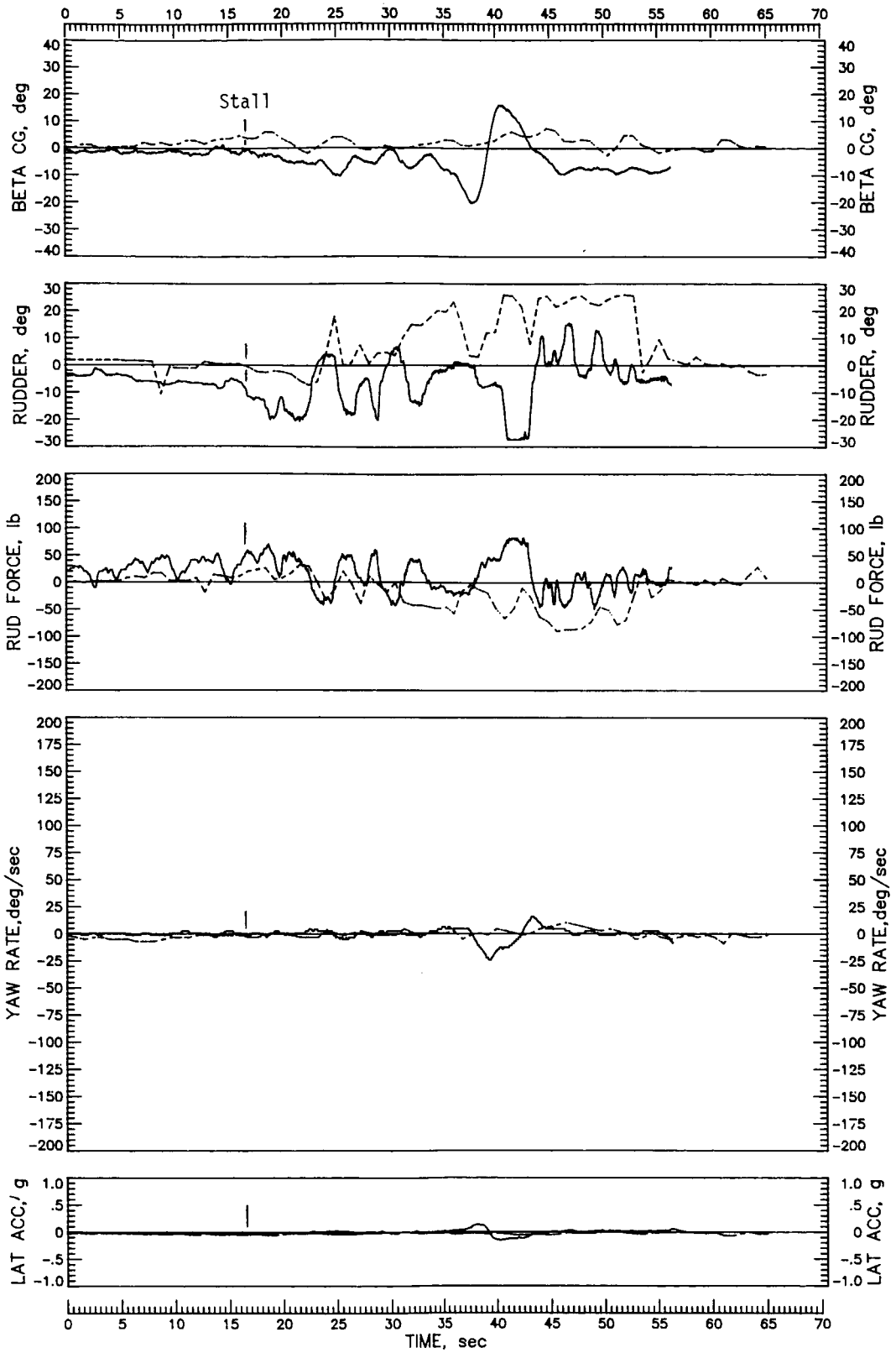

Figure 14. Continued.

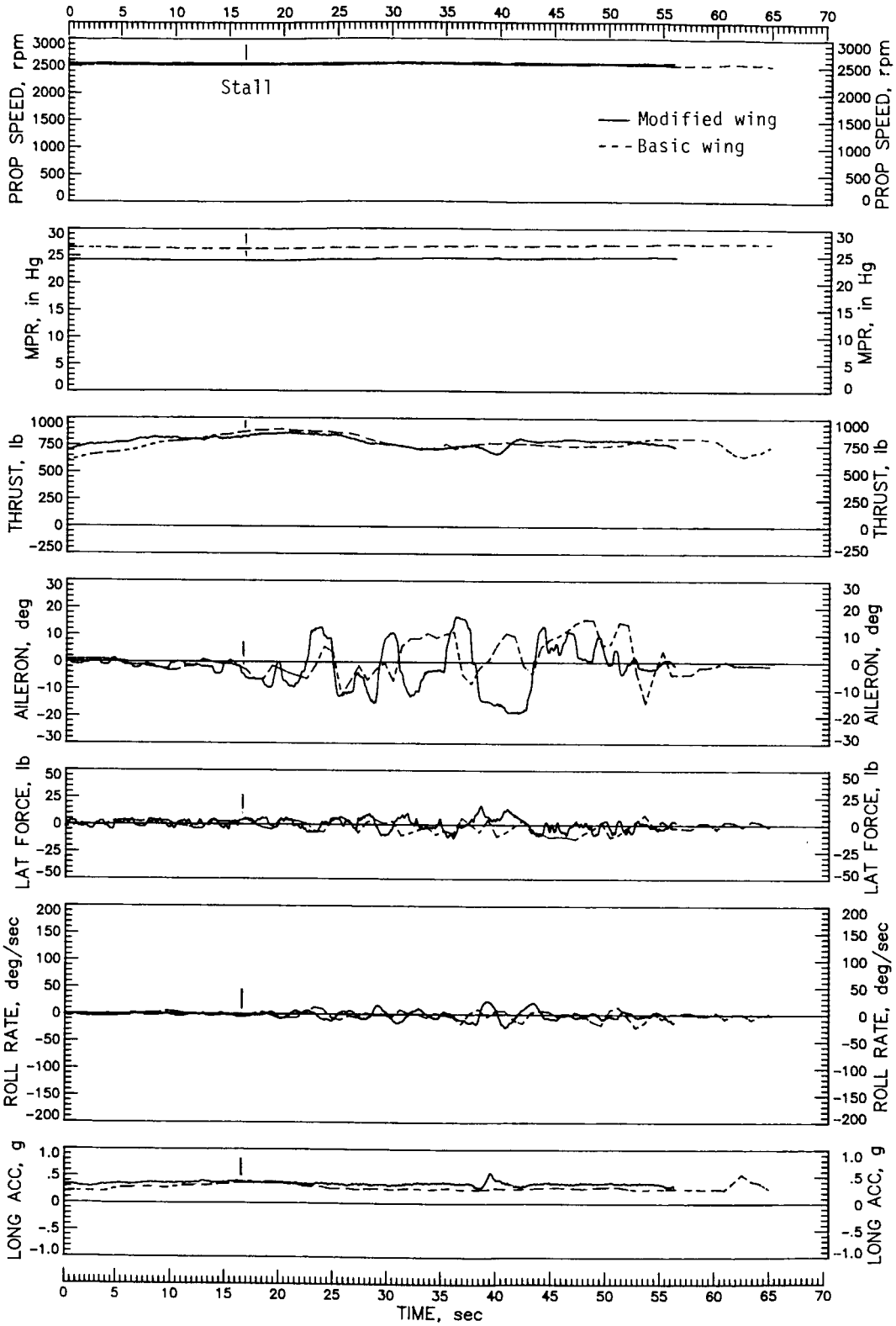

Figure 14. Continued.

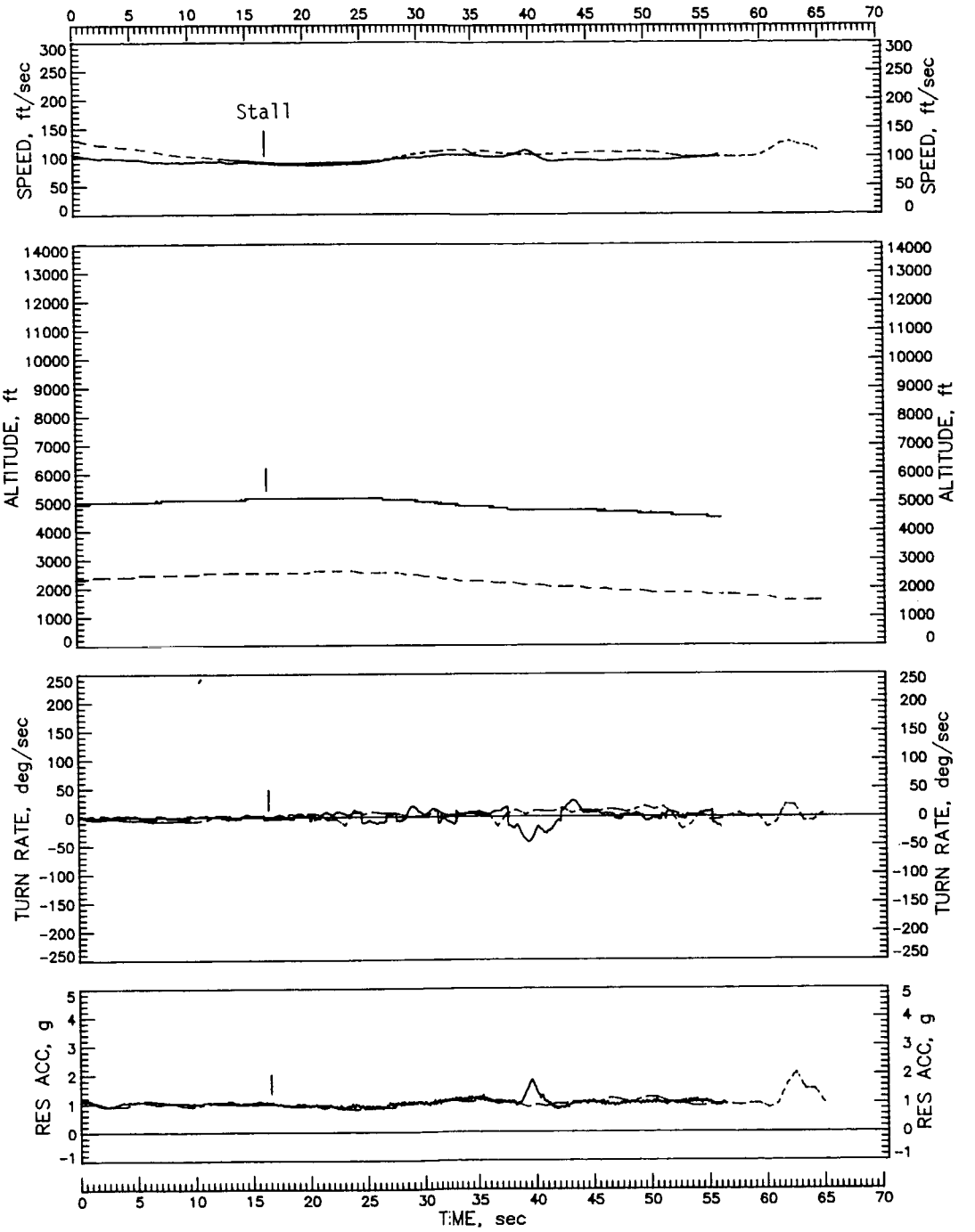

Figure 14. Concluded.

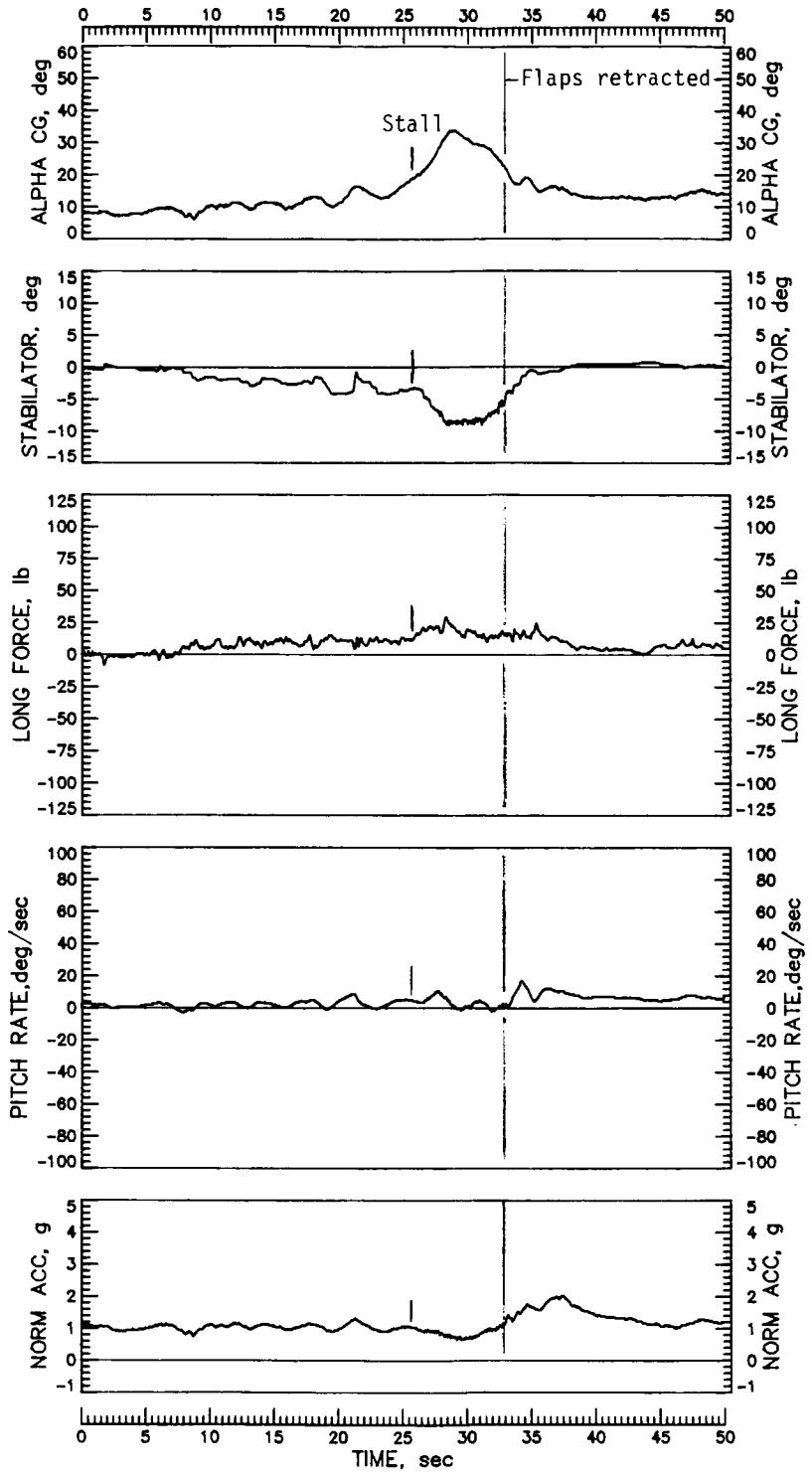

Figure 15. Maximum-power stall of modified airplane from 30° banked skidding left turn with flaps extended 40° and gear retracted. Test weight = 2438 lb; c.g. = 0.2777$\bar{c}$.

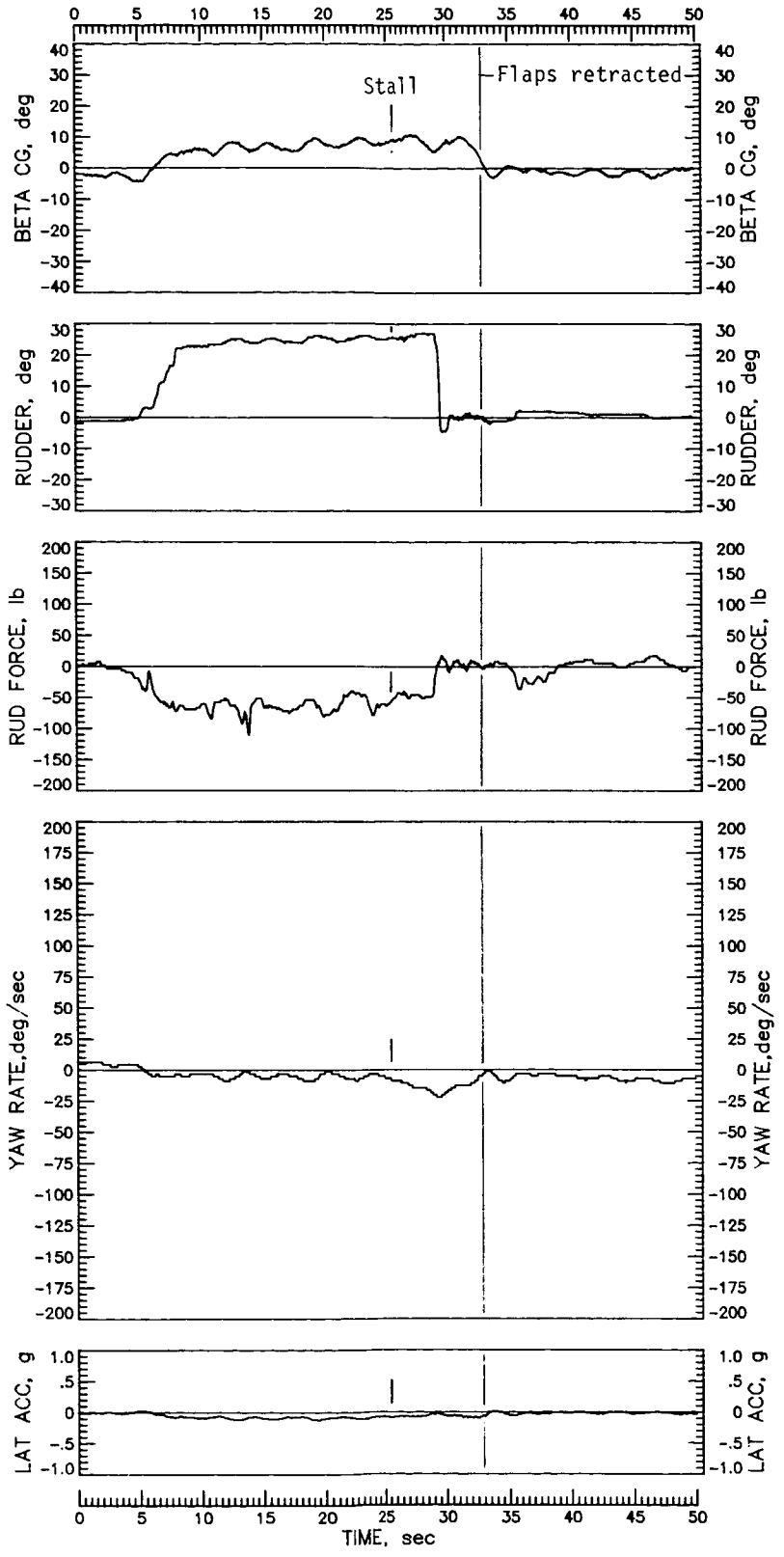

Figure 15. Continued.

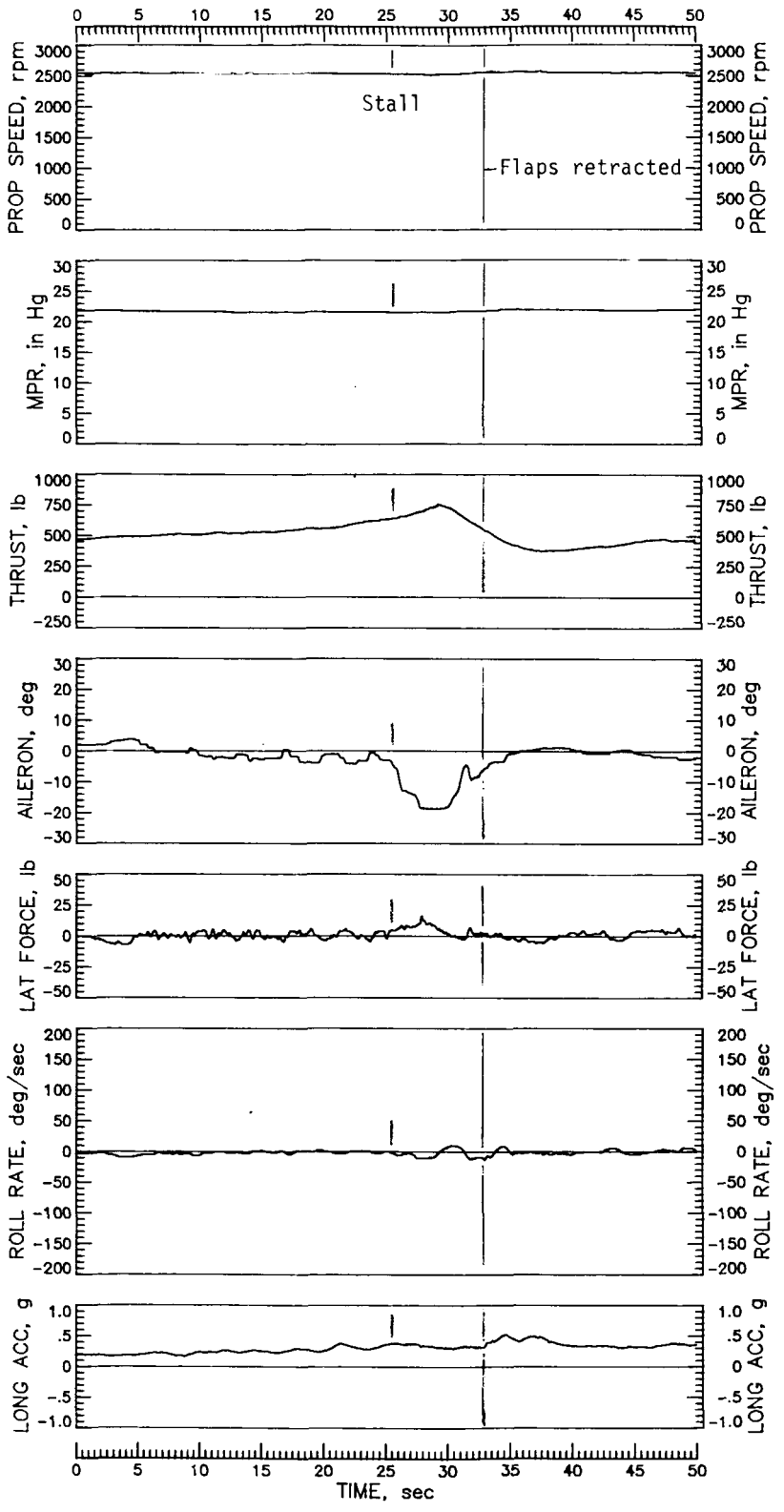

Figure 15. Continued.

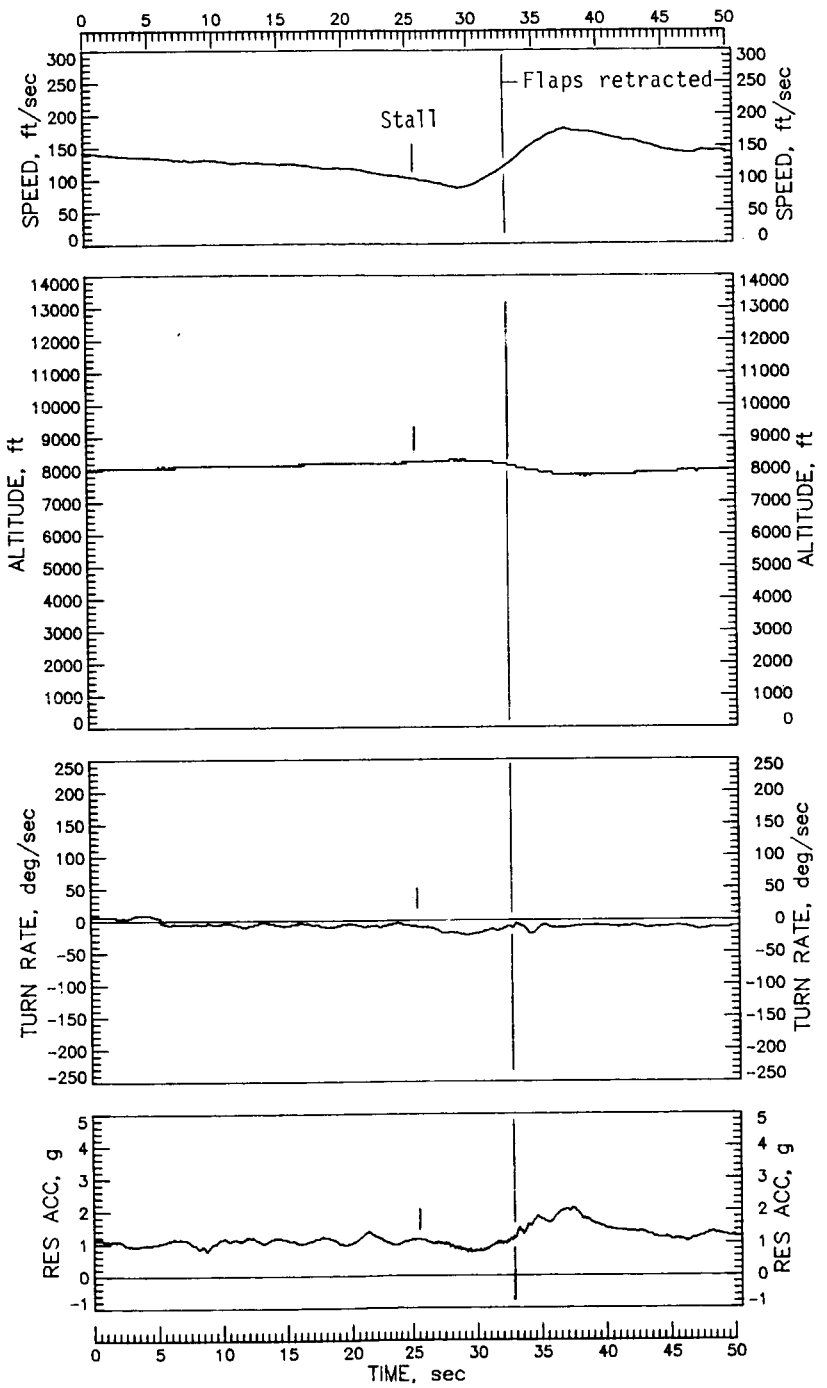

Figure 15. Concluded.

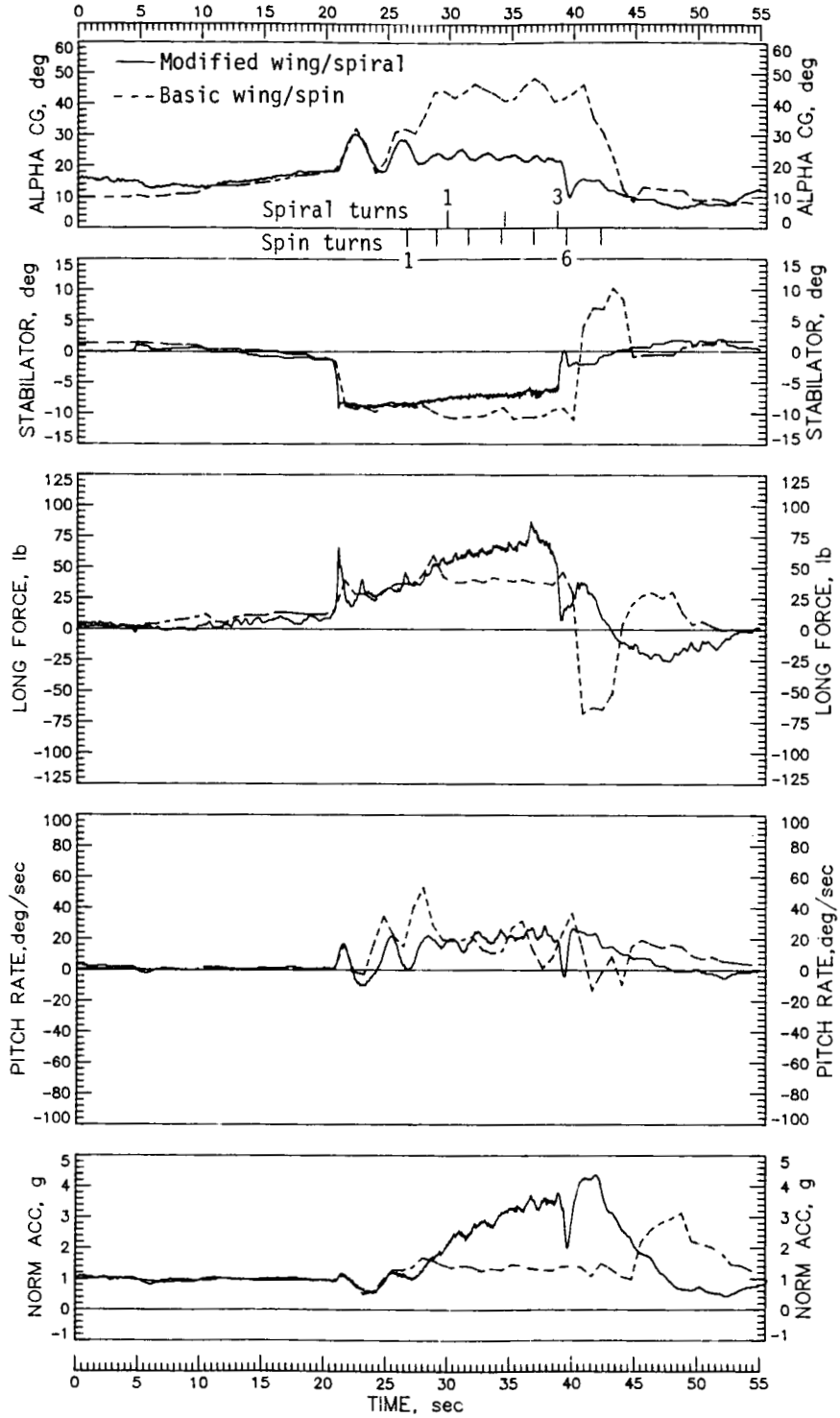

Figure 16. Comparison of response of basic and modified airplane to pro-spin control inputs at idle power, ailerons neutral, flaps and gear retracted. Test weight = 2438 lb; c.g. = $0.2777\bar{c}$.

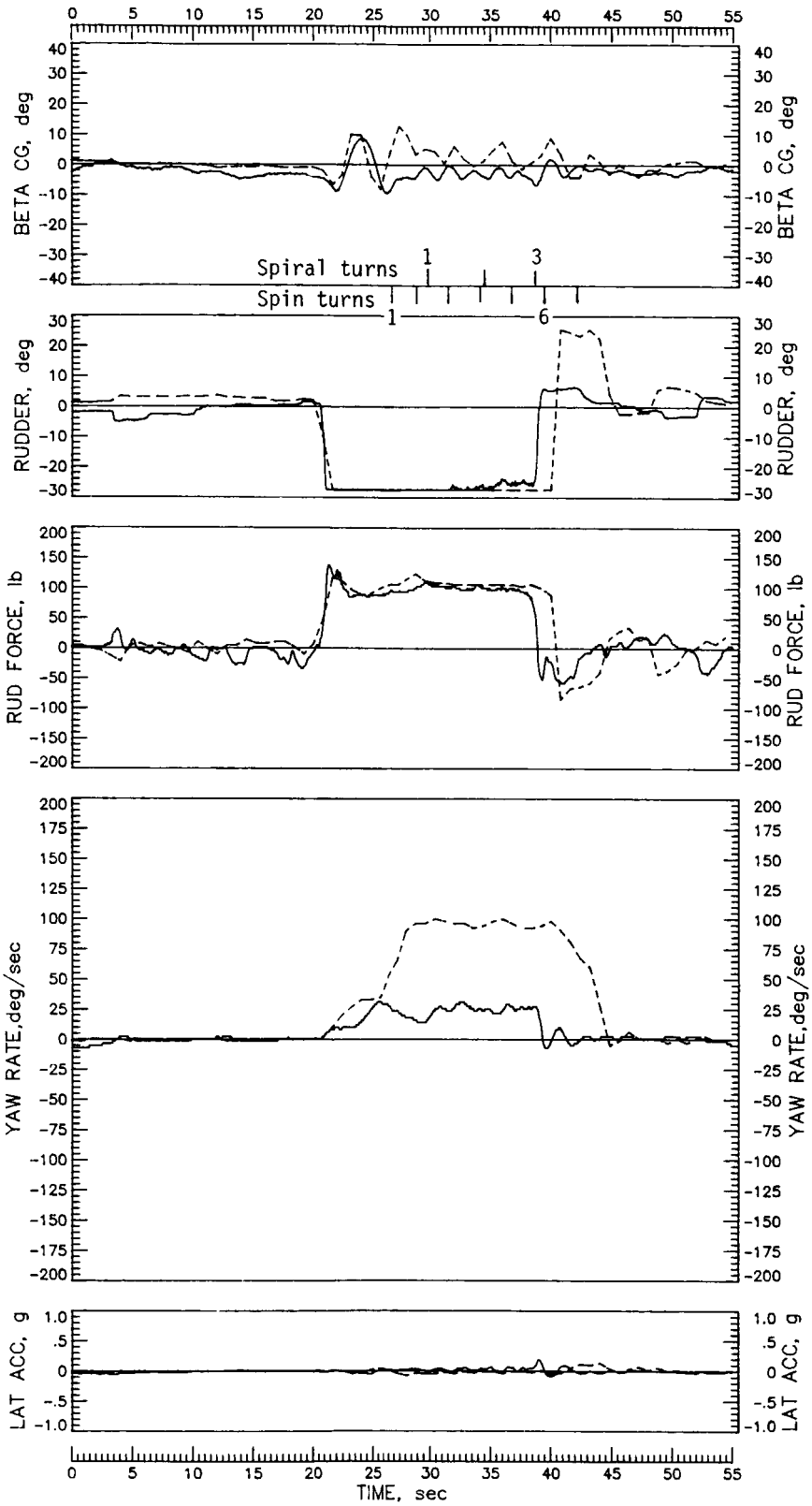

Figure 16. Continued.

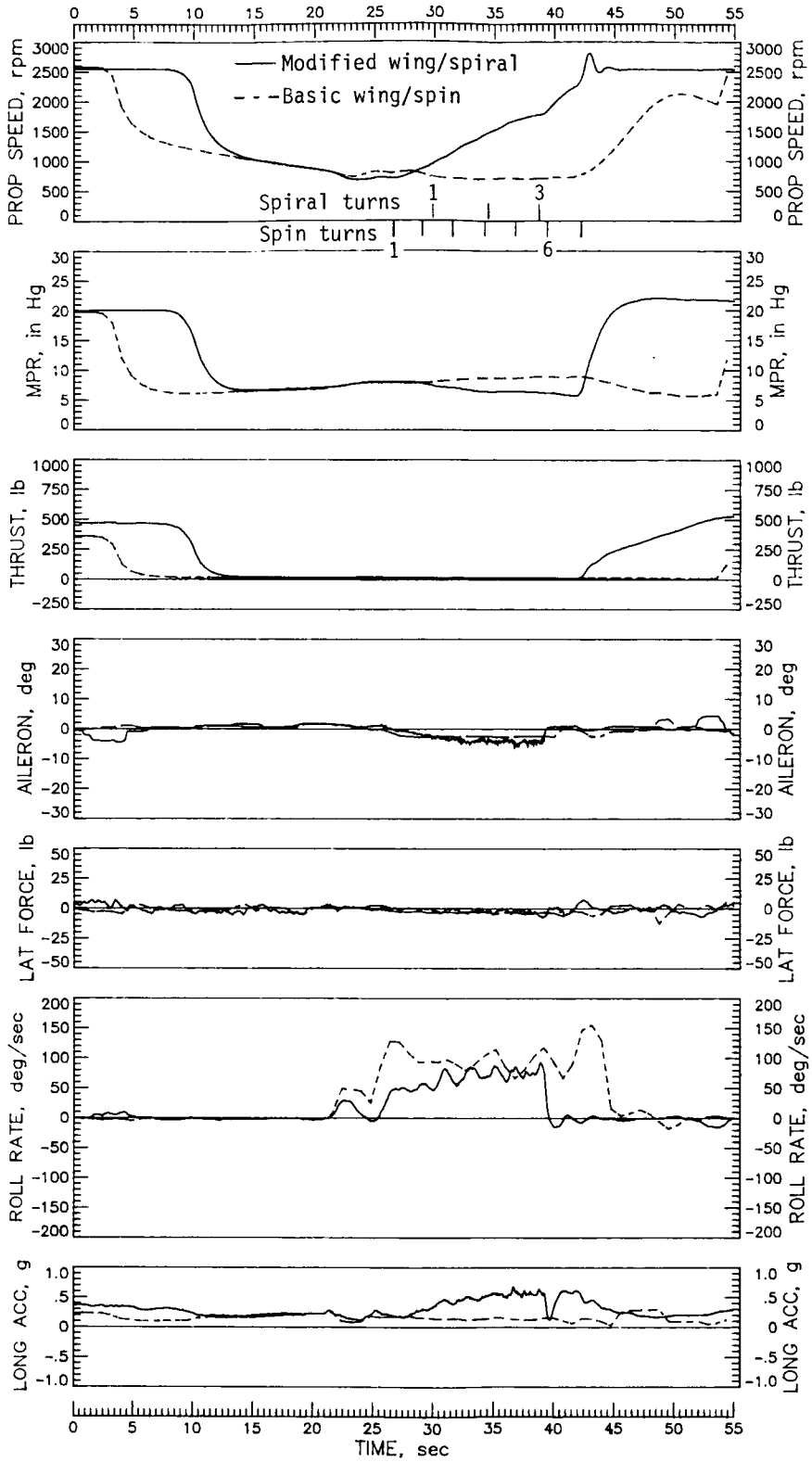

Figure 16. Continued.

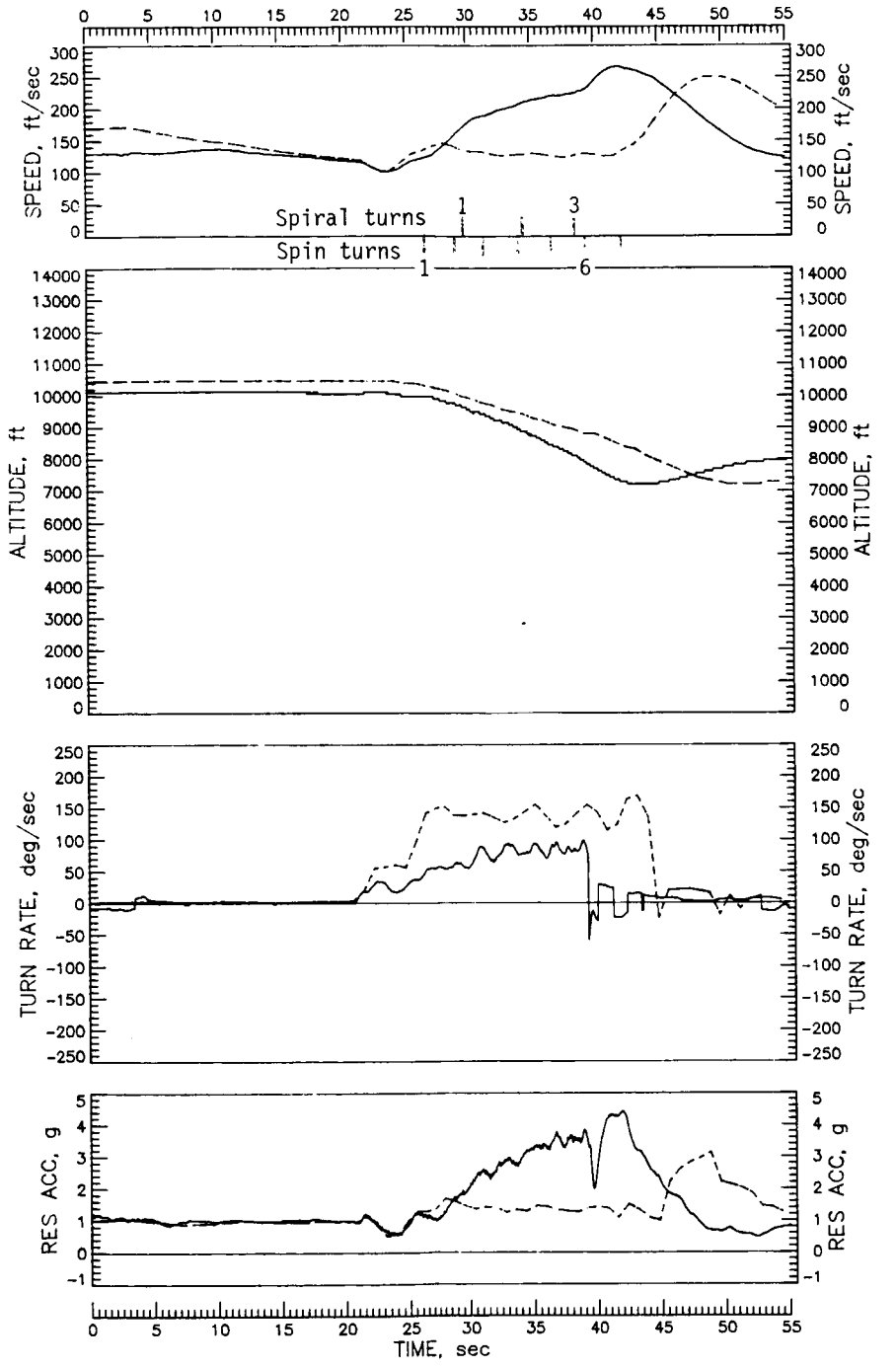

Figure 16. Concluded.

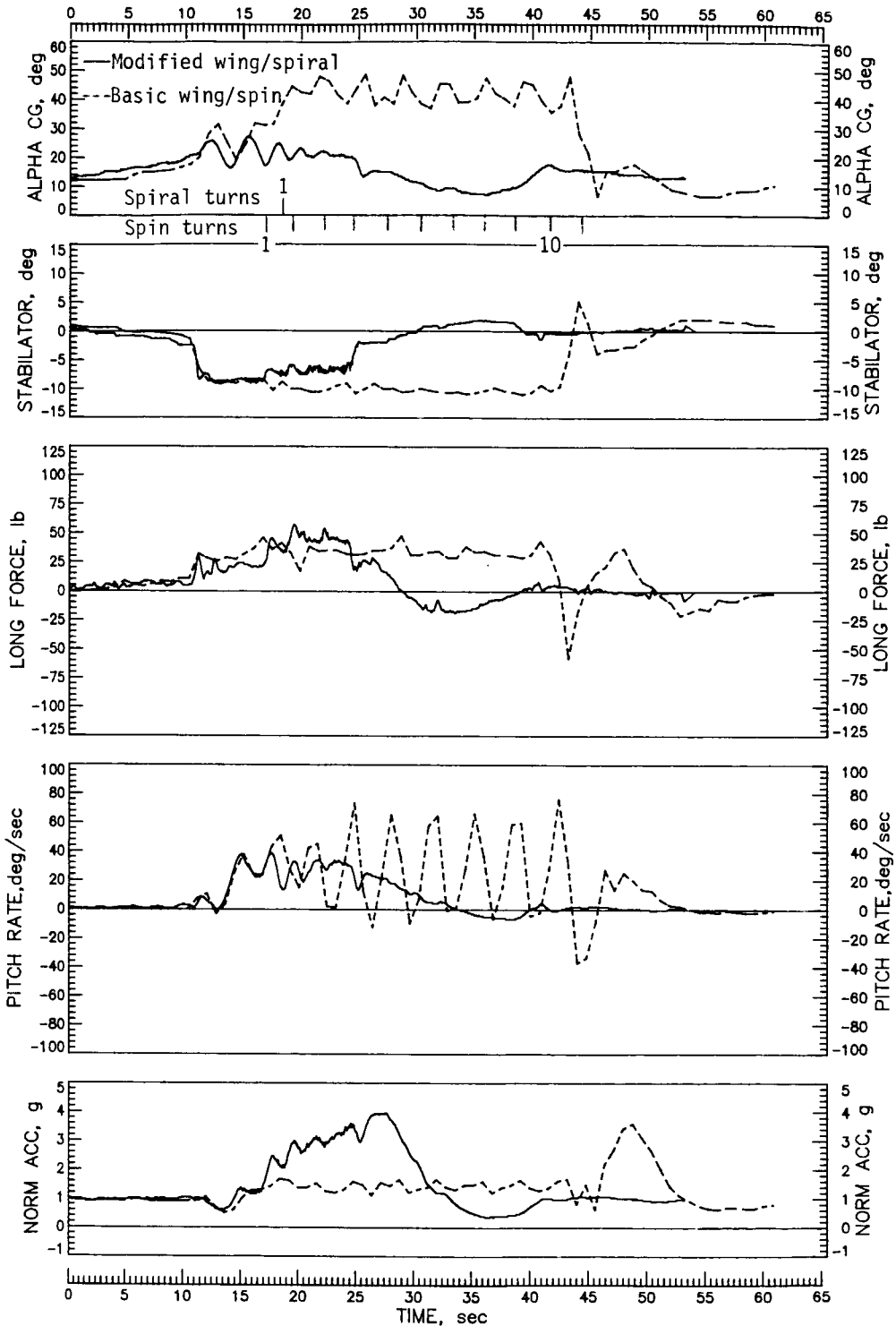

Figure 17. Comparison of response of basic and modified airplane to pro-spin control inputs at idle power, ailerons with the spin, flaps and gear retracted. Test weight = 2438 lb; c.g. = $0.2777\bar{c}$.

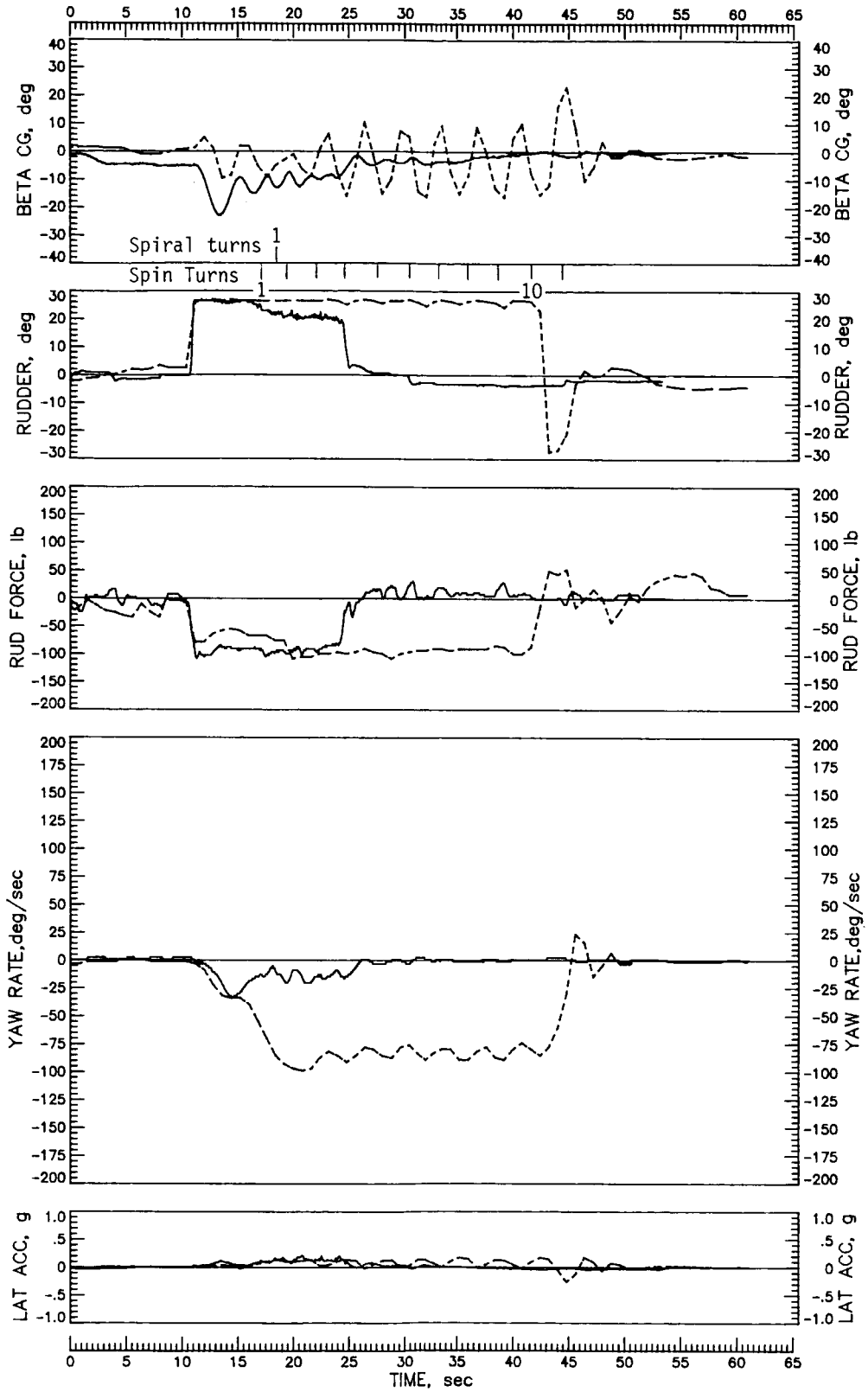

Figure 17. Continued.

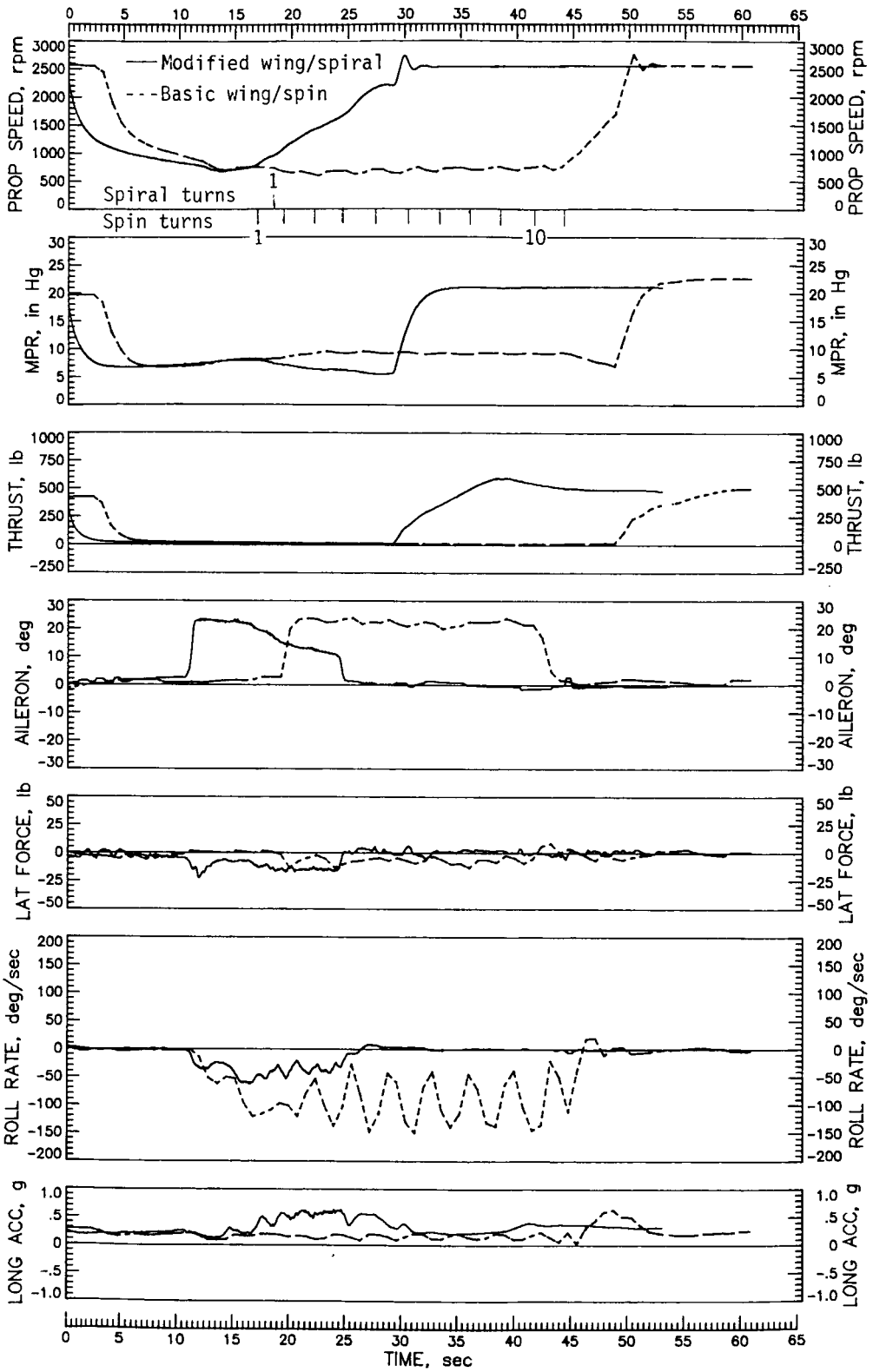

Figure 17. Continued.

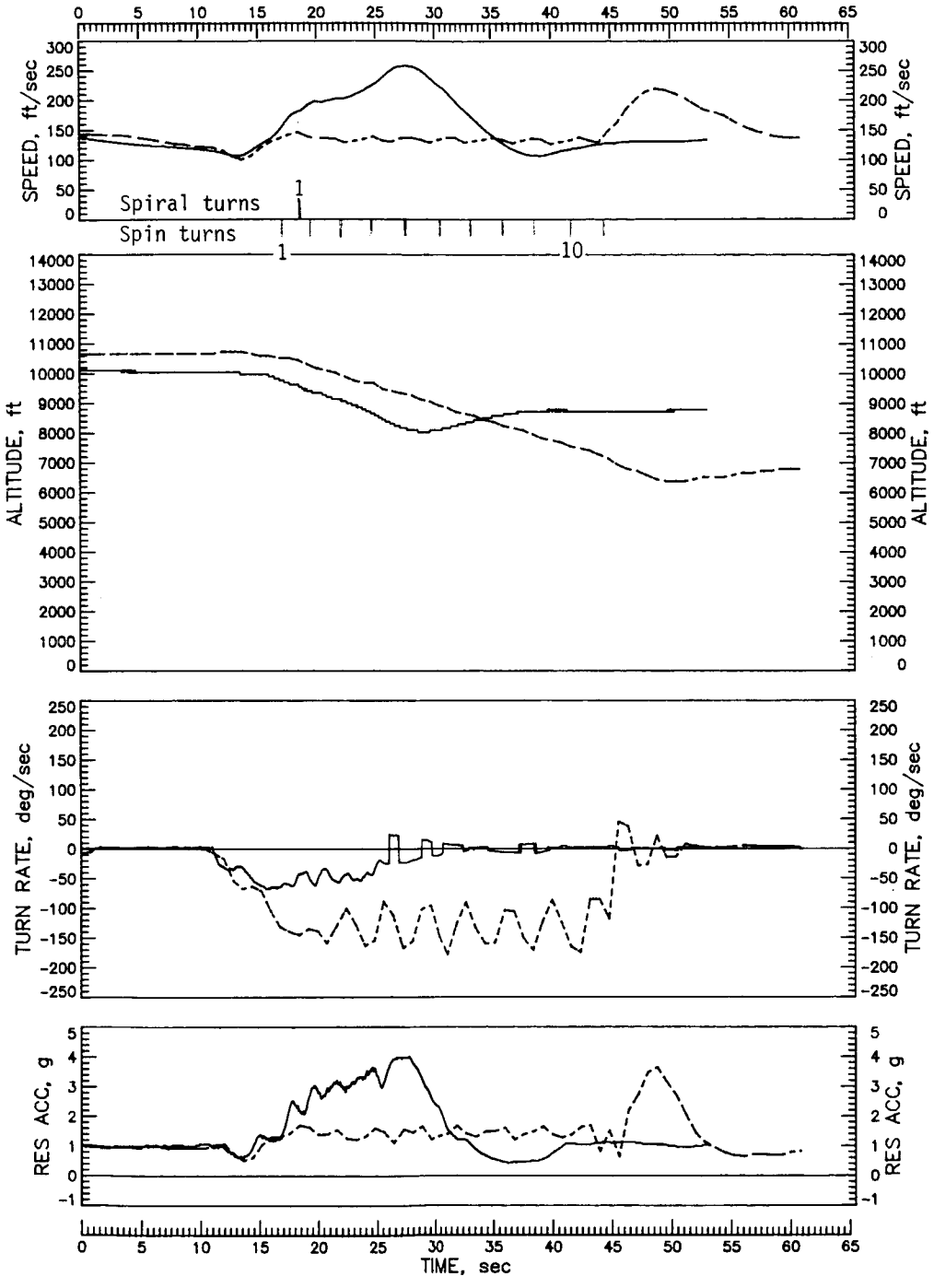

Figure 17. Concluded.

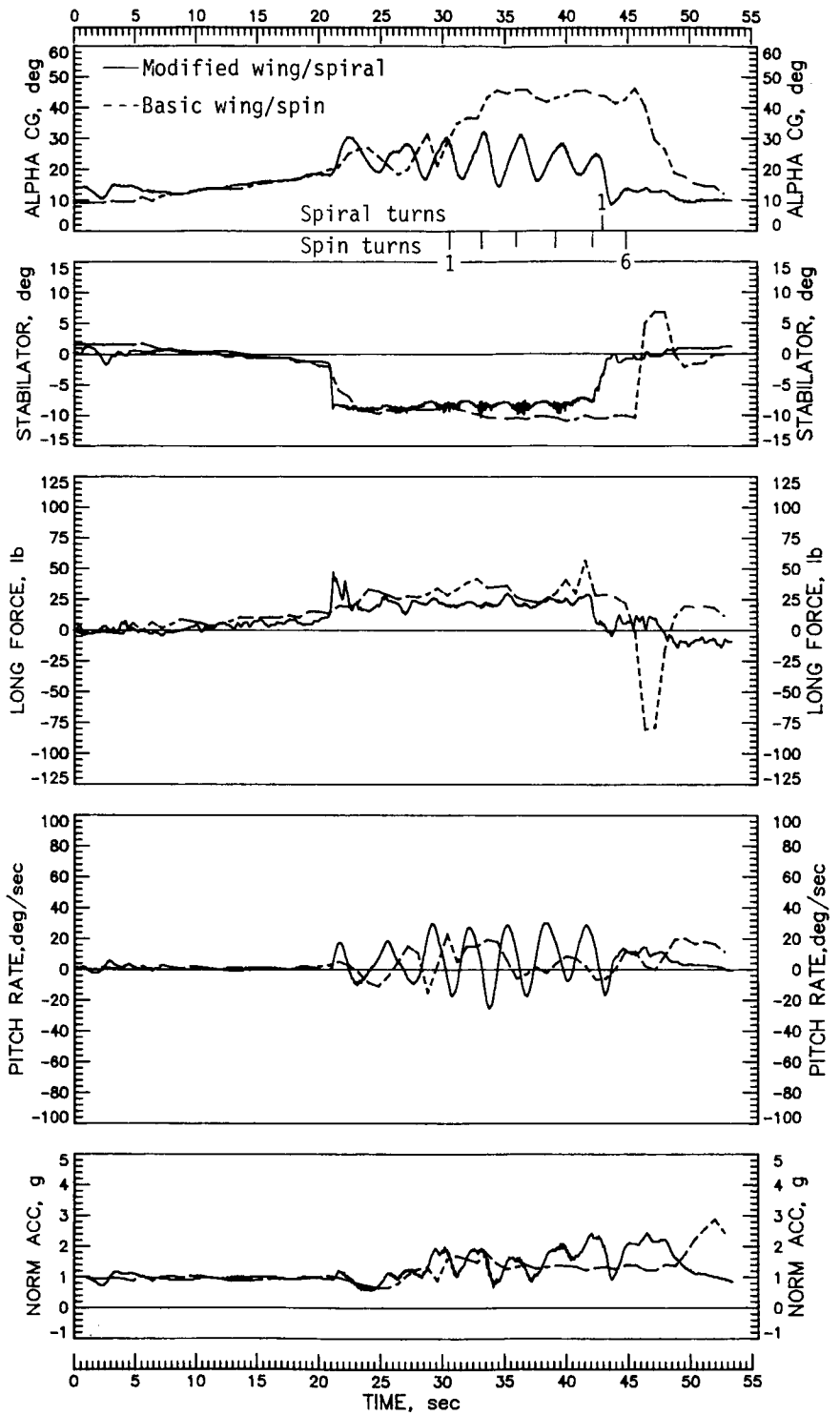

Figure 18. Comparison of response of basic and modified airplane to pro-spin control inputs at idle power, ailerons against the spin, flaps and gear retracted. Test weight = 2438 lb; c.g. = $0.2777\bar{c}$.

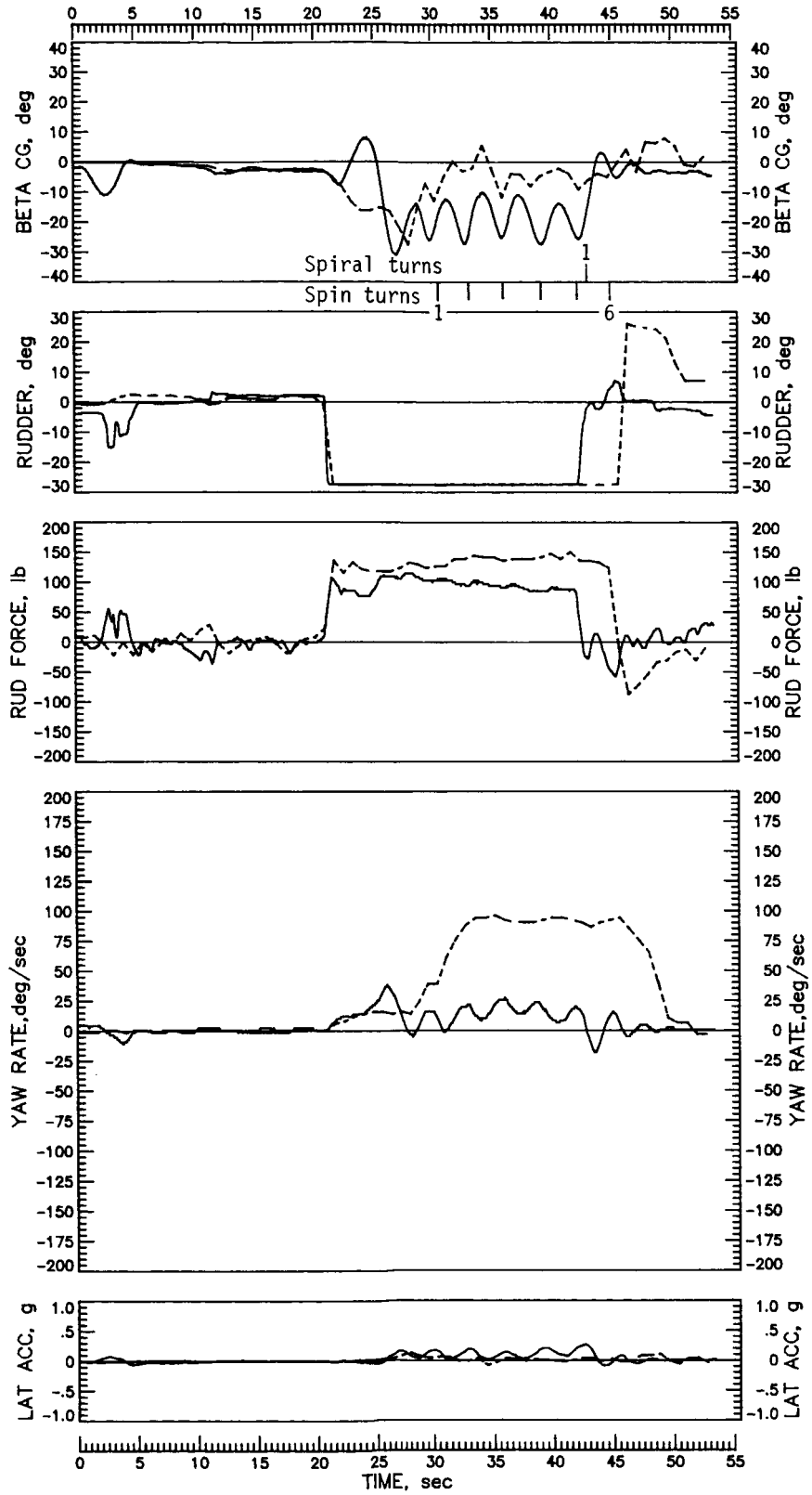

Figure 18. Continued.

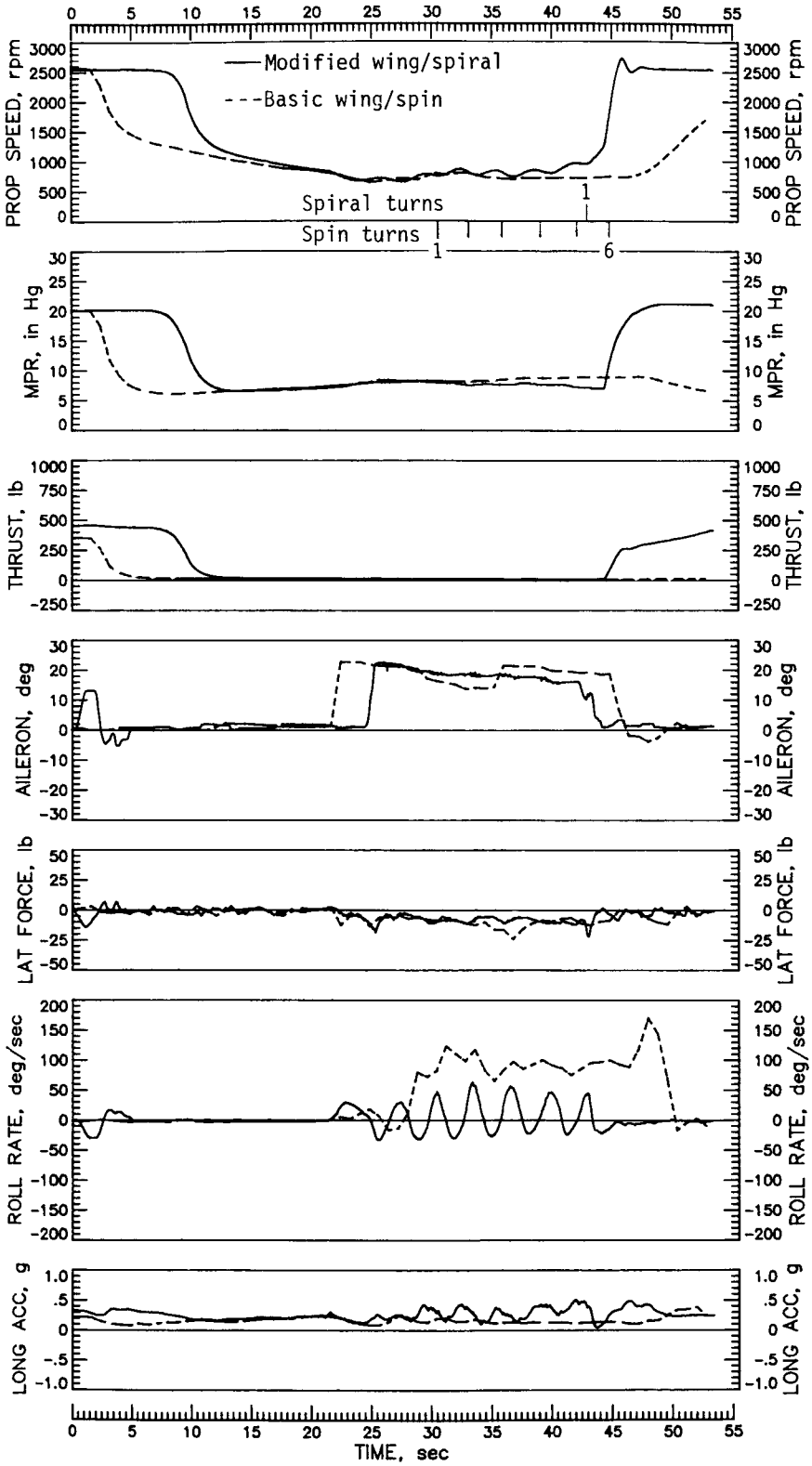

Figure 18. Continued.

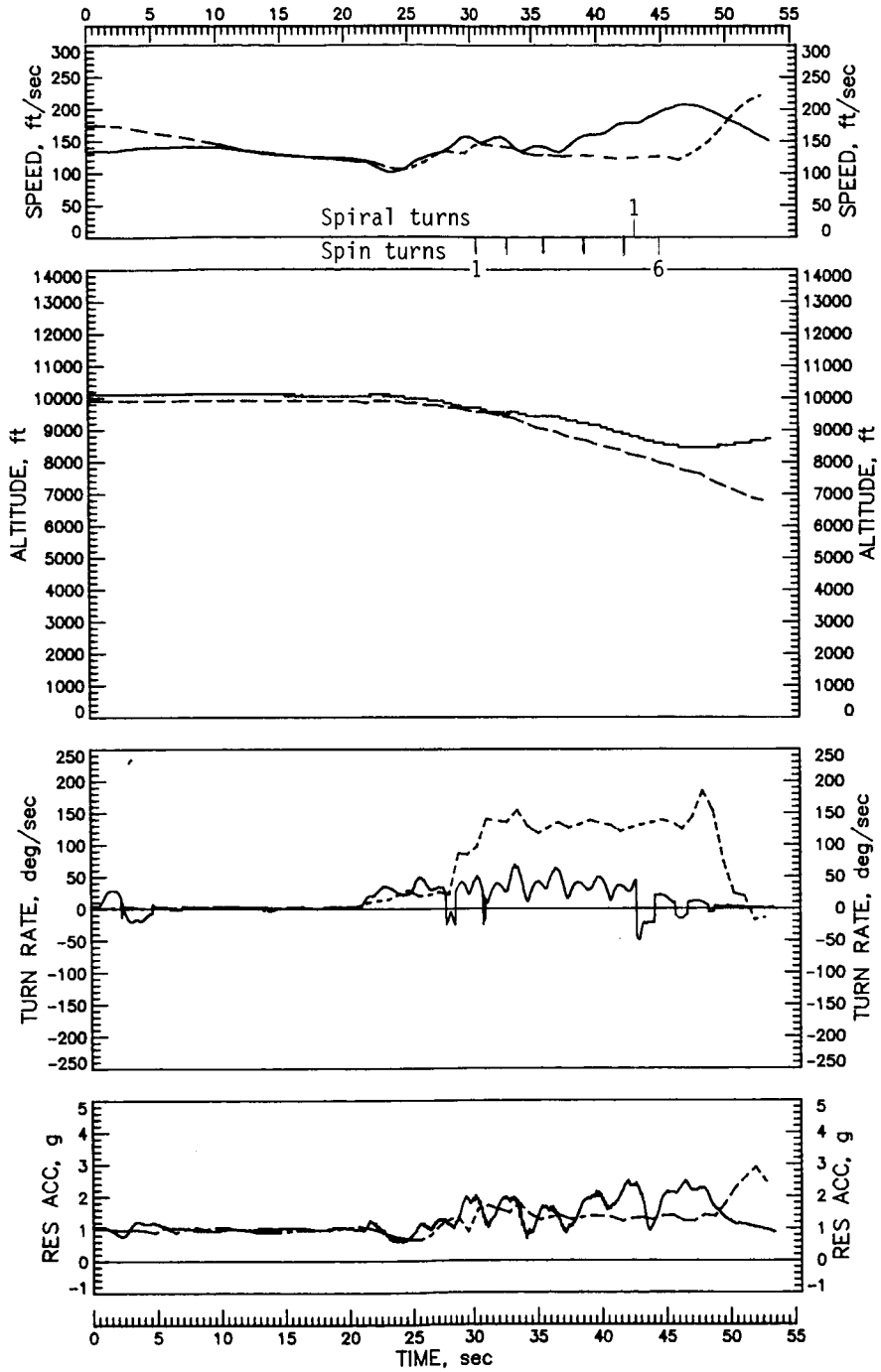

Figure 18. Concluded.

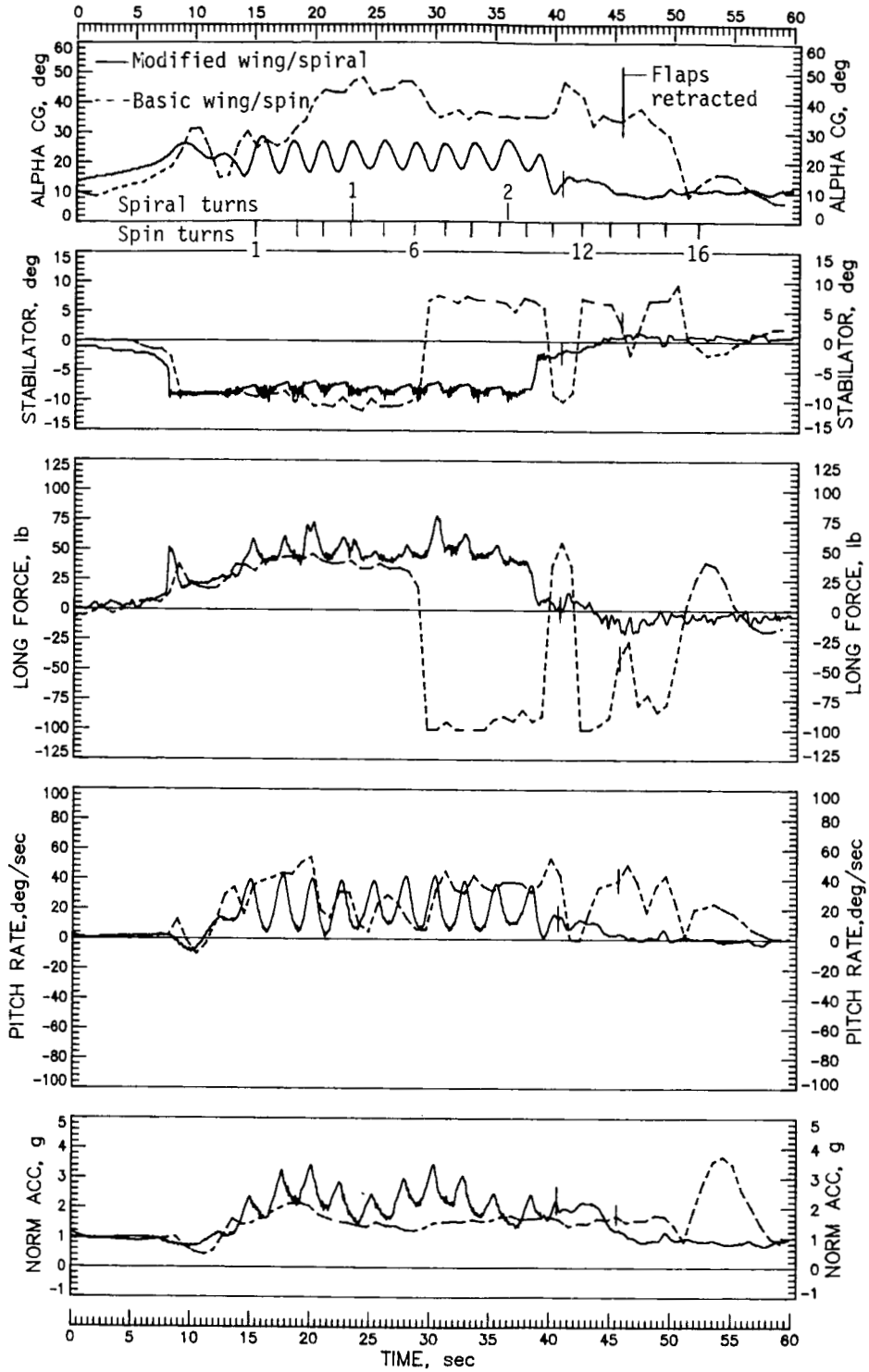

Figure 19. Comparison of response of basic and modified airplane to pro-spin control inputs at idle power, ailerons neutral, flaps deflected 40°, gear retracted. Test weight = 2438 lb; c.g. = 0.2777$\bar{c}$.

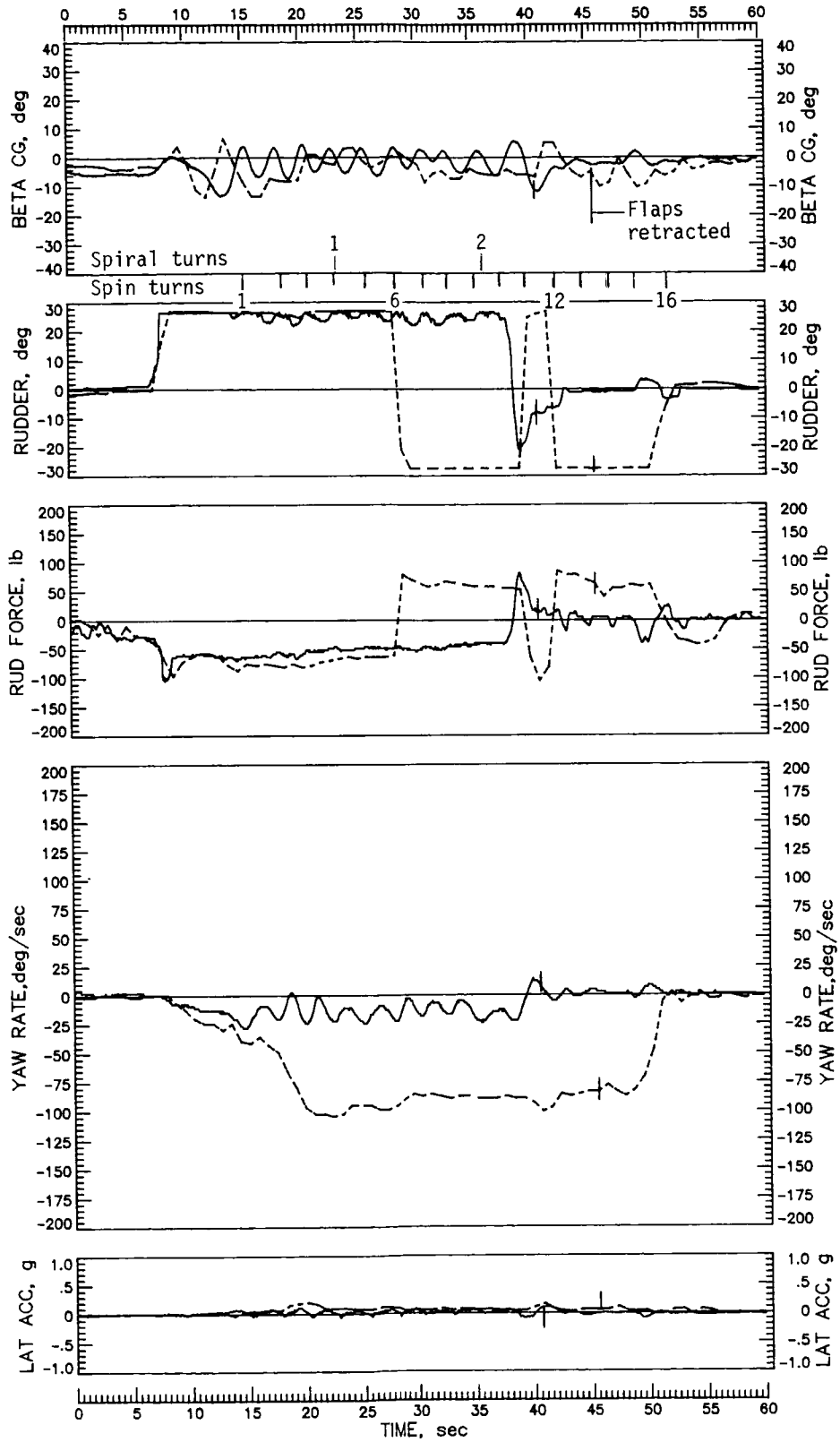

Figure 19. Continued.

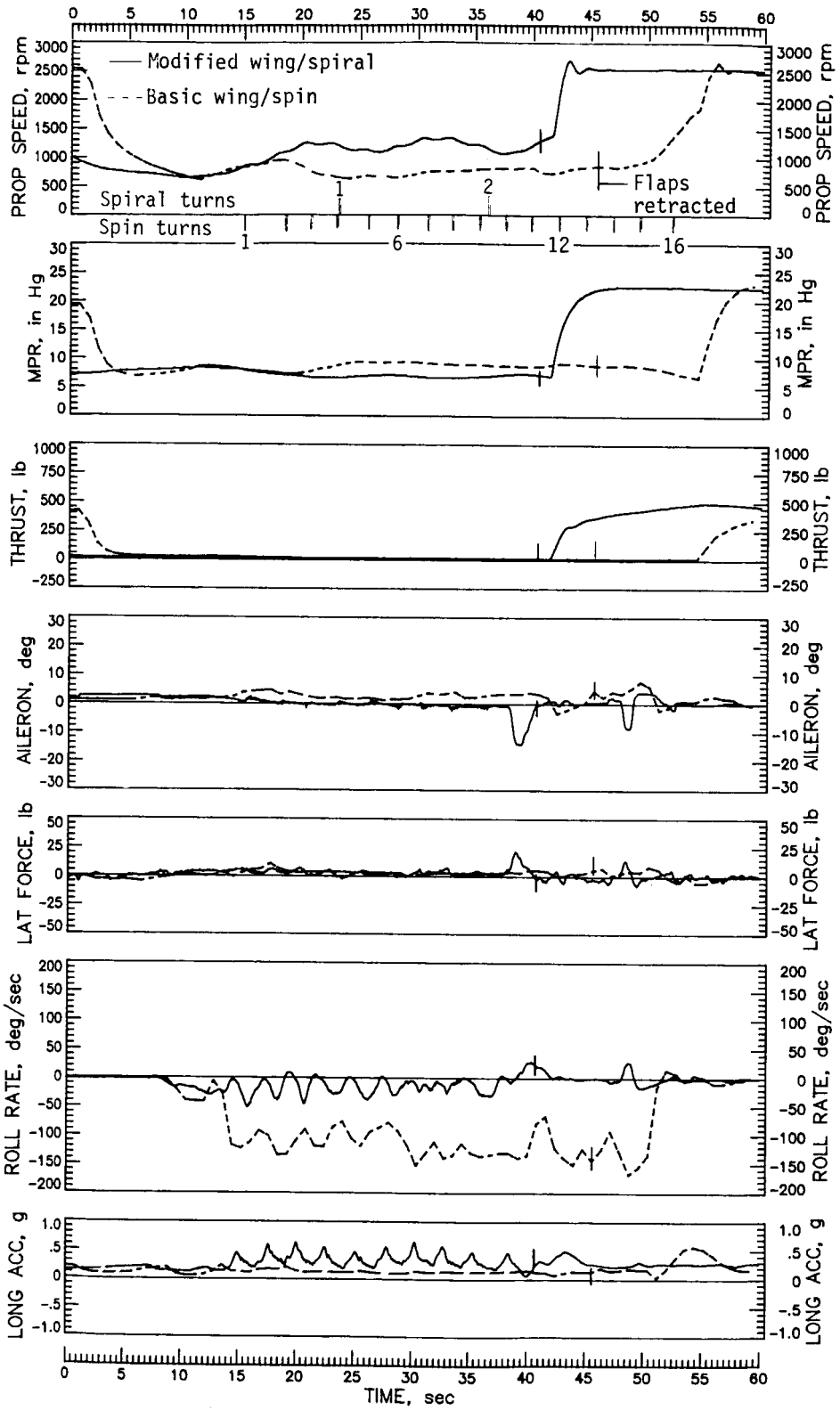

Figure 19. Continued.

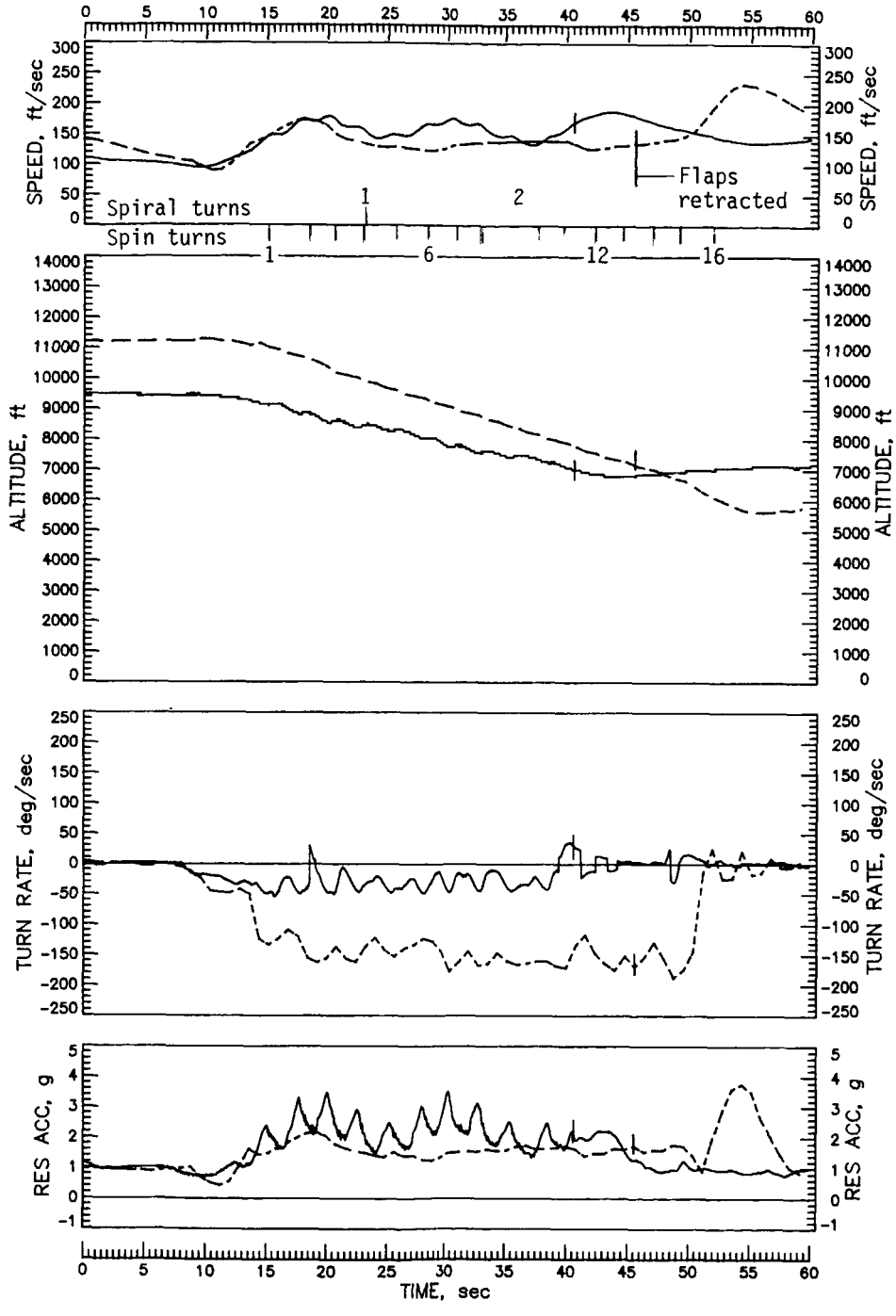

Figure 19. Concluded.

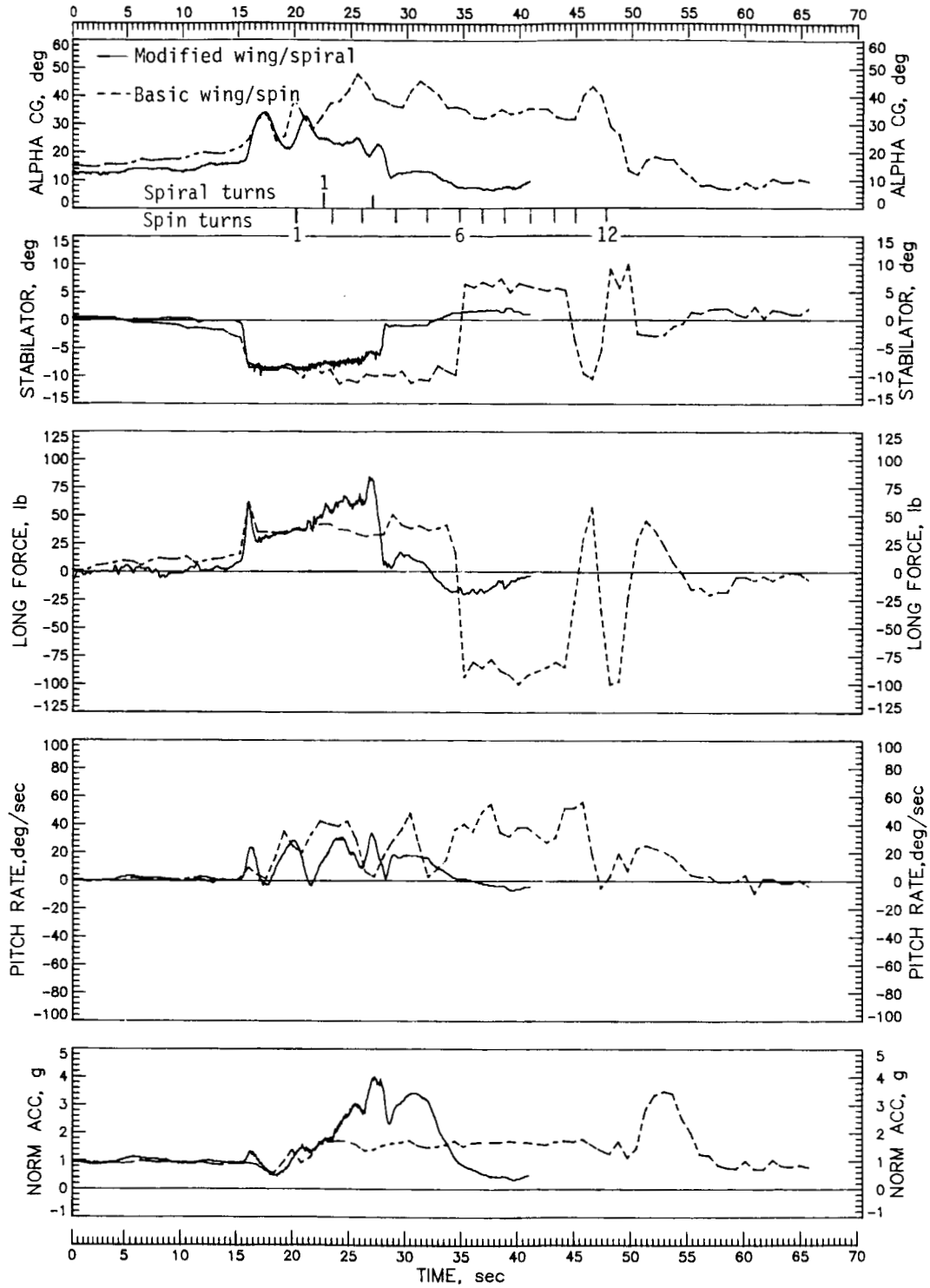

Figure 20. Comparison of response of basic and modified airplane to pro-spin control inputs at maximum power, ailerons neutral, flaps and gear retracted. Test weight = 2438 lb; c.g. = $0.2777\bar{c}$.

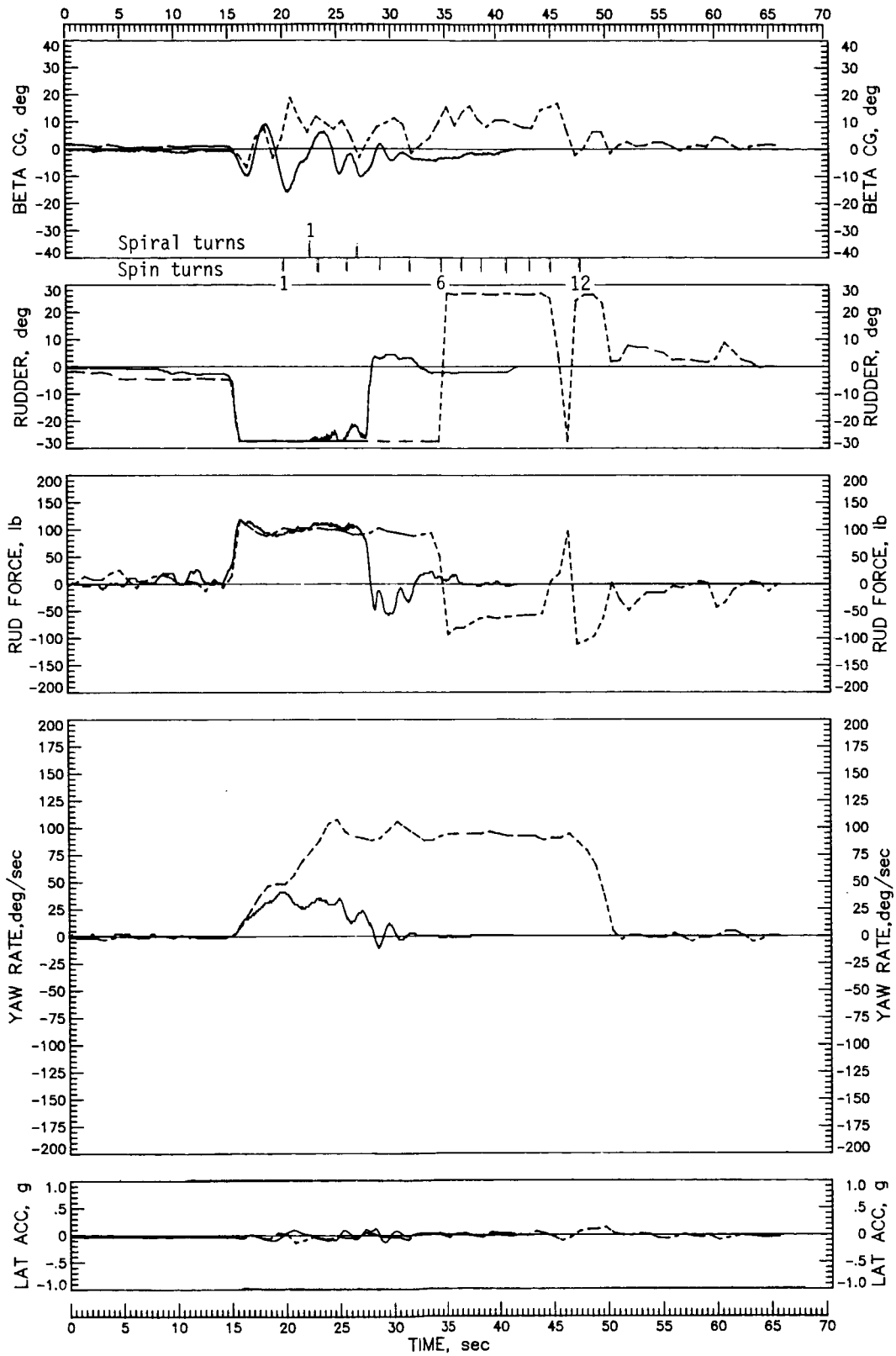

Figure 20. Continued.

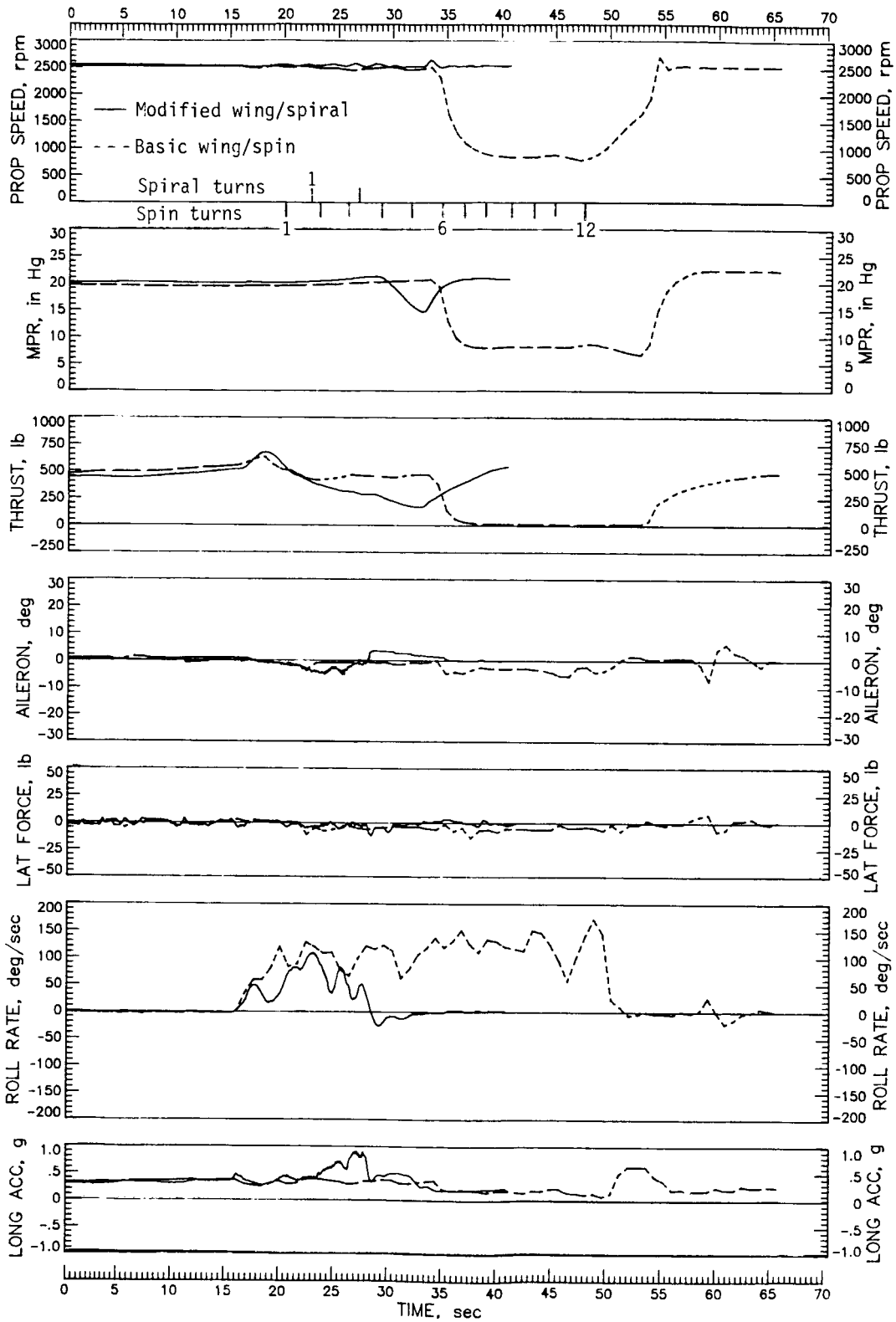

Figure 20. Continued.

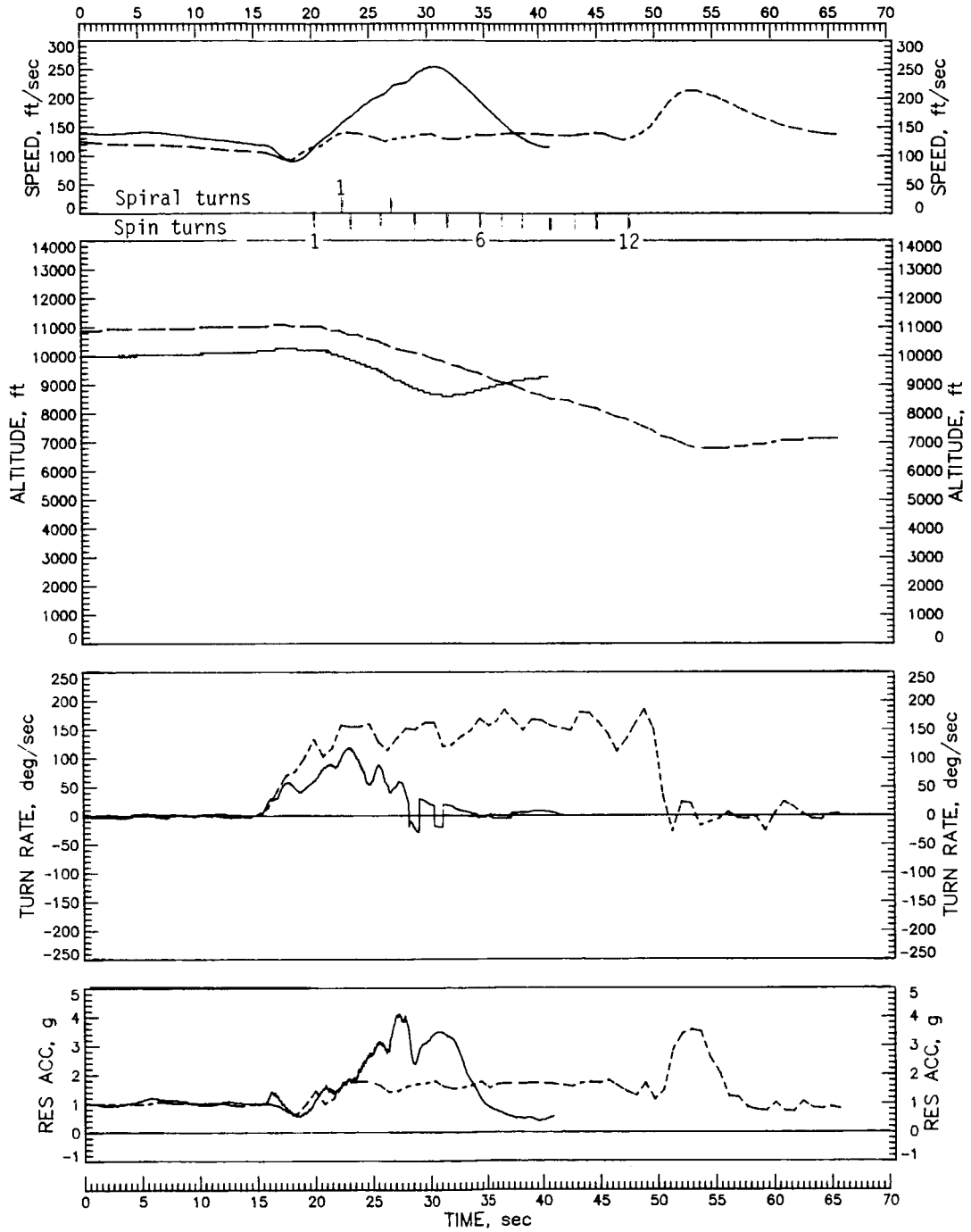

Figure 20. Concluded.

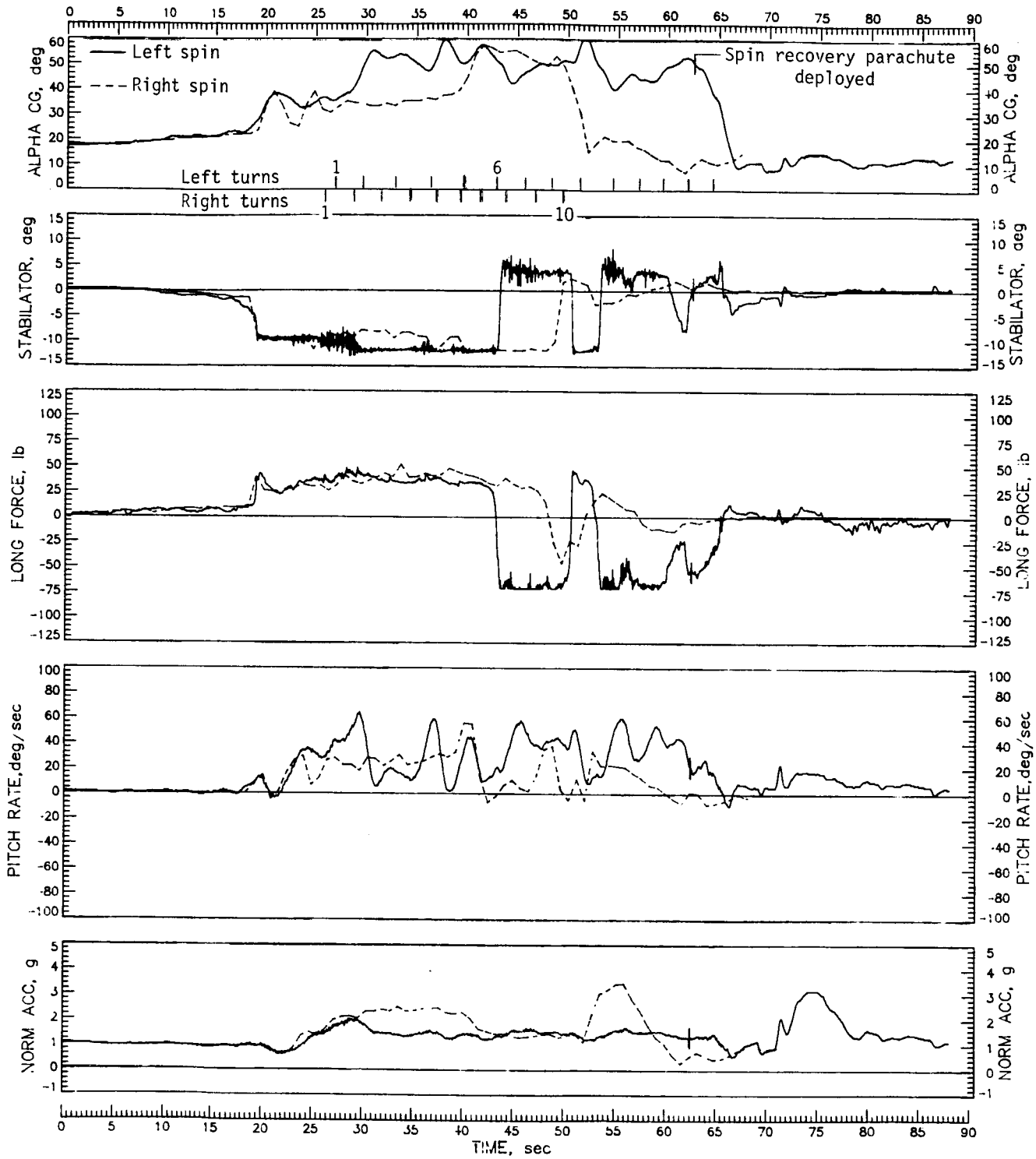

Figure 21. Right and left spins of modified airplane at maximum power entered from 1g, wings-level flight, ailerons neutral, flaps and gear retracted. Test weight = 2690 lb; c.g. = 0.3207$\bar{c}$.

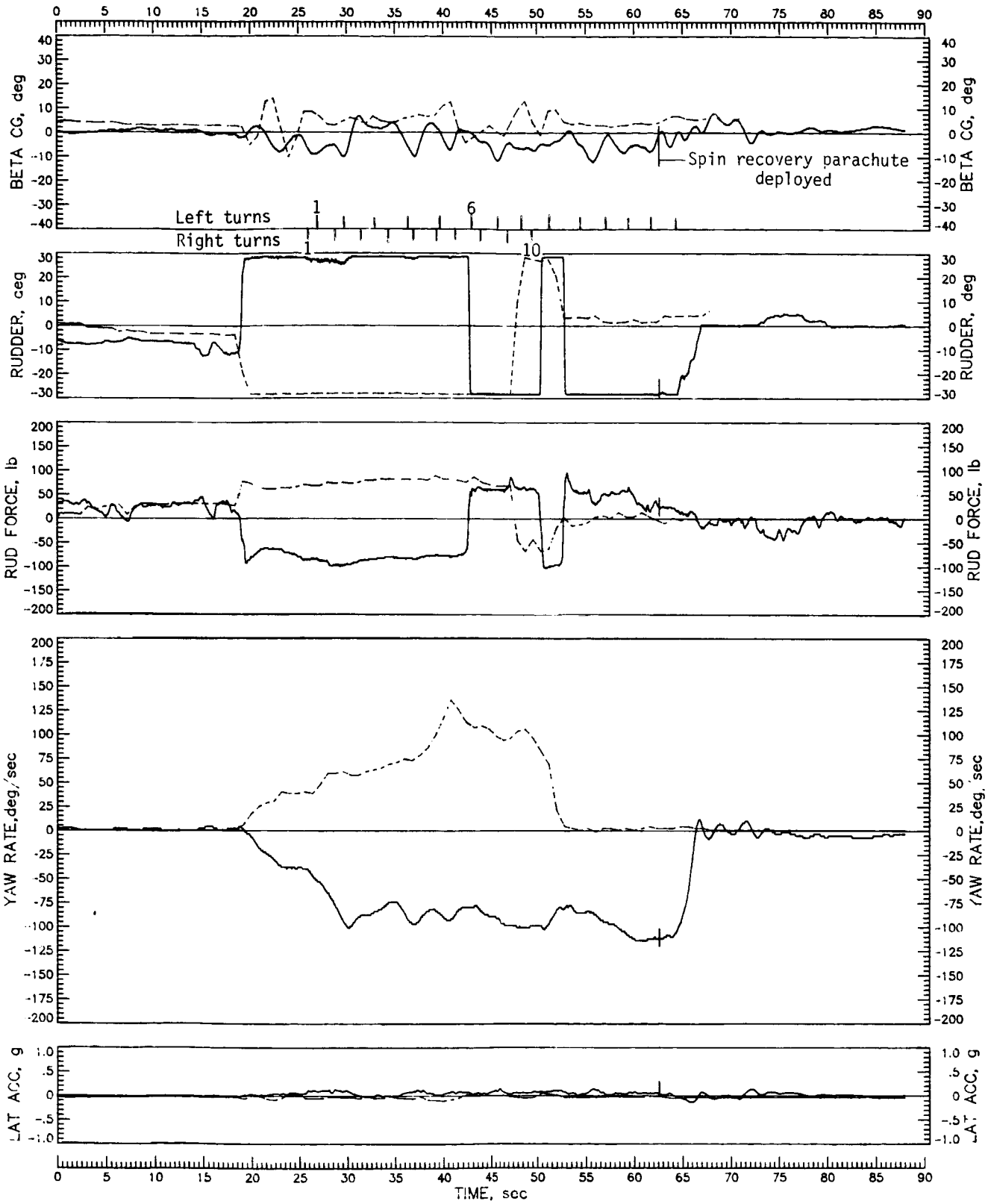

Figure 21. Continued.

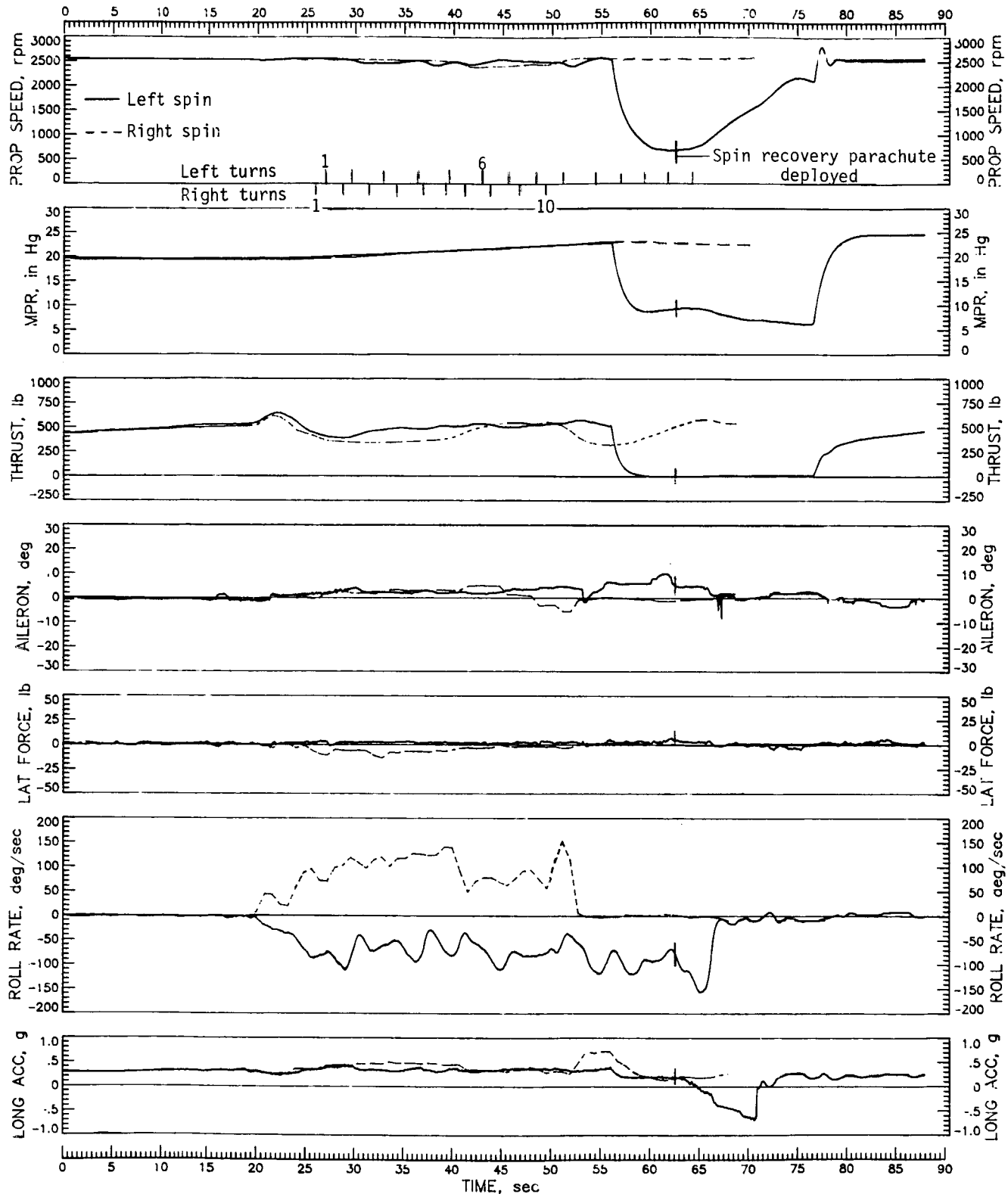

Figure 21. Continued.

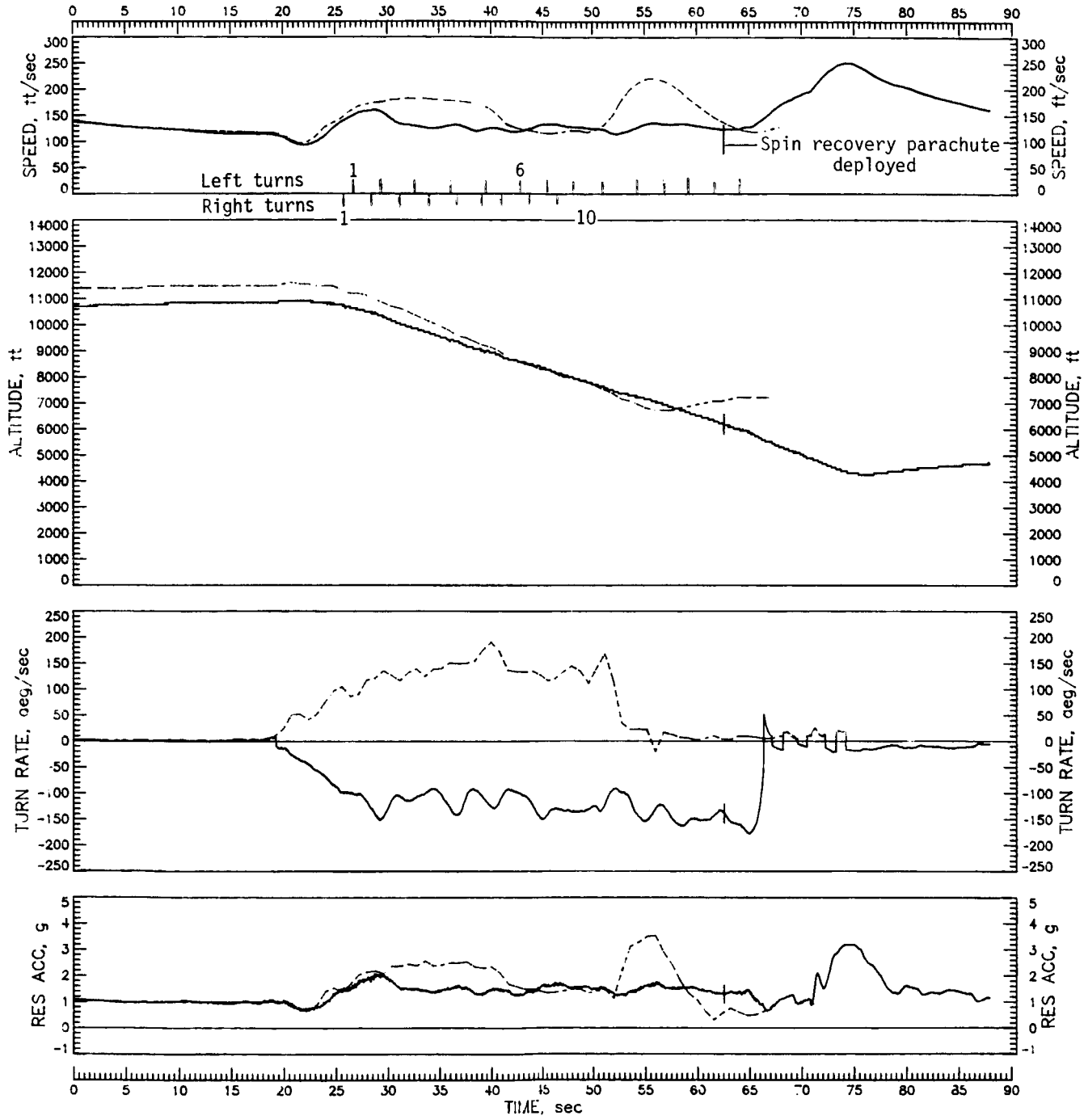

Figure 21. Concluded.

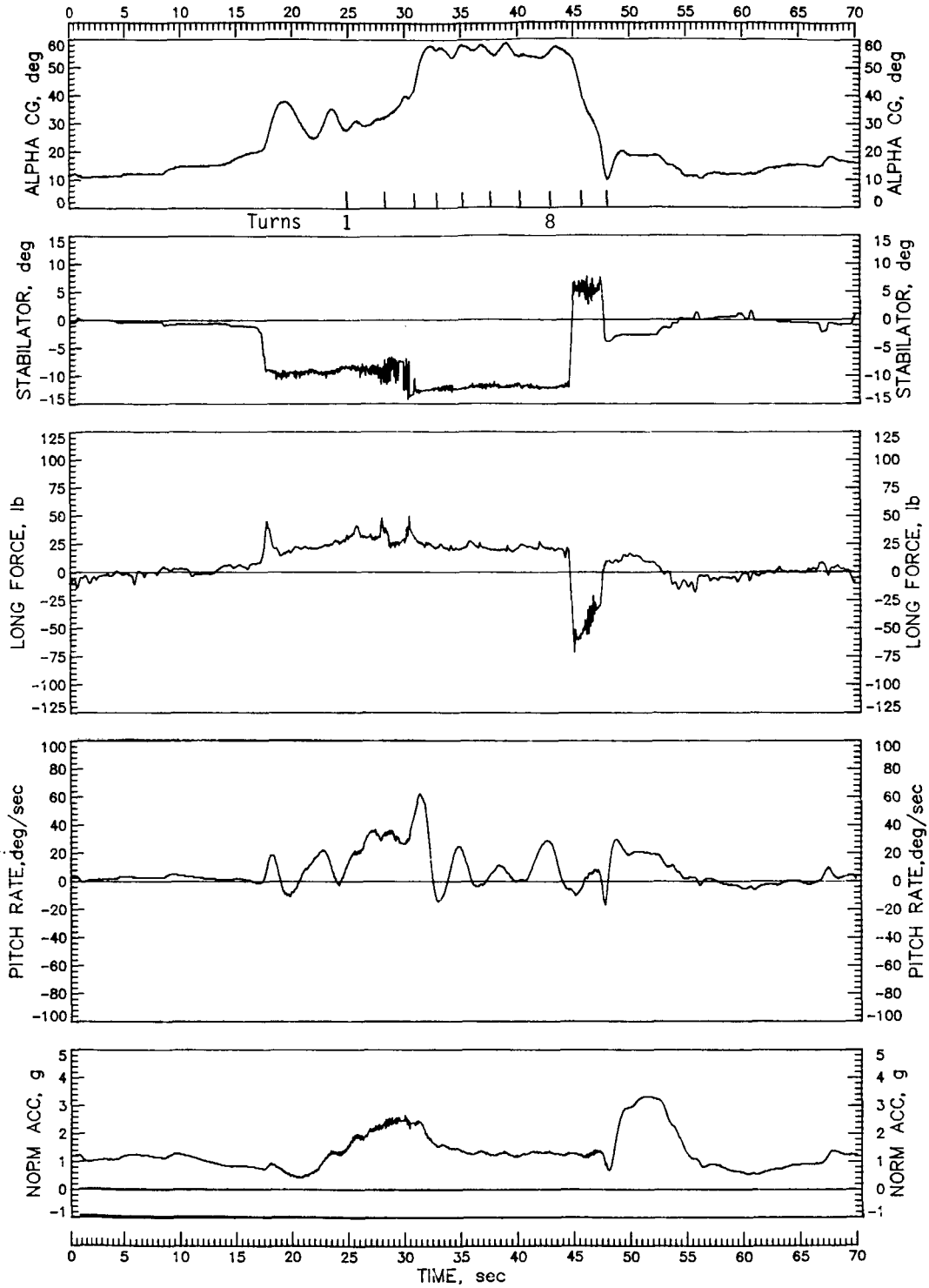

Figure 22. Right spin of modified airplane at maximum power entered from 1g, wings-level flight, ailerons neutral, flaps and gear retracted. Test weight = 2829 lb; c.g. = 0.2787$\bar{c}$.

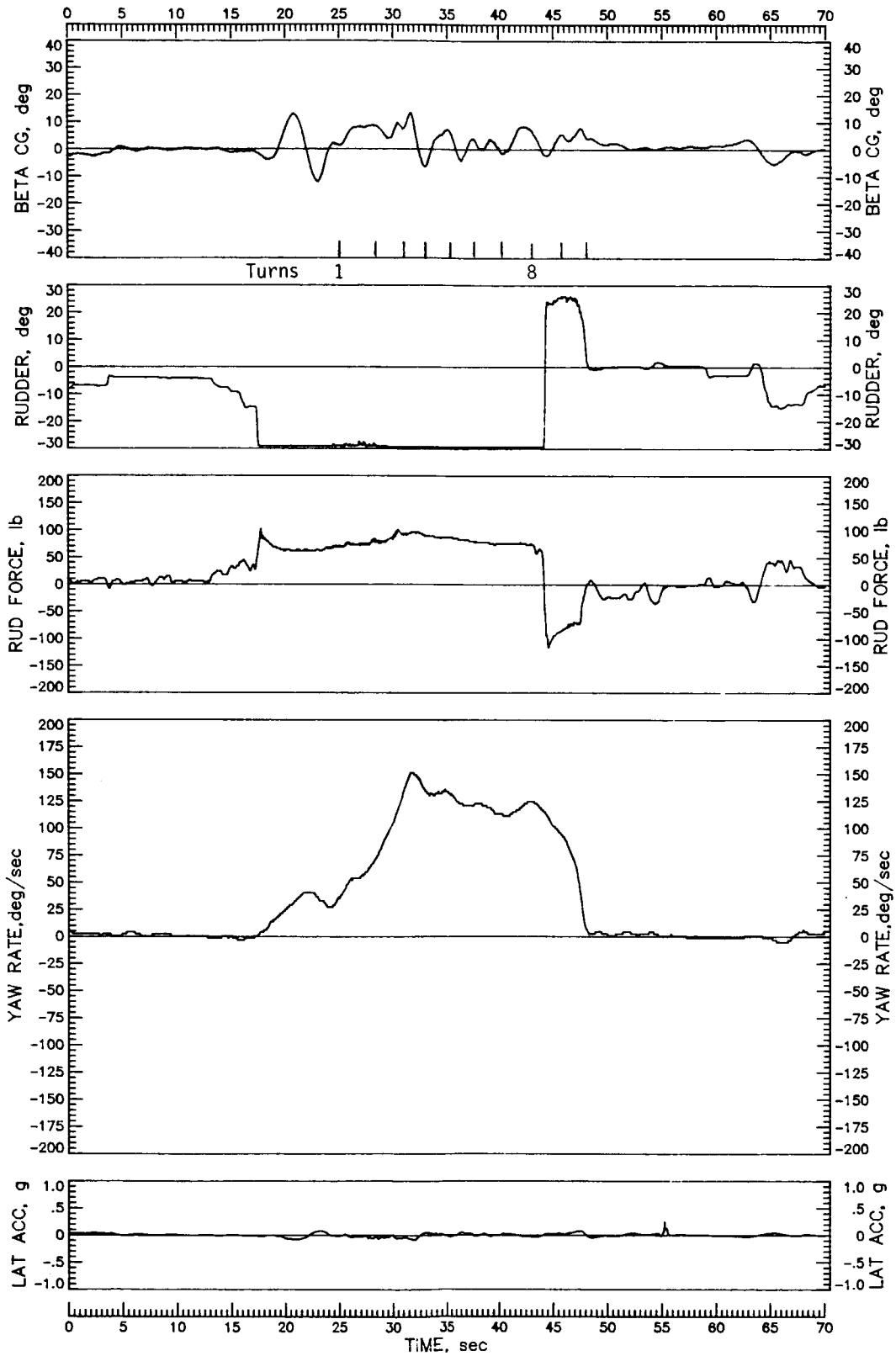

Figure 22. Continued.

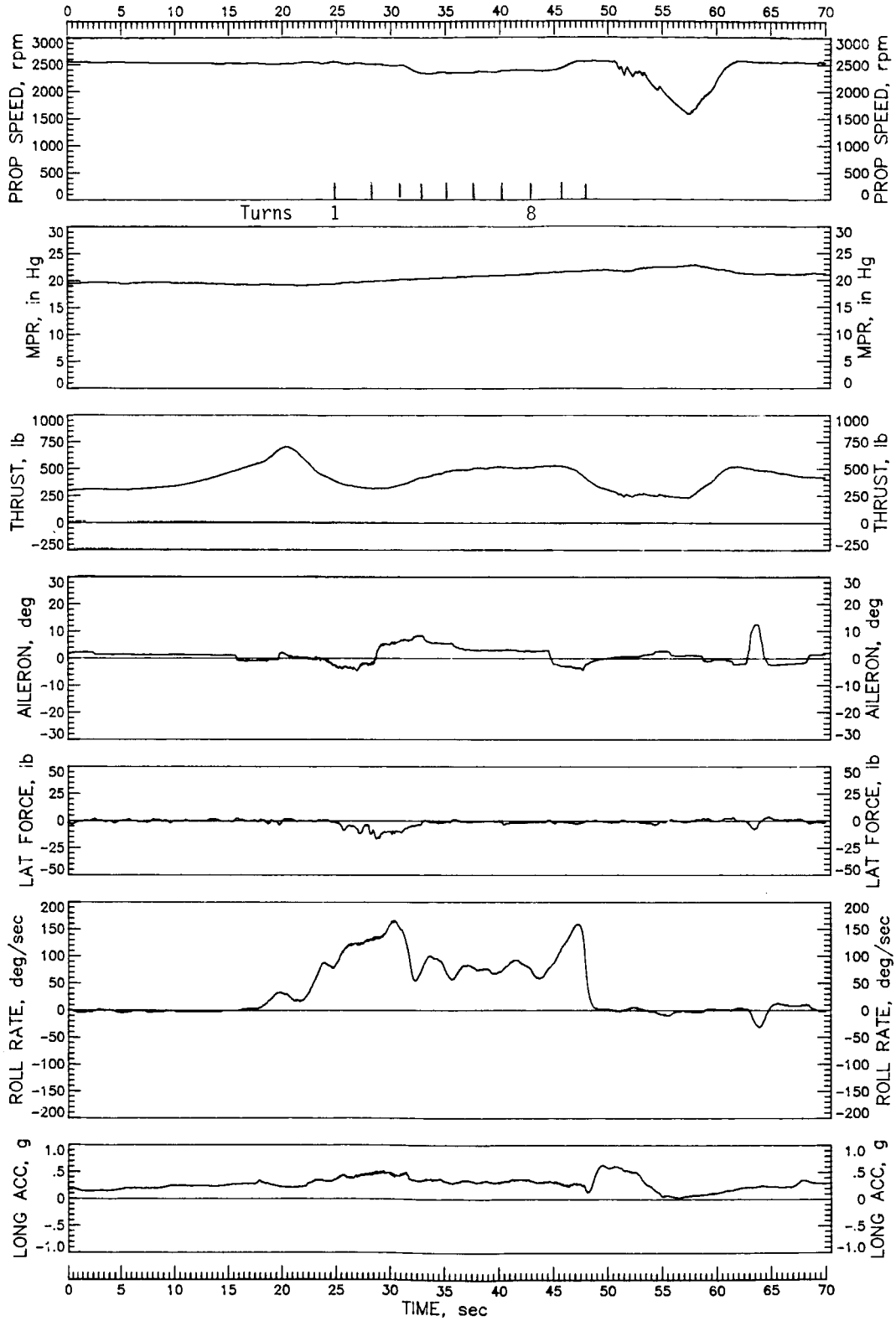

Figure 22. Continued.

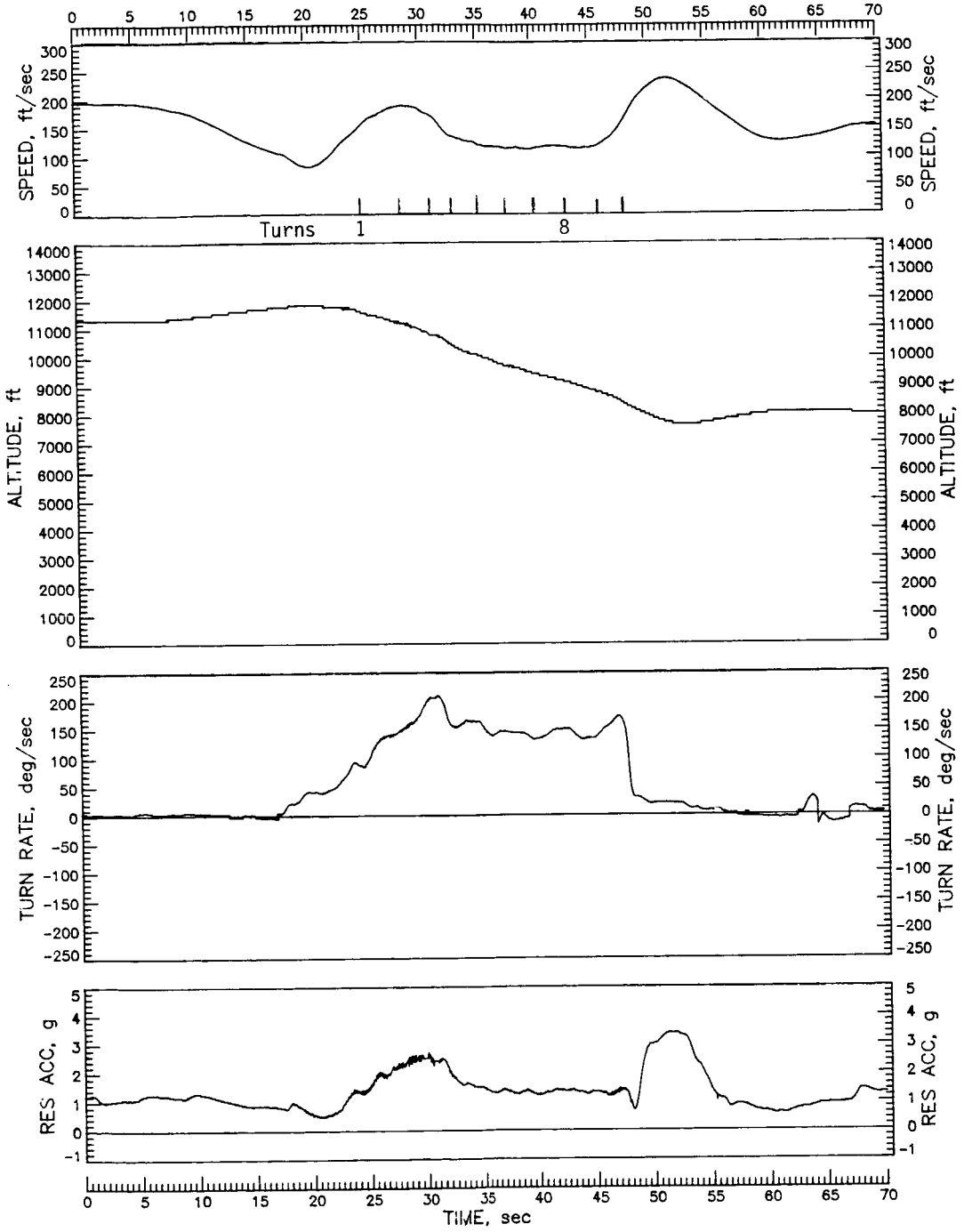

Figure 22. Concluded.

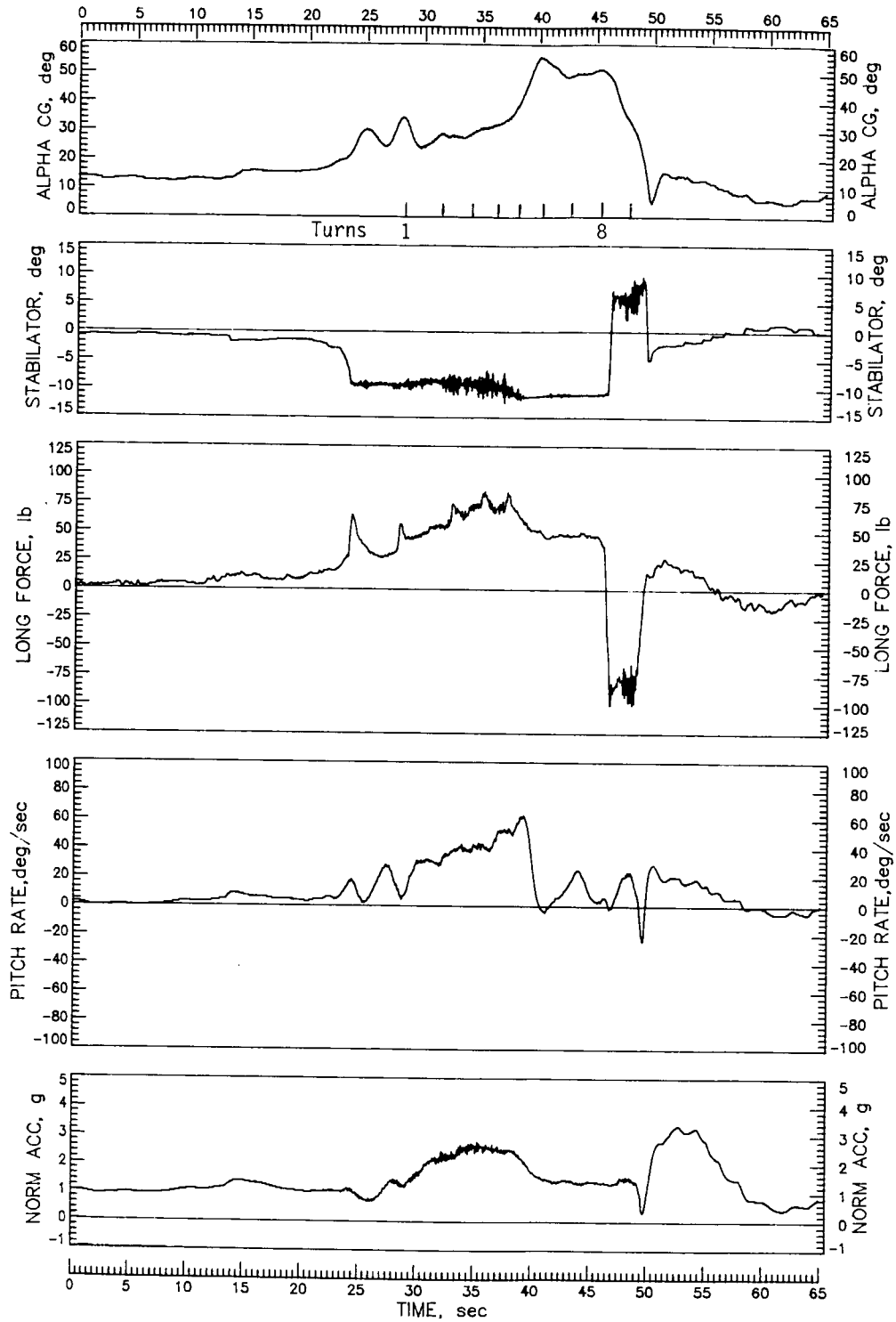

Figure 23. Right spin of modified airplane at maximum power entered from 30° banked turn, ailerons neutral, flaps and gear retracted. Test weight = 2670 lb; c.g. = $0.2842\bar{c}$.

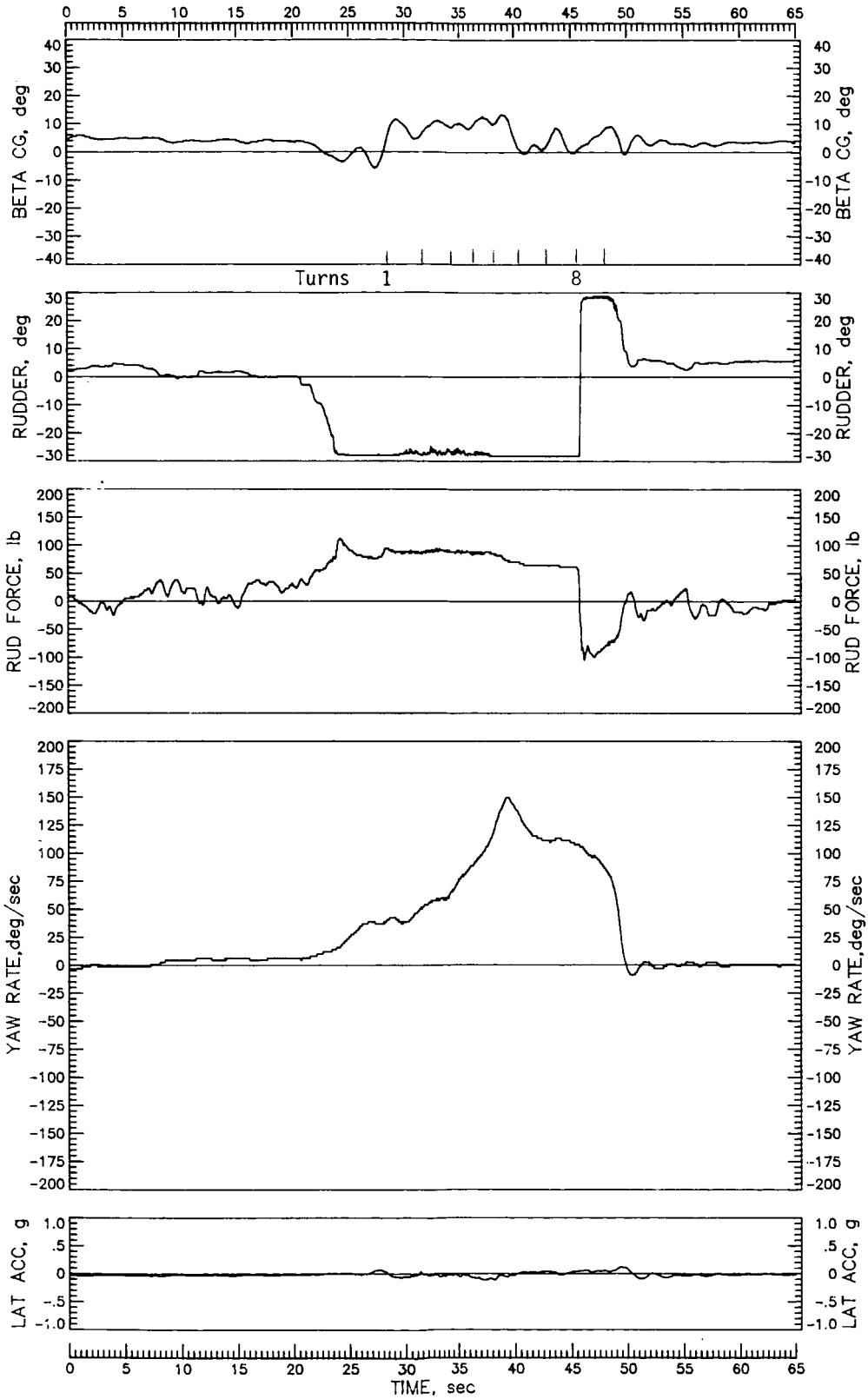

Figure 23. Continued.

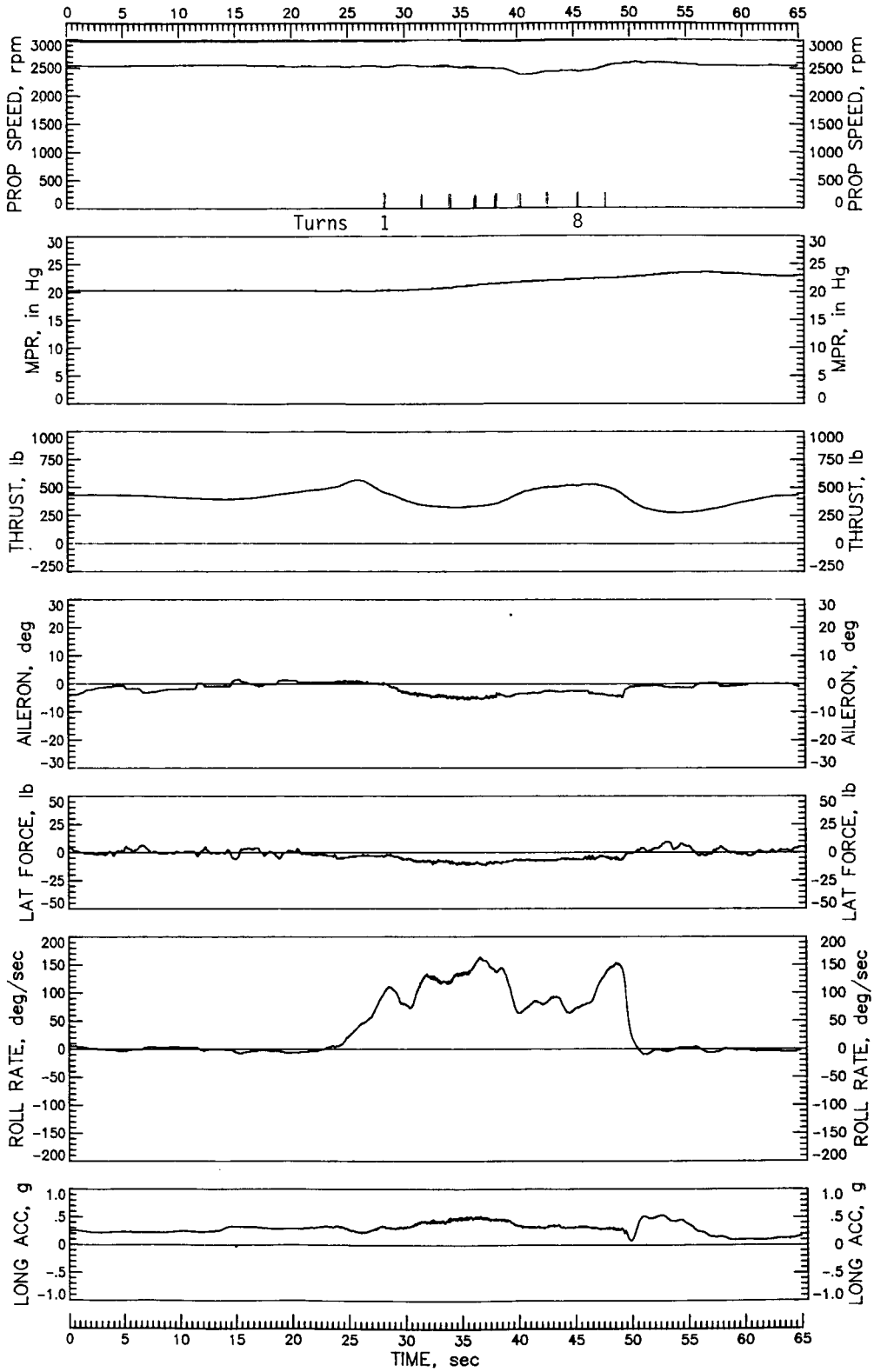

Figure 23. Continued.

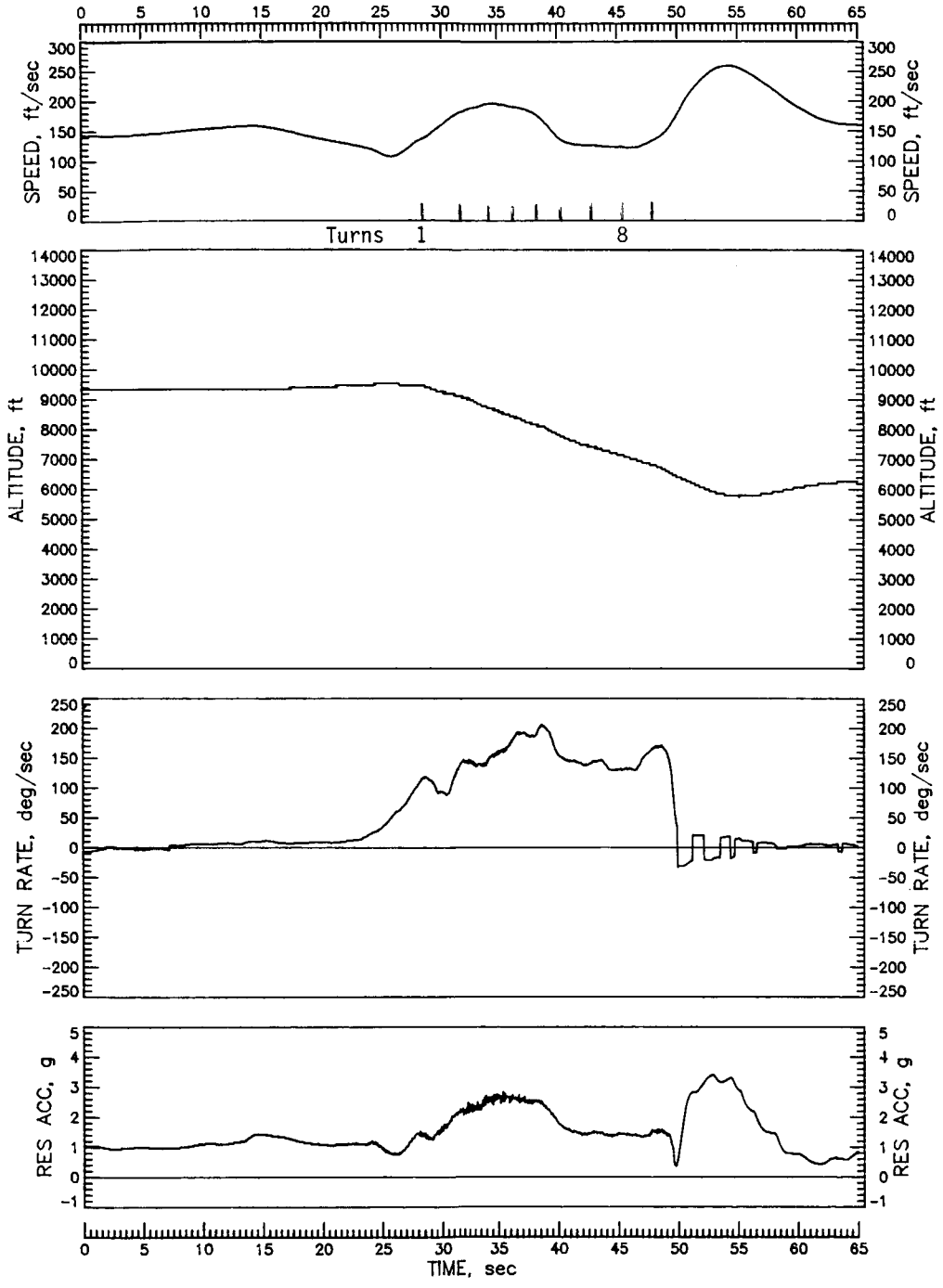

Figure 23. Concluded.

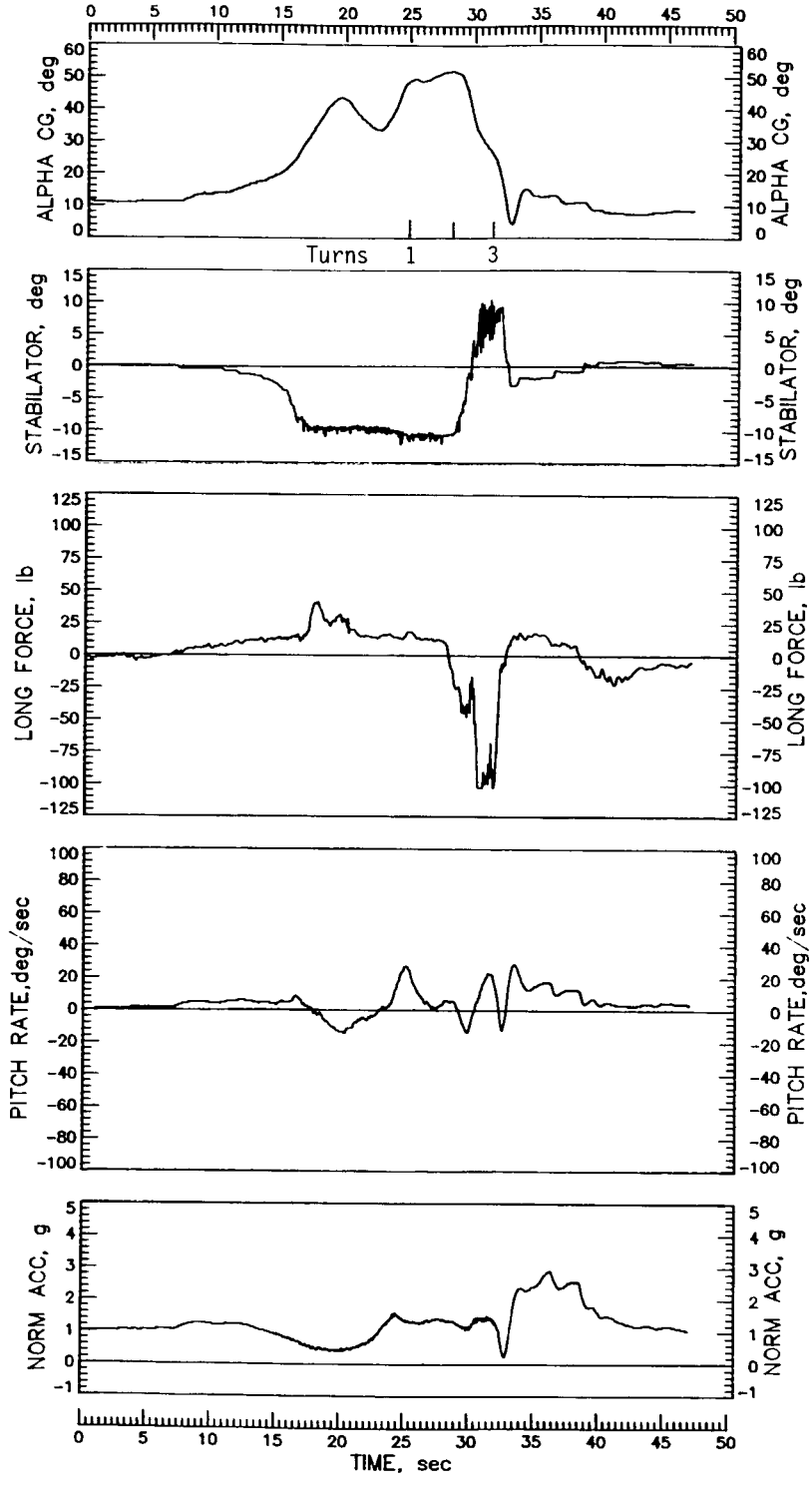

Figure 24. Left spin of modified airplane at maximum power entered from zoom maneuver, ailerons against the spin, flaps and gear retracted. Test weight = 2677 lb; c.g. = $0.2823\bar{c}$.

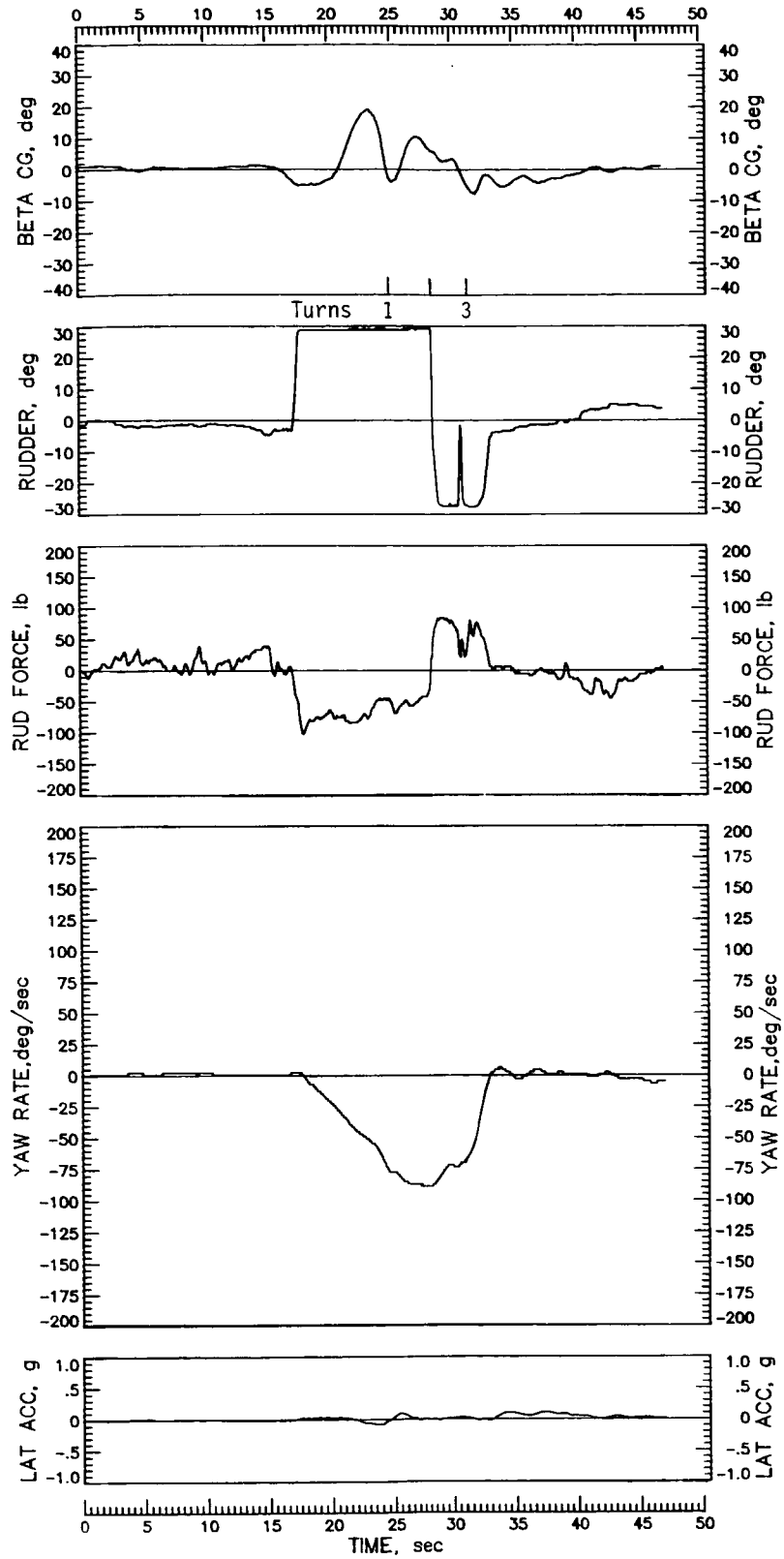

Figure 24. Continued.

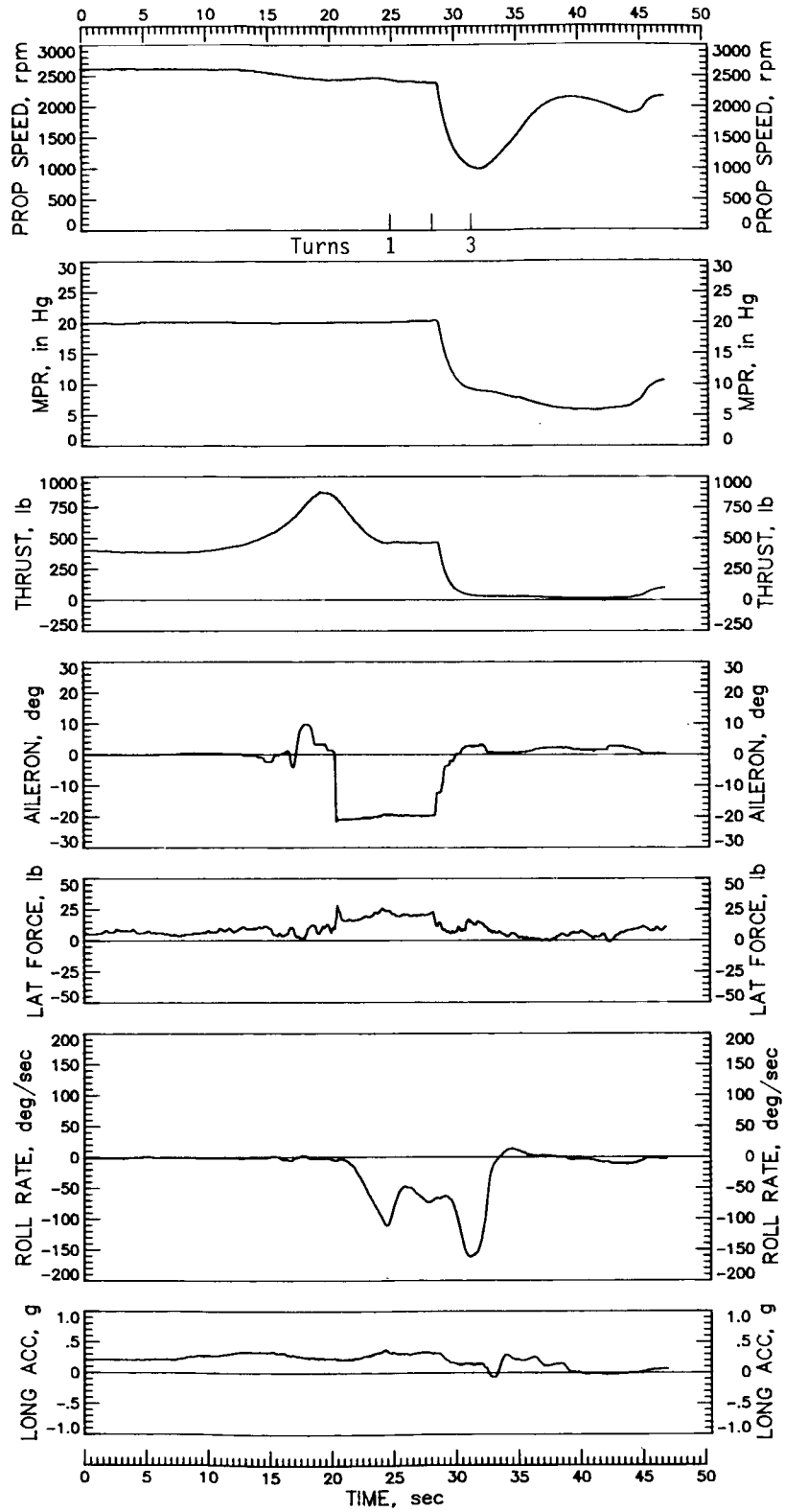

Figure 24. Continued.

C-2

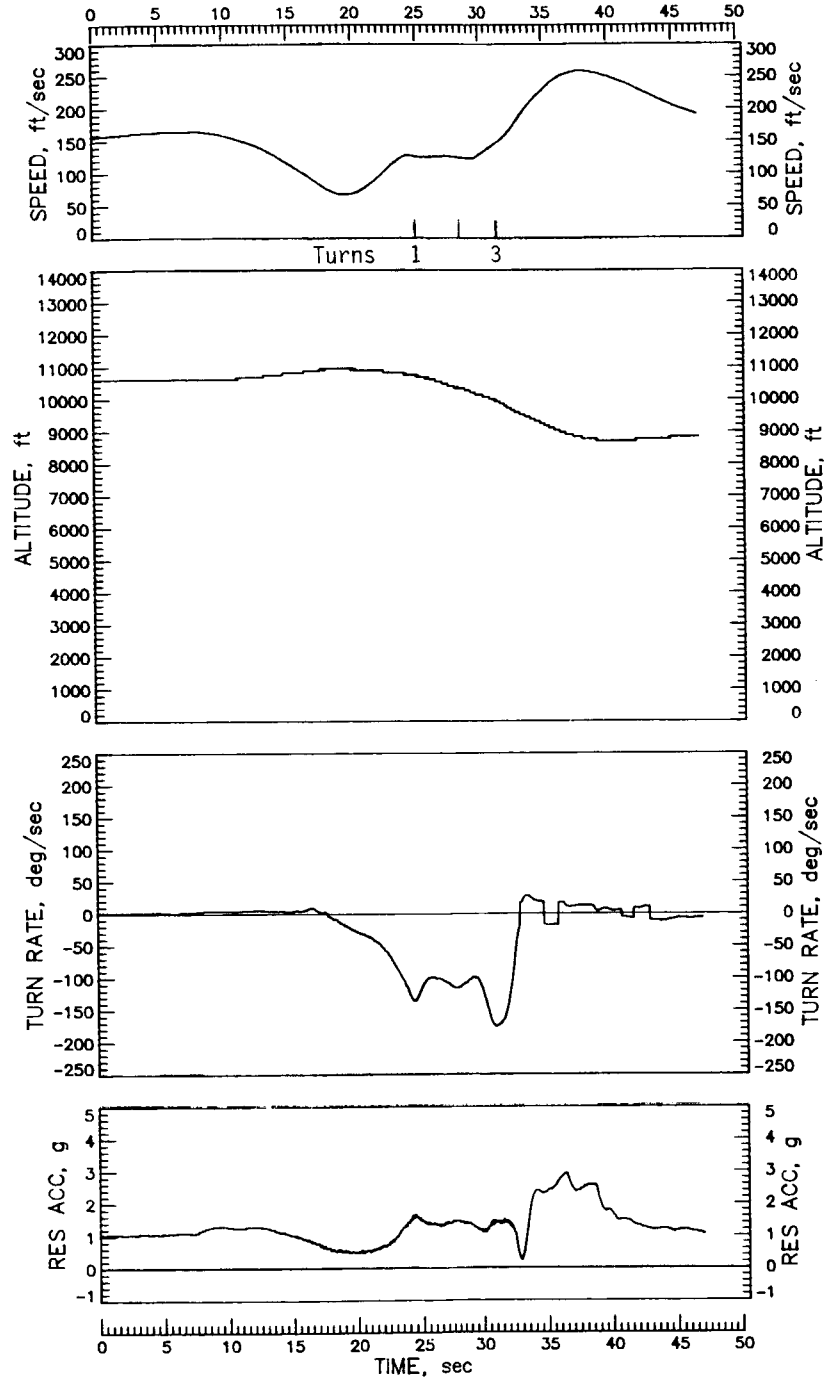

Figure 24. Concluded.

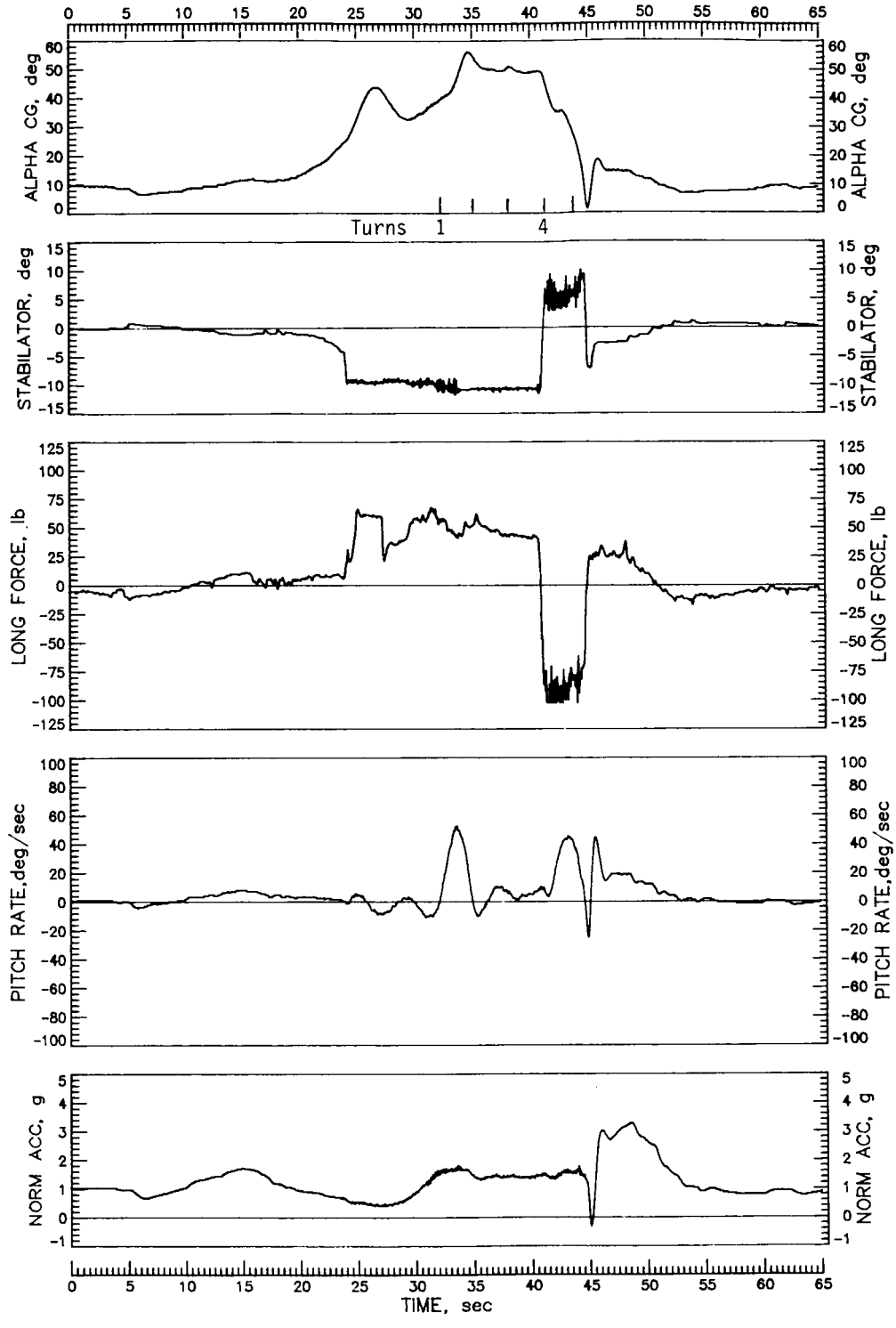

Figure 25. Left spin of modified airplane at maximum power entered from zoom maneuver, ailerons against the spin, flaps and gear retracted. Test weight = 2678 lb; c.g. = 0.2594$\bar{c}$.

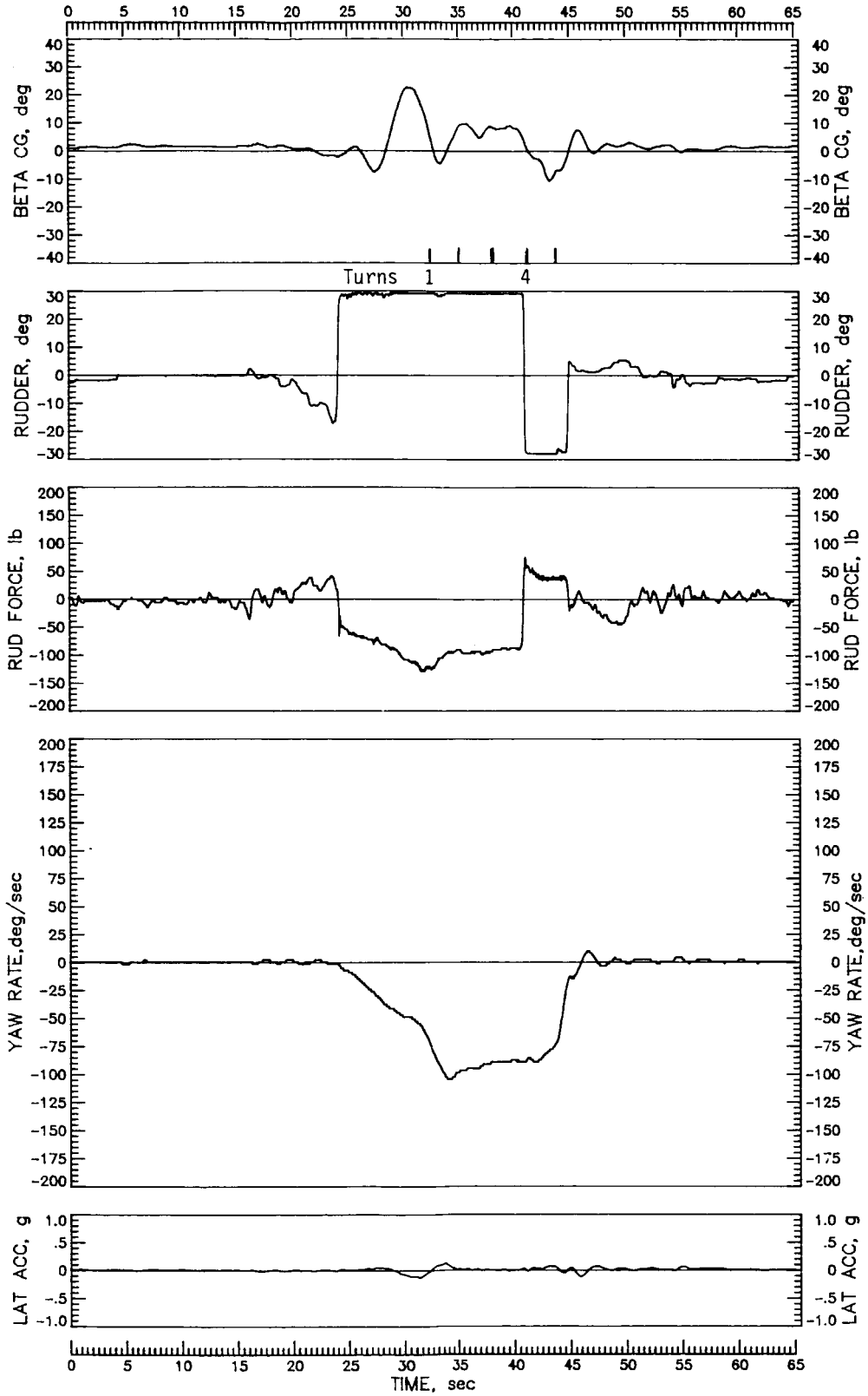

Figure 25. Continued.

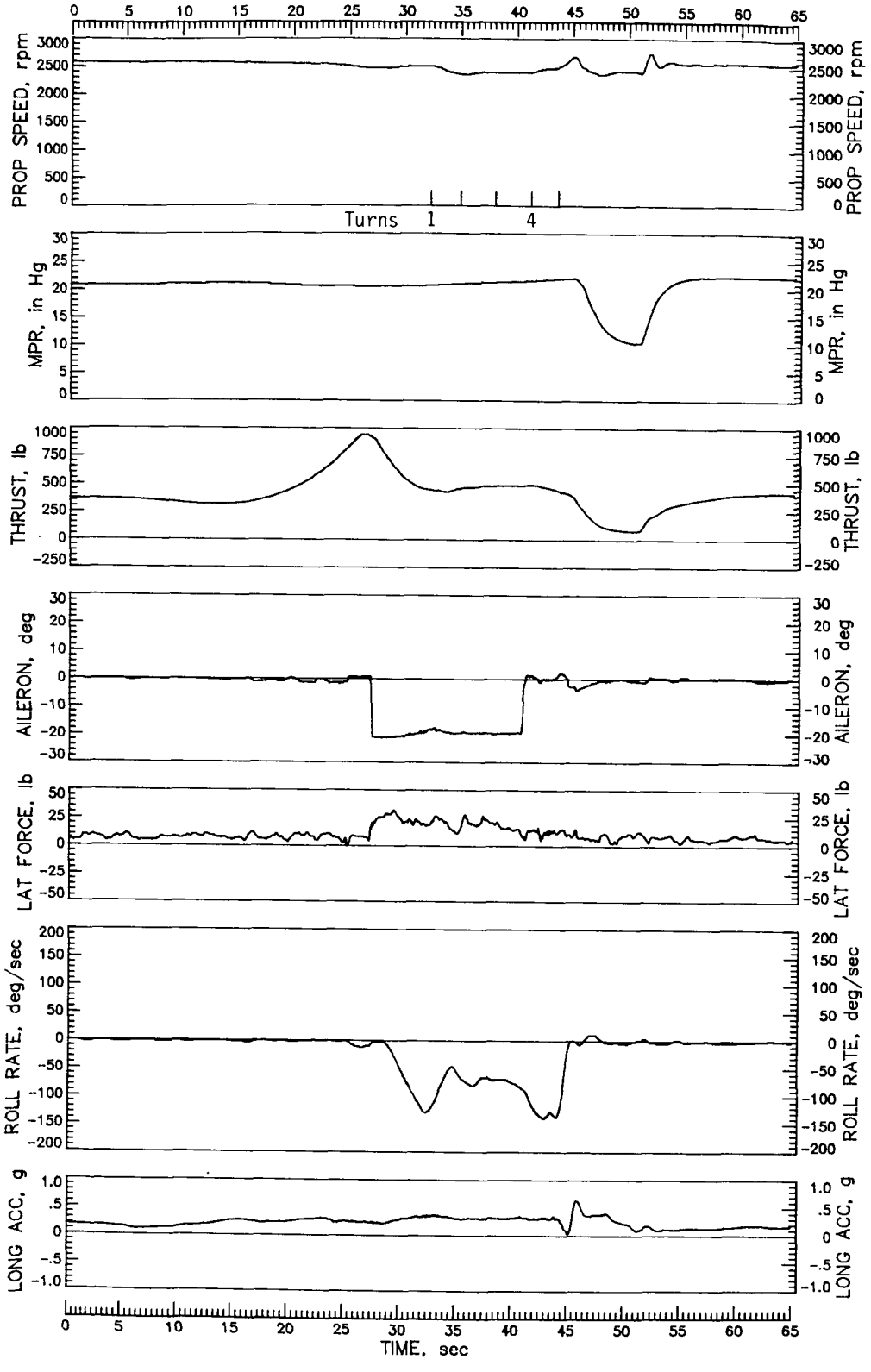

Figure 25. Continued.

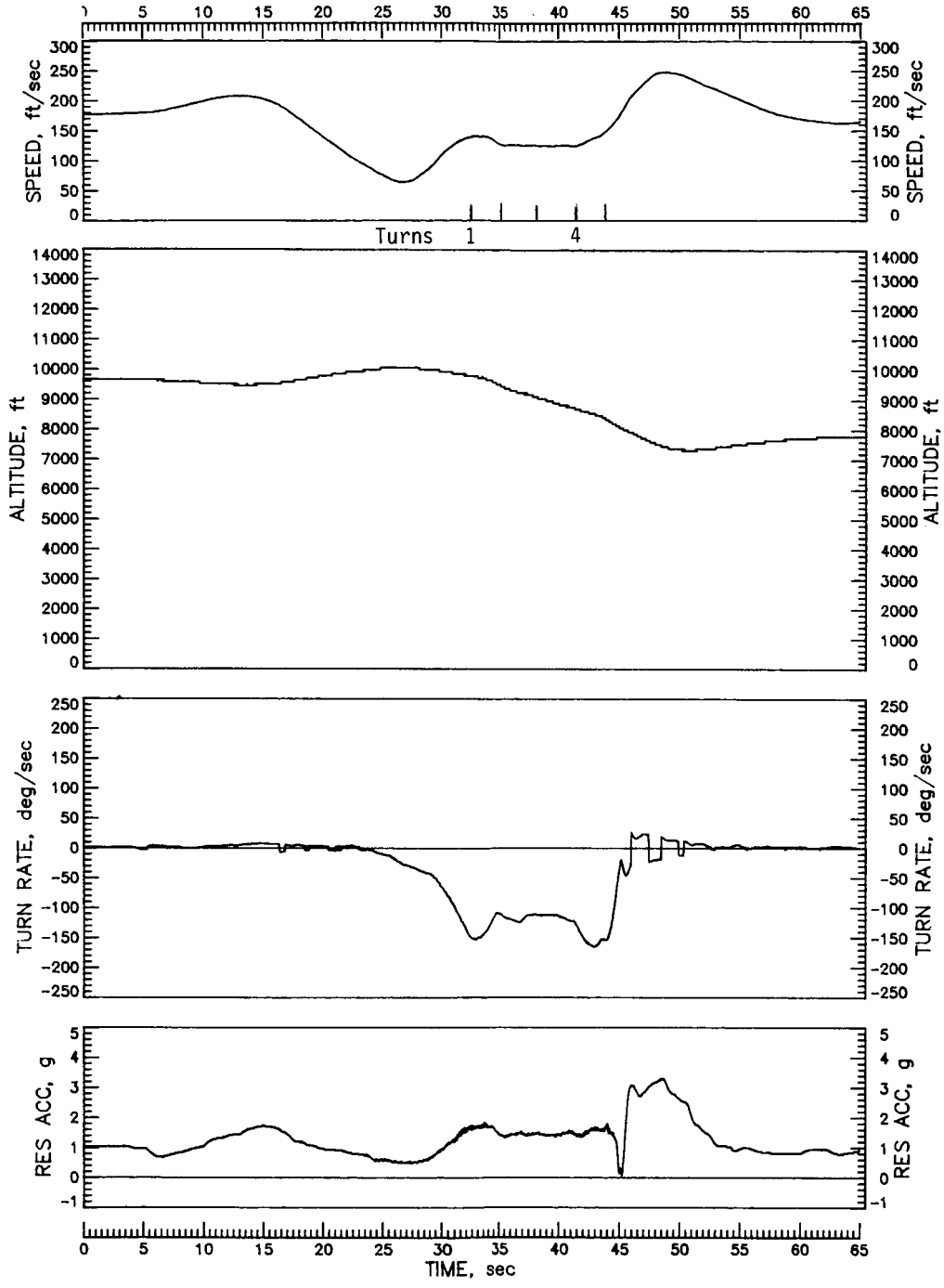

Figure 25. Concluded.

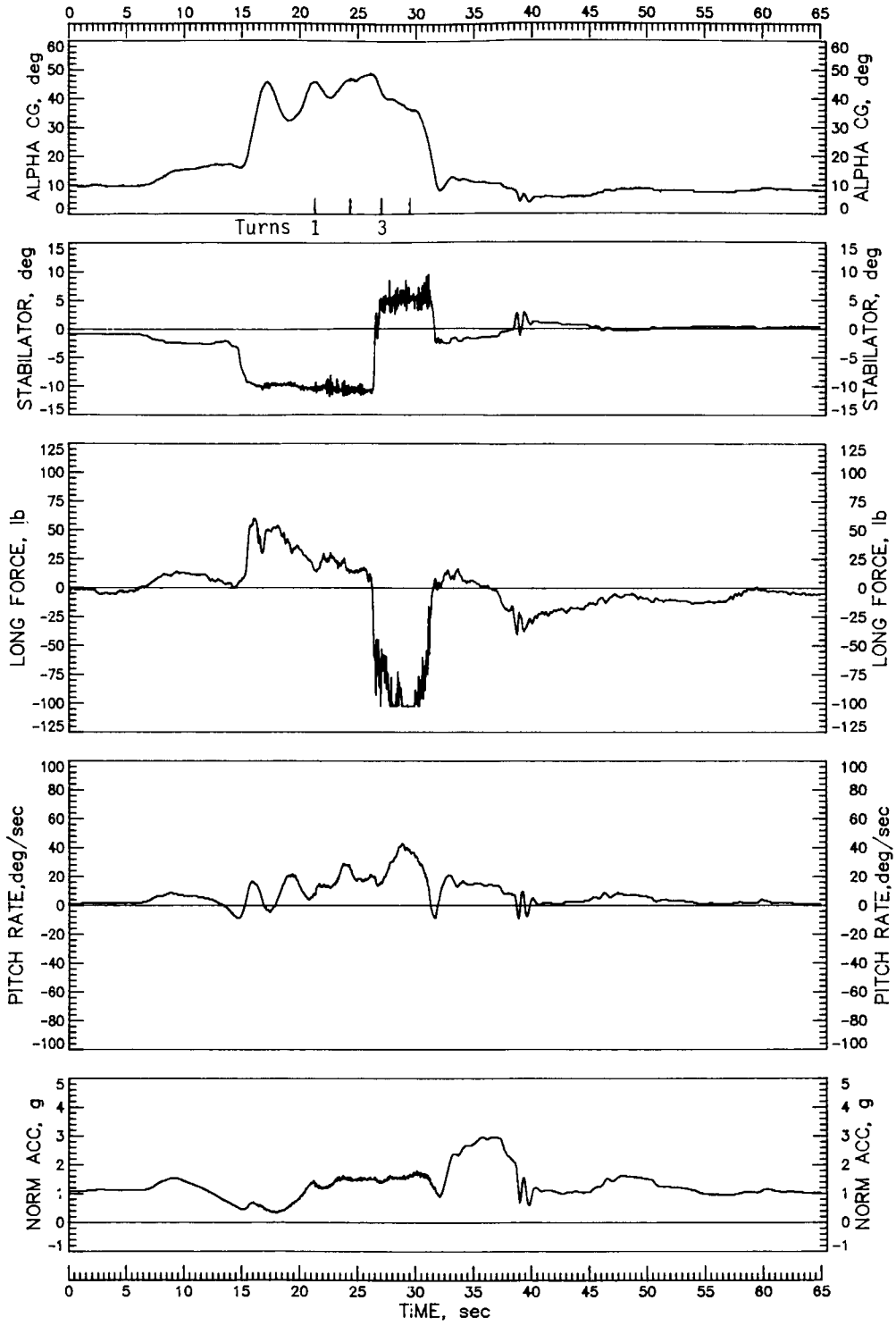

Figure 26. Left spin of modified airplane at maximum power entered from zoom maneuver, ailerons against the spin, flaps and gear retracted. Test weight = 2678 lb; c.g. = $0.2397\bar{c}$.

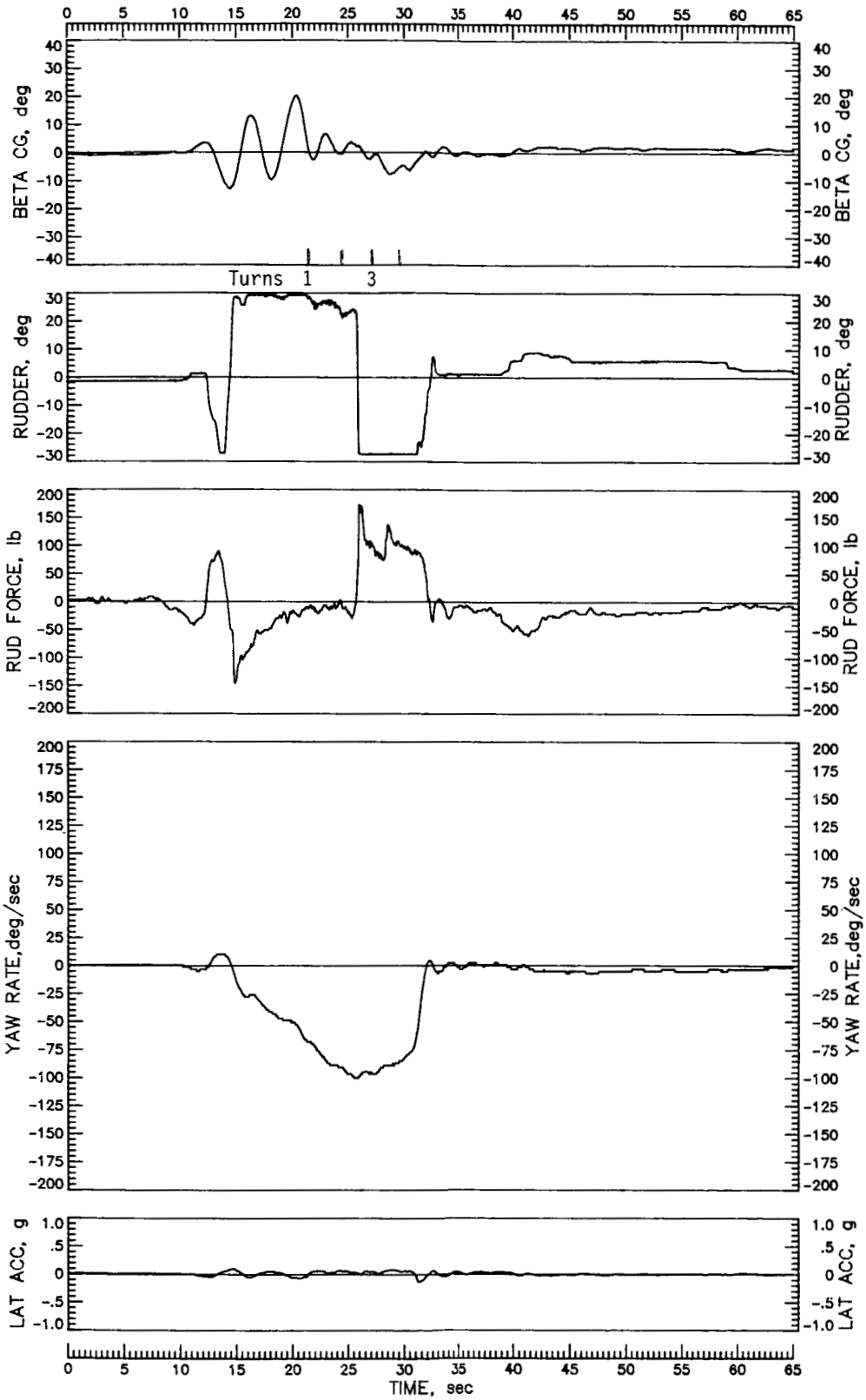

Figure 26. Continued.

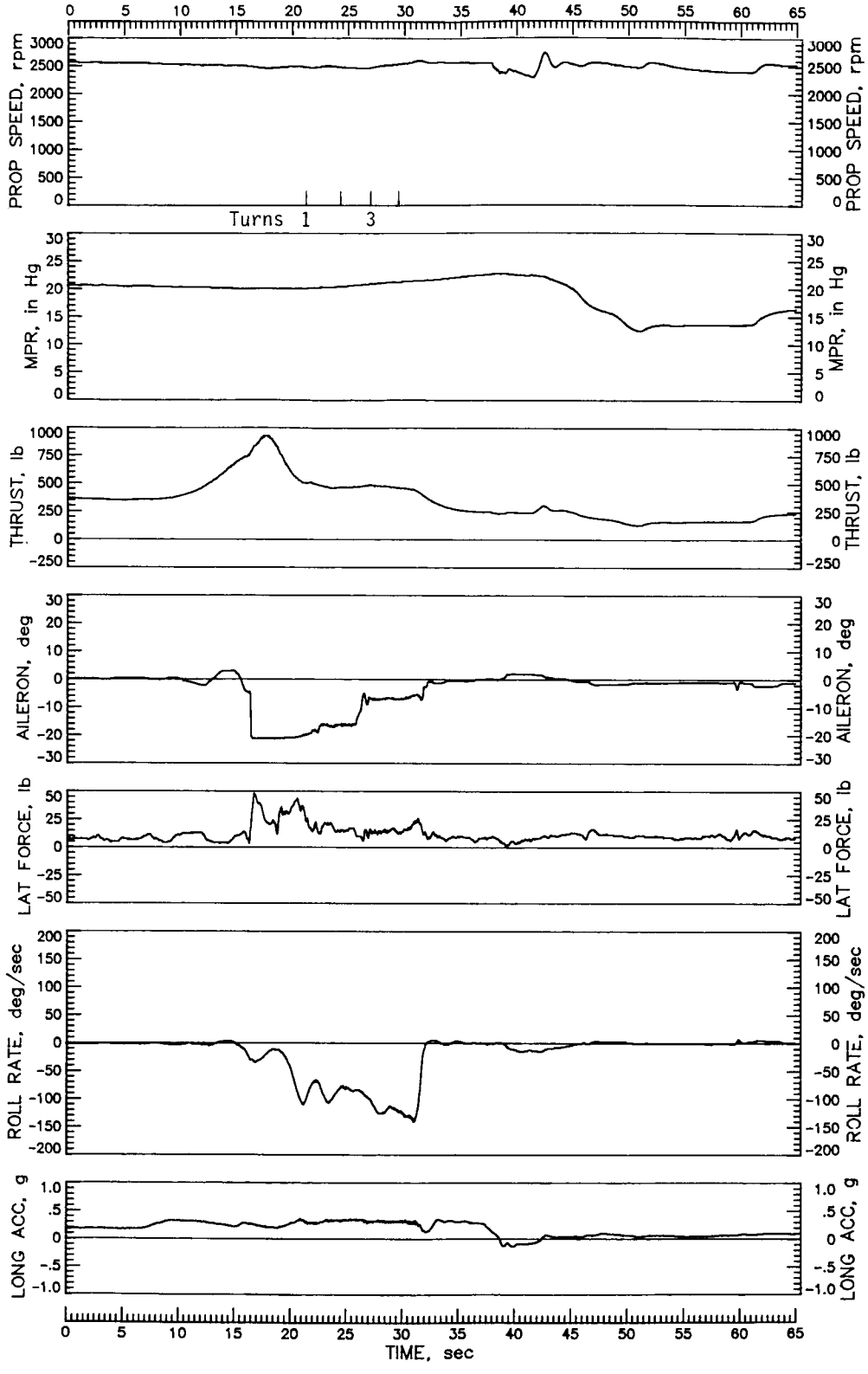

Figure 26. Continued.

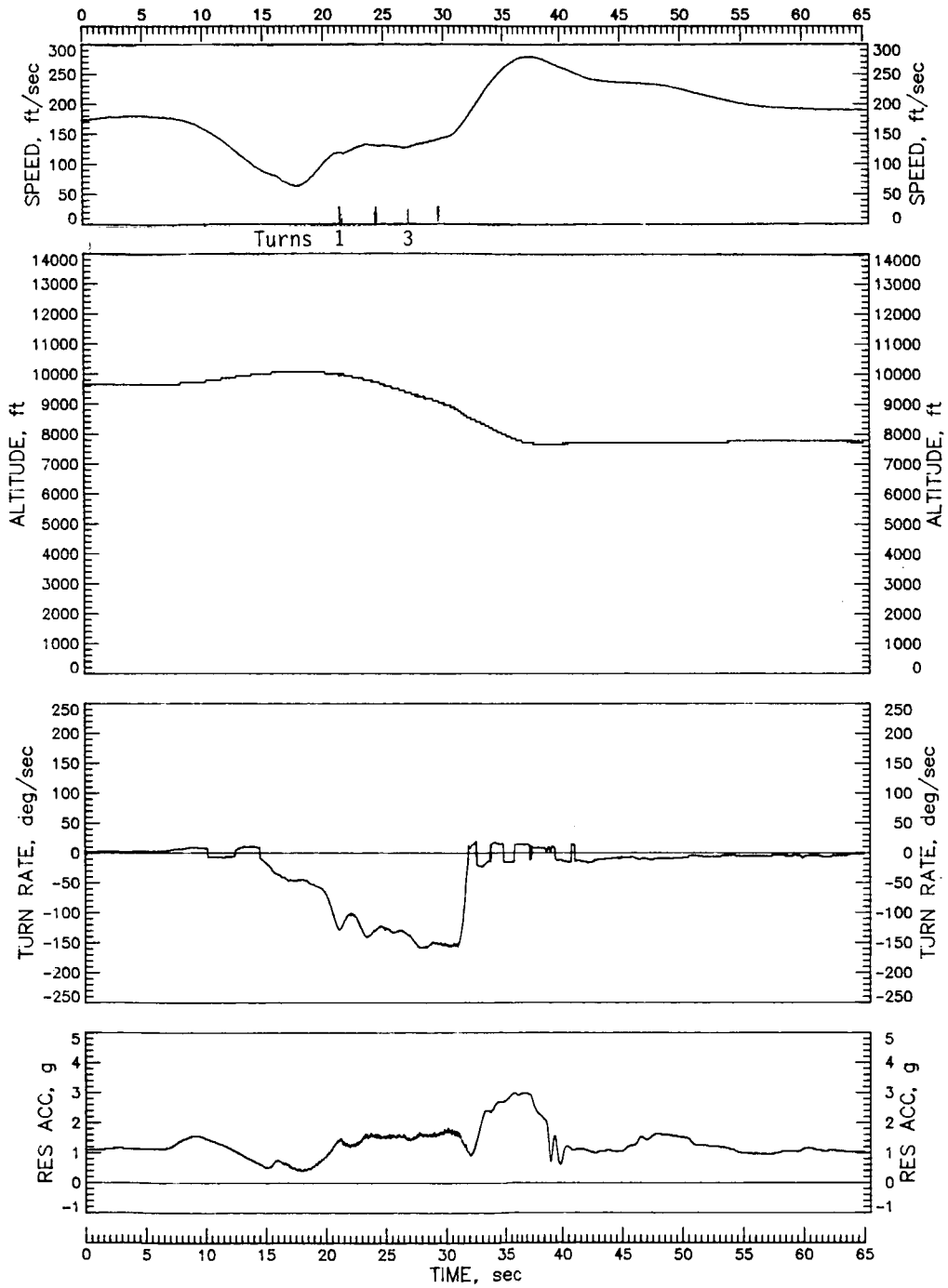

Figure 26. Concluded.

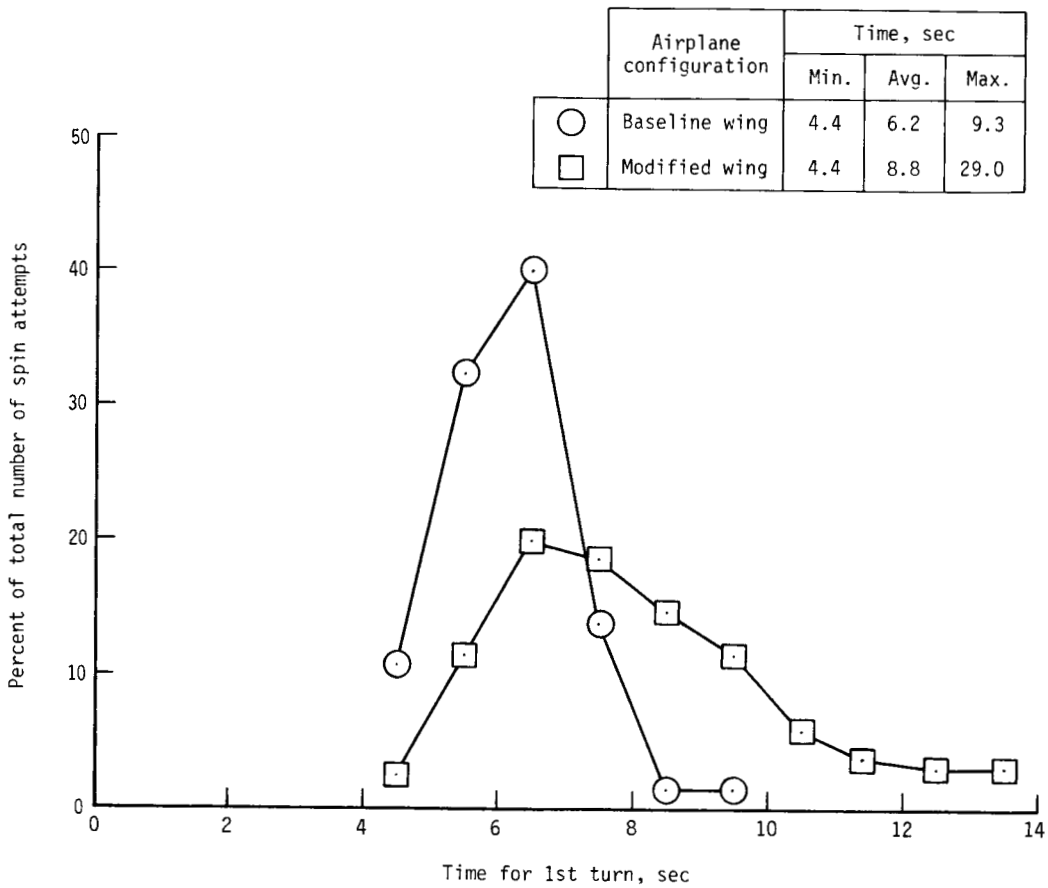

Figure 27. Distributions of times for first turn of rotation following pro-spin control input.

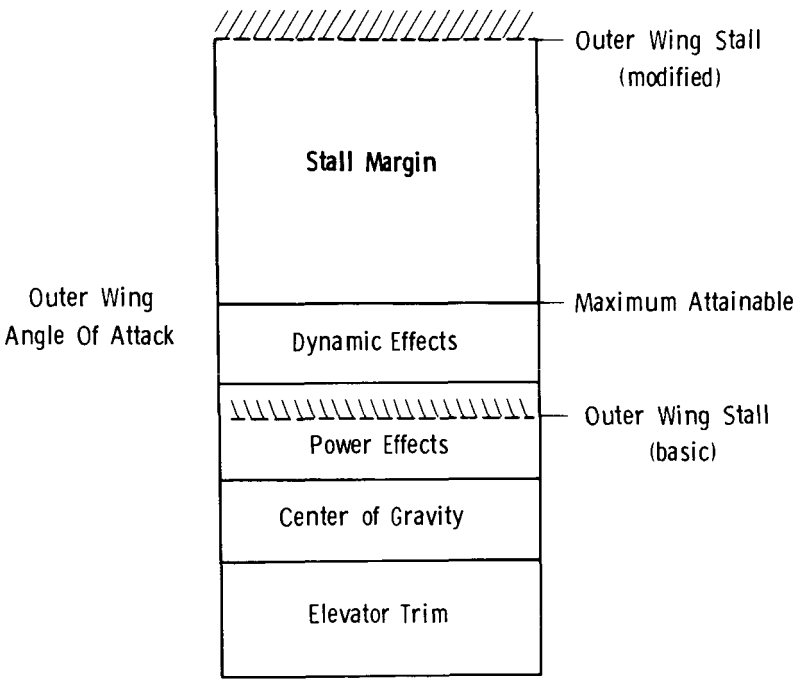

Figure 28. Maximum attainable angle of attack and stall-margin concept.

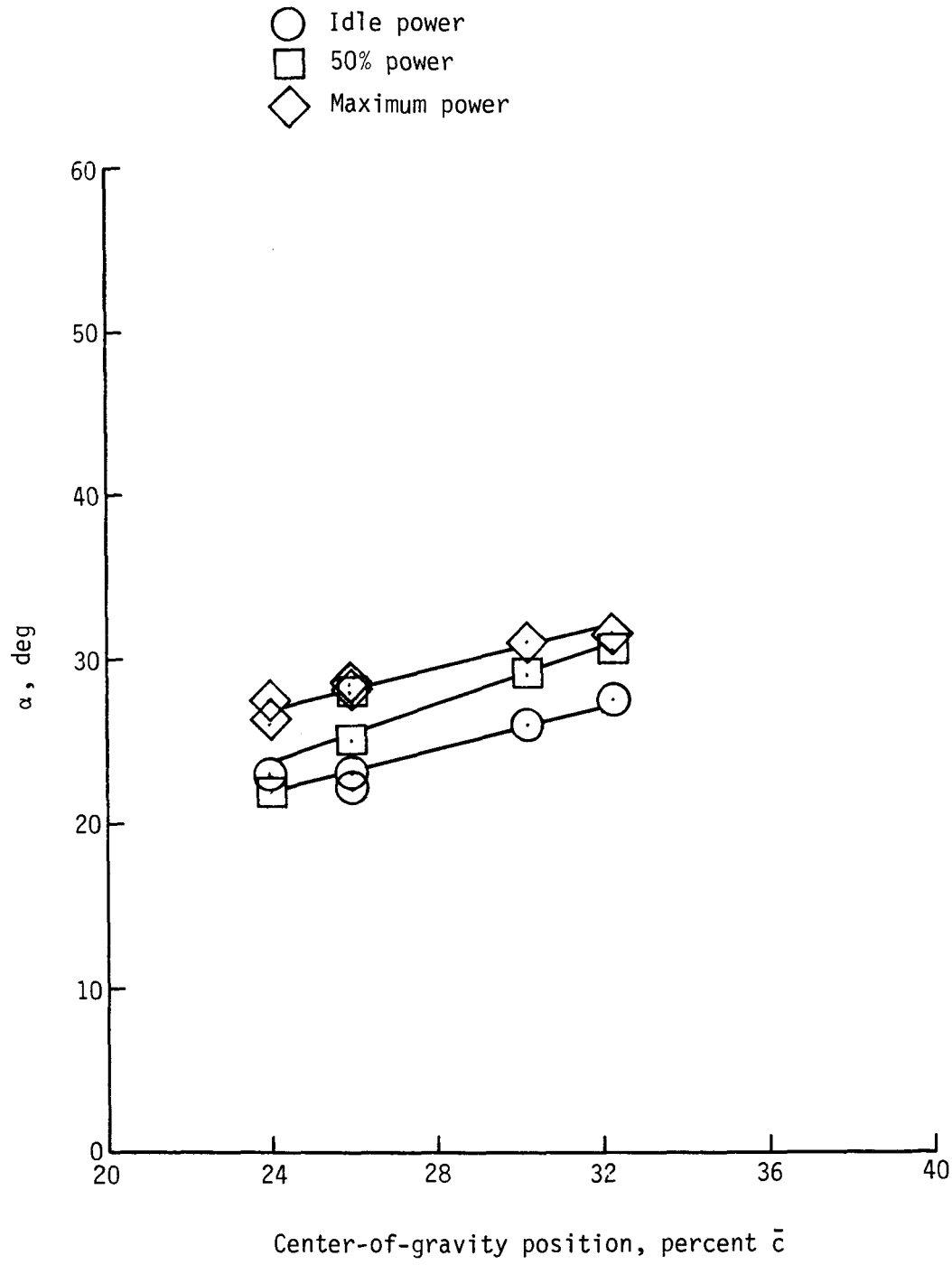

(a) Flaps retracted.

Figure 29. Variation of maximum trim angle of attack with center-of-gravity position for full trailing-edge-up stabilator deflection.

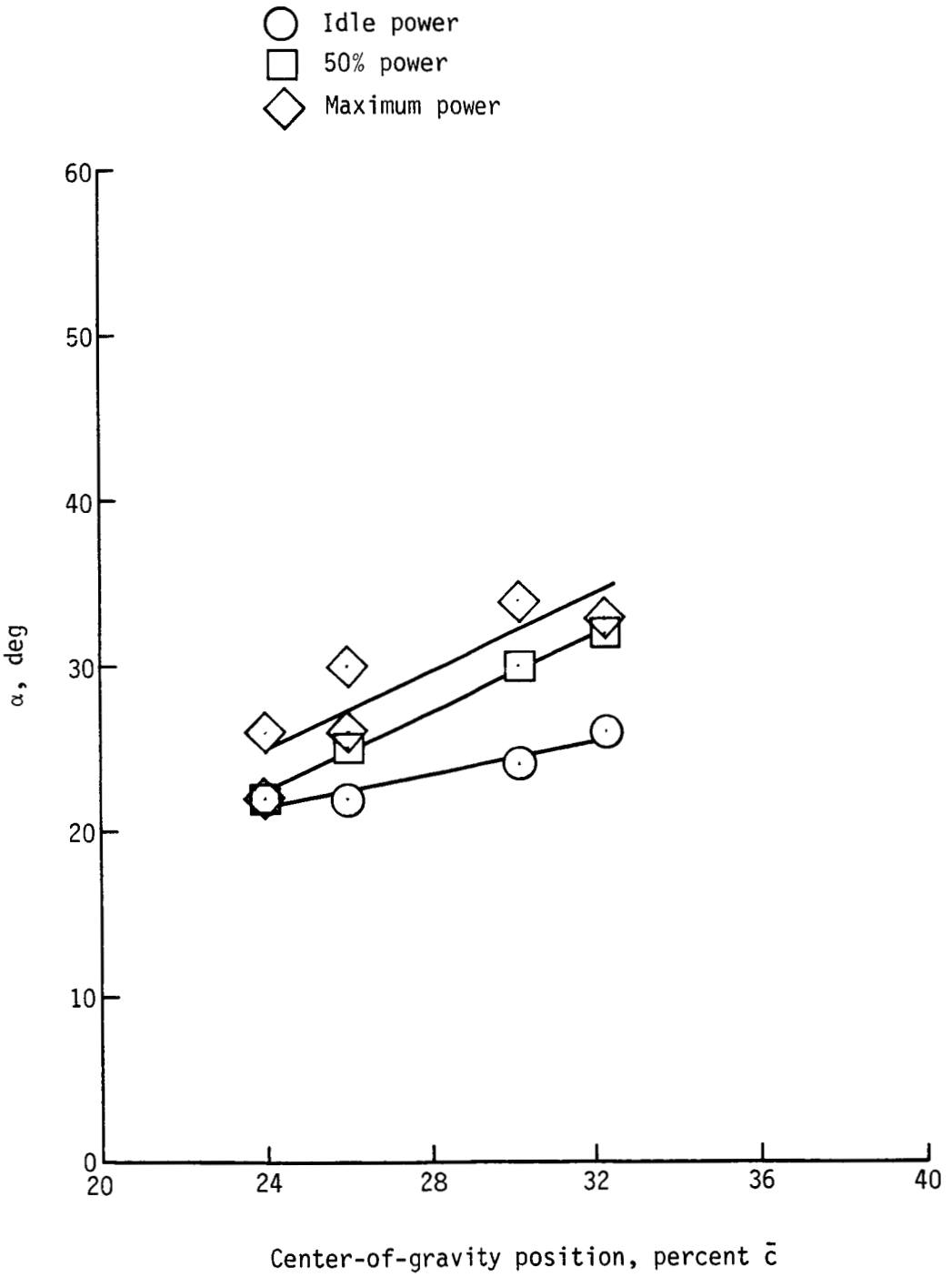

(b) Flaps deflected 40°.

Figure 29. Concluded.

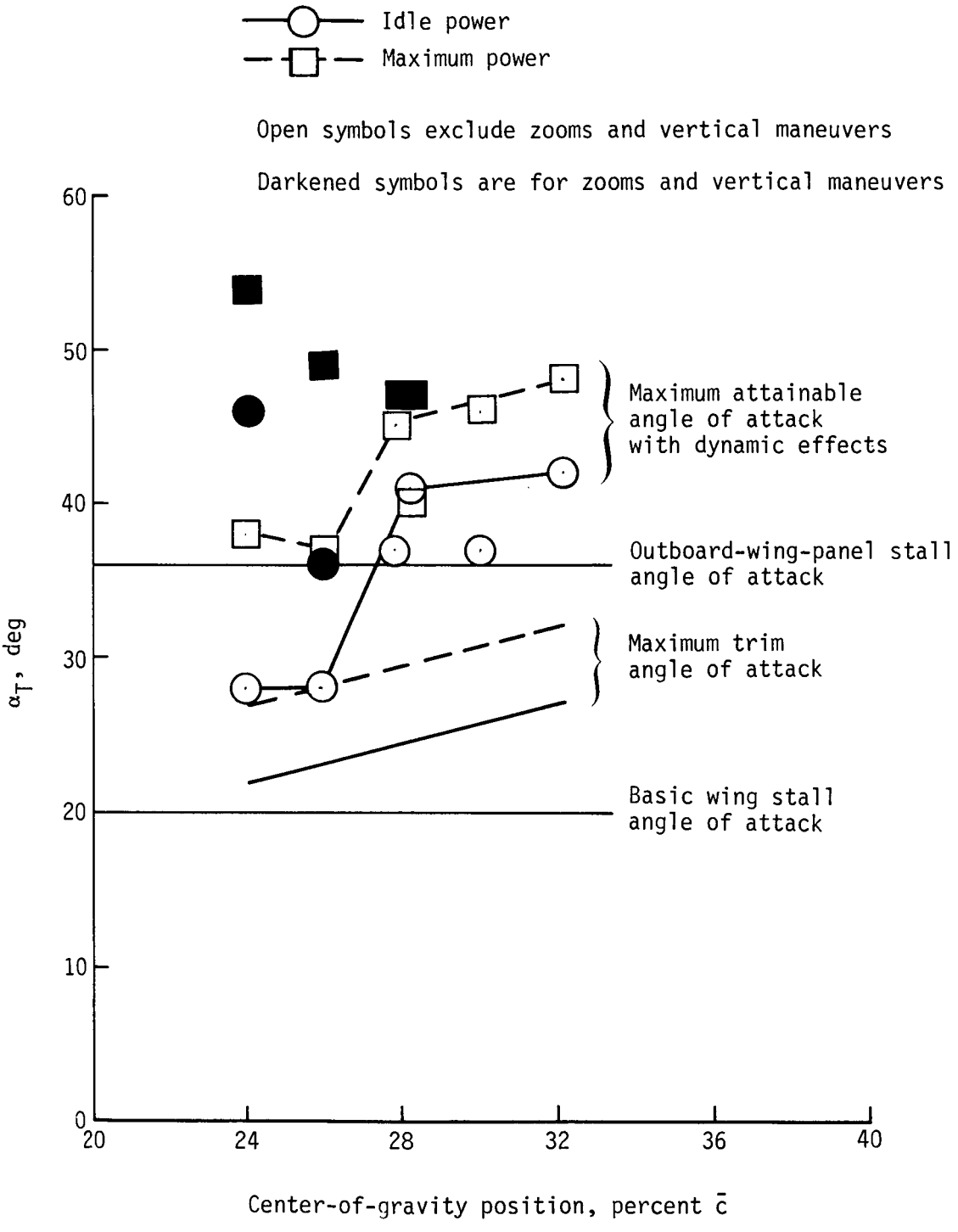

(a) Flaps retracted.

Figure 30. Variation of maximum attainable outer-wing angle of attack with center-of-gravity position.

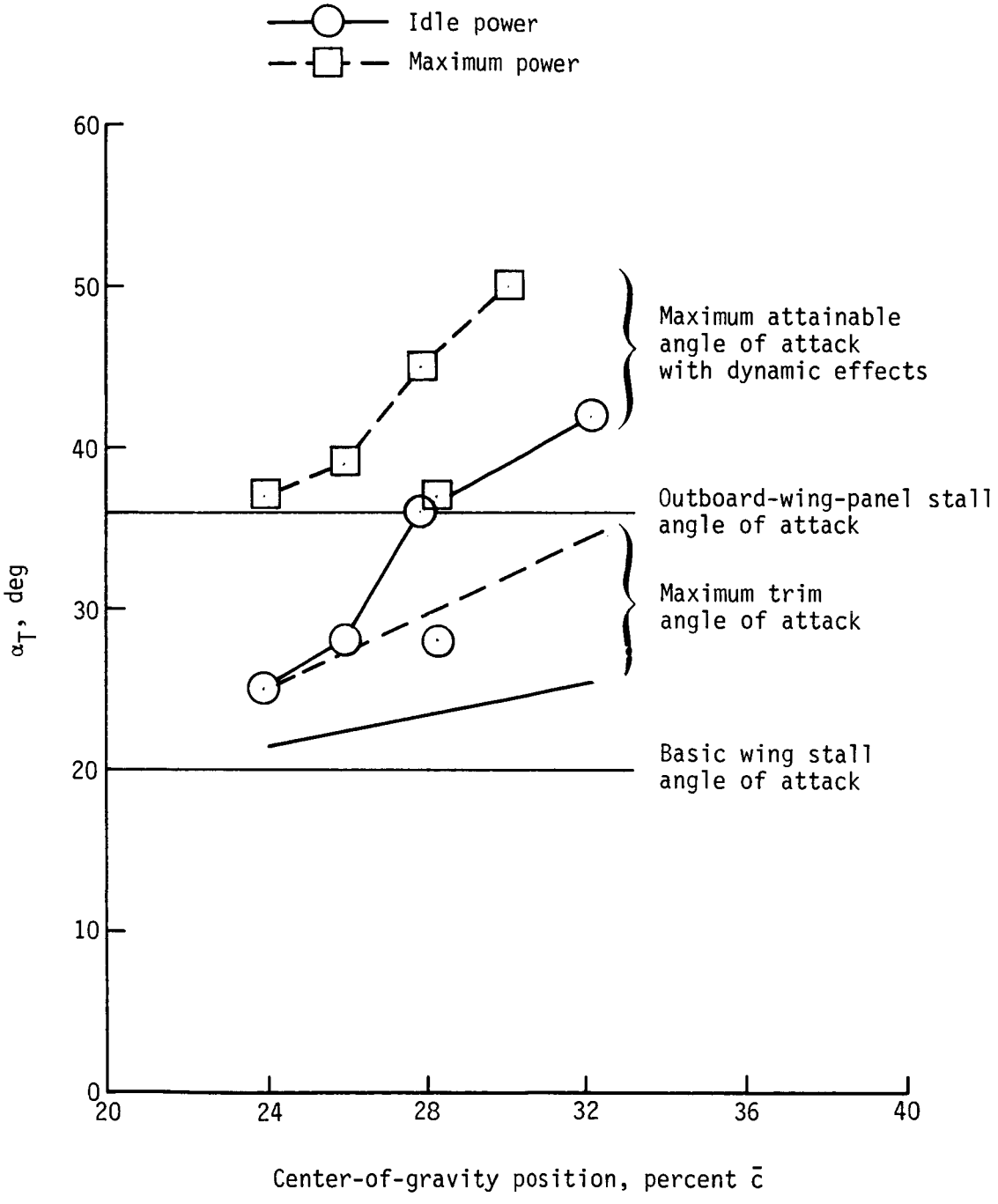

(b) Flaps deflected 40°.

Figure 30. Concluded.

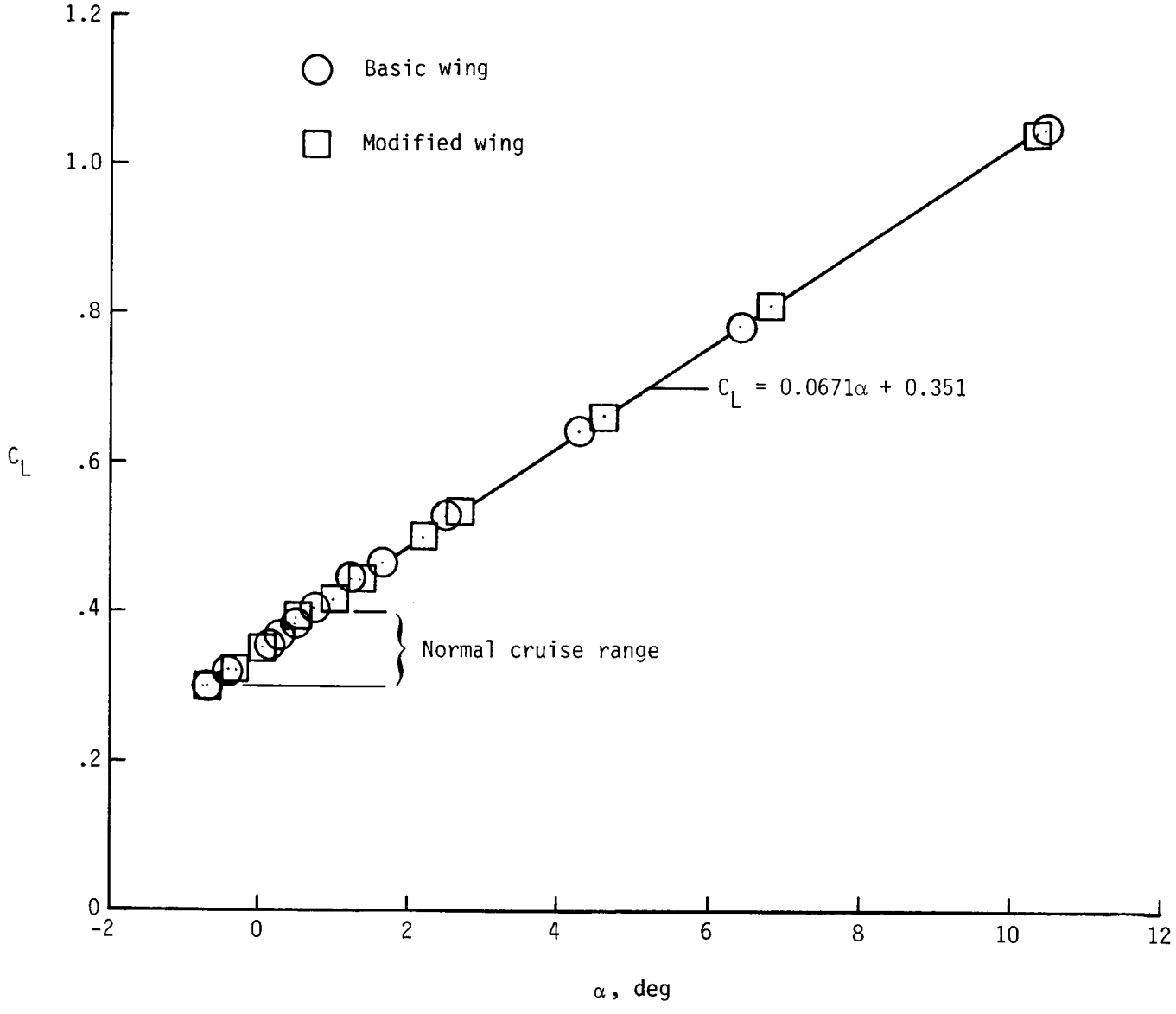

Figure 31. Airplane lift characteristics with and without wing-leading-edge modification.

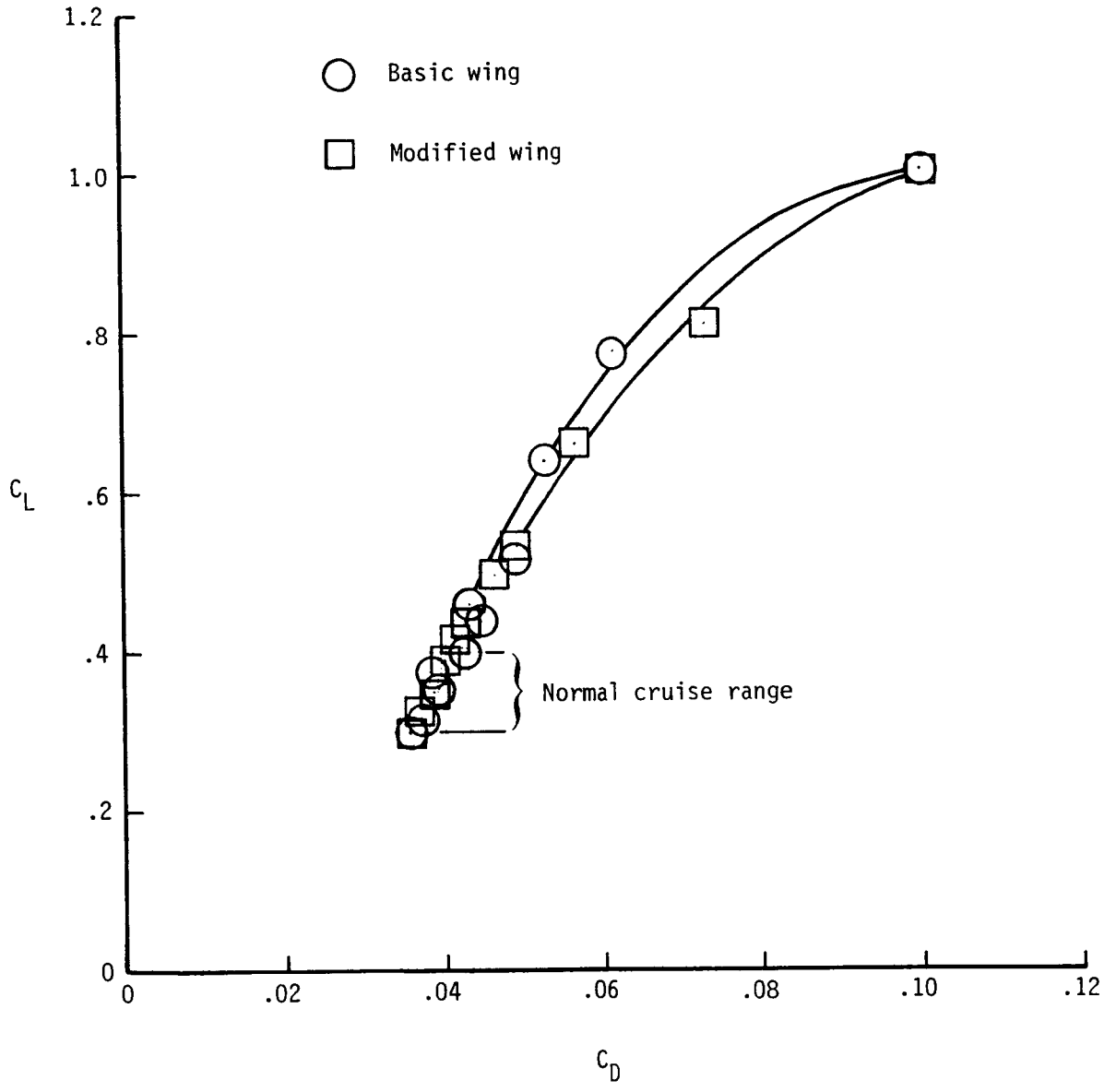

Figure 32. Airplane drag characteristics with and without wing-leading-edge modification.

NASA
National Aeronautics and Space Administration

Report Documentation Page

1. Report No.	2. Government Accession No.	3. Recipient's Catalog No.
NASA TP-2691		

4. Title and Subtitle	5. Report Date
Flight Investigation of the Effects of an Outboard Wing-Leading-Edge Modification on Stall/Spin Characteristics of a Low-Wing, Single-Engine, T-Tail Light Airplane	July 1987
	6. Performing Organization Code
7. Author(s)	8. Performing Organization Report No.
H. Paul Stough III, Daniel J. DiCarlo, and James M. Patton, Jr.	L-16243
9. Performing Organization Name and Address	10. Work Unit No.
NASA Langley Research Center Hampton, VA 23665-5225	505-61-41-01
	11. Contract or Grant No.
12. Sponsoring Agency Name and Address	13. Type of Report and Period Covered
National Aeronautics and Space Administration Washington, DC 20546-0001	Technical Paper
	14. Sponsoring Agency Code

15. Supplementary Notes

16. Abstract

Flight tests were performed to investigate the change in stall/spin characteristics due to the addition of an outboard wing-leading-edge modification to a four-place, low-wing, single-engine, T-tail, general aviation research airplane. Stalls and attempted spins were performed for various weights, center-of-gravity positions, power settings, flap deflections, and landing-gear positions. Both stall behavior and spin resistance were improved compared with the baseline airplane. The baseline airplane would readily spin for all combinations of power settings, flap deflections, and aileron inputs, but the modified airplane did not spin at idle power or with flaps extended. With maximum power and flaps retracted, the modified airplane did enter spins with abused loadings or for certain combinations of maneuver and control input. The modified airplane tended to spin at a higher angle of attack than the baseline airplane.

17. Key Words (Suggested by Authors(s))	18. Distribution Statement
Stall Spin Wing design Light airplane General aviation	Unclassified—Unlimited Subject Category 05

19. Security Classif.(of this report)	20. Security Classif.(of this page)	21. No. of Pages	22. Price
Unclassified	Unclassified	116	A06

For sale by the National Technical Information Service, Springfield, Virginia 22161-2171